

# **Higher Order Time Discretization of Compartmentalized Reservoirs**

by

©Dan Wang

A thesis submitted to the

School of Graduate Studies

in partial fulfillment of the requirements for the degree of

**Master of Oil and Gas Engineering**

**Faculty of Engineering and Applied Science**

Memorial University of Newfoundland

Oct 2016

St. John's Newfoundland and Labrador

## ABSTRACT

Reservoir tank modeling has traditionally been employed to simplify complicated reservoir simulation models and to reduce computational time whilst maintaining model accuracy. In this thesis, we refine this concept by replacing a simple tank model with a system of ordinary differential equations (ODEs) to model the dynamic changes of well inflow, aquifer influx, fluid compressibility, and pore volume. A dual time step method is used to solve the system of equations, which is not included in the existing model. Well transmissibility and aquifer sizes are kept constant during small time steps in which pressures and flow rates are solved. The new pressure is then used to update the well indices and aquifer size over larger time steps. This new model is transient during a single large time step calculation and hence represents an enhancement over standard finite difference method formulations.

The reservoir is subdivided into a number of subvolumes representing individual reservoir compartments and aquifers, which may or may not be in communication. Using the concepts of transmissibility and compressibility, the complex 3D reservoir system is converted into a model that establishes flow into wells and between compartments. Pressure loss due to friction along the well is also fully integrated in the model. The multiple reservoir compartments and flowing wellbore are coupled to provide influx and inter-compartment fluid transfer. Employing the fourth-order Runge-Kutta Method, the ordinary differential equations generated by the system of reservoir units, are solved accurately and efficiently.

The new method is verified by comparing it with a standard reservoir simulation launcher (Eclipse Trademark of Schlumberger Technology Corporation). Case studies are utilized to illustrate the results of the method which predict oil/gas production with water encroachment from an aquifer. Sensitivity analysis is performed to understand the relationships between input variables and output results in the model. For black oil reservoirs, this model incorporates wellbore friction and up to fifty reservoir compartments, which allows us to more accurately predict the reservoir performance. In addition, this model incorporates and compares the effects of compressibility for gas reservoirs, the results show that for those gas reservoirs with high rock compressibility, the gas reservoir model with water compressibility and pore volume term considered must be used in order to obtain more realistic simulation results.

## ACKNOWLEDGEMENTS

The author would like to express the generous and unwavering support of my supervisors, **Dr. Lesley James** and **Dr. Thormod Johansen** for providing outstanding technical guidance to this body of work. Thanks to their great patience and kind support through each step of this thesis.

The author would also like to express my appreciation to Norah Hyndman for helping with thesis corrections.

Additionally, I would like to acknowledge my research colleagues. Thanks for their suggestions and encouragement.

A special acknowledgement is extended to my parents and loving husband Xiang Shan.

Their supporting, concerning, and selfless giving are the best treasures in my present life.

# Nomenclature

## List of Abbreviations, Symbols and Nomenclature

### Abbreviations

BWDA	Bottom waterdrive aquifer
EWDA	Edge waterdrive aquifer
<b>FVF</b>	<b>Formation volume factor</b>
HCPV	Hydrocarbon pore volume
LWDA	Linear waterdrive aquifer
MBA	Material balance analysis
MCC	Multiple communicating compartmentalized reservoir model
MNC	Multiple non-communicating compartmentalized reservoir model
ODE	Ordinary differential equation
OIIP	Oil initially in place
PVC	Pore volume compressibility
RCs	Reservoir compartments
STC	Stock tank condition
<b>STOIIP/STGIIP</b>	<b>Stock tank oil/gas initially in place</b>
THP	Tubing head pressure

## English Symbols with SI Units

$a$	Half major axis in the ellipse	-
$A$	Cross section area of the pipe	$\text{m}^2$
$A_c$	Cross sectional area	$\text{m}^2$
$B$	Formation volume factor	-
$B_g$	Gas formation volume factor	-
$B_w$	Water formation volume factor	$\text{Rm}^3 / \text{Sm}^3$
$c_a$	Aquifer compressibility	$\text{kPa}^{-1}$
$c_t$	Total compressibility	$\text{kPa}^{-1}$
$c_g$	Gas compressibility	$\text{kPa}^{-1}$
$c_o$	Oil compressibility	$\text{kPa}^{-1}$
$c_r$	Rock compressibility	$\text{kPa}^{-1}$
$c_w$	Water compressibility	$\text{kPa}^{-1}$
$D$	Wellbore diameter	$\text{m}$
$D_h$	Hydraulic diameter	$\text{m}$
$E_0$	Oil expansion	$\text{m}^3 / \text{m}^3$
$f$	Friction factor	-
$g$	Gravity acceleration	$\text{m}^2 / \text{s}$
$G$	Stock tank gas initially in place	$\text{Sm}^3$
$G_p$	Cumulative gas produced at stock tank condition	$\text{Sm}^3$
$h$	Reservoir thickness	$\text{m}$

$J_w$	Well transmissibility	$\text{Sm}^3/(\text{kPa}\cdot\text{day})$
$i$	Number of Reservoir Compartments	-
$J_a$	Aquifer transmissibility	$\text{Sm}^3/(\text{kPa}\cdot\text{day})$
$J_c$	Inter-compartment transmissibility	$\text{Sm}^3/(\text{kPa}\cdot\text{day})$
$J_{wj}^*$	Simplified gas well transmissibility	$\text{Sm}^3/(\text{kPa}\cdot\text{day})$
$K$	Absolute permeability	mD
$K_h$	Horizontal permeability	mD
$K_v$	Vertical permeability	mD
$L$	Distance	m
$m$	Pseudo-pressure	kPa
$M$	Molecular mass of reservoir gas	g/mol
$M_G$	Molecular mass of surface gas	g/mol
$n$	Total number of the RCs	-
$N$	Initial oil in place	$\text{Sm}^3$
$\bar{p}$	Average initial aquifer pressure	kPa
$P_0$	Pressure at standard condition	kPa
$P_c$	Critical pressure	kPa
$P_i$	Initial aquifer pressure	kPa
$\Delta P$	Pressure drop at the reservoir/aquifer interface	kPa
$P_{ra}$	Abandonment reservoir pressure	kPa
$P_{ref}$	Reference pressure	kPa
$P_r$	Average reservoir pressure	kPa
$P_w$	Bottom hole pressure	kPa

$P_{w\_bl}$	Pressure loss in the blank pipe segment	kPa
$P_{wf}$	Wellbore pressure	kPa
$q$	Flowrate	Sm <sup>3</sup> /day
$q_{wf}$	Wellbore flowrate	Sm <sup>3</sup> /day
$Q_o$	Cumulative oil production	Sm <sup>3</sup>
$r_a$	Radius of the aquifer	m
$r_e$	Radius of the reservoir	m
<b>R</b>	<b>Gas Constant</b>	<b>J/(Kg*K)</b>
Re	Renolds number	-
$S_{cw}$	Connate water saturation	-
$S_g$	Gas saturation	-
$S_o$	Oil saturation	-
$S_w$	Water saturation	-
$t$	Time	day
$T_0$	Temperature at standard condition	K
$T_c$	Critical temperature	K
$t_D$	Dimensionless time	-
$T_r$	Reservoir temperature	K
$v$	Velocity	m/s
$V_a$	Aquifer volume	m <sup>3</sup>
$\Delta V_{cw}$	Expansion of connate water in gas zone	m <sup>3</sup>
$V_r$	In-situ saturated volume in the reservoir	m <sup>3</sup>

$\Delta W$	Influx of water from the aquifer	$m^3$
$W_A$	Aquifer size	$Rm^3$
$W_{awe}$	Cumulative water influx	$Rm^3$
$W_e$	Water influx	$m^3$
$W_e$	Cumulative water influx from aquifer to reservoir	$m^3$
$W_{eD}$	Dimensionless water influx	-
$W_{ei}$	Initial encroachable water	$m^3$
$W_i$	Initial water volume in the aquifer	$Rm^3$

### **Greek Symbols with SI Units**

$\alpha$	Poiseuille number	-
$\mu$	Viscosity of the fluid	Pa.s
$\mu_w$	Water viscosity	Pa.s
$\rho$	Density	$kg/m^3$
$\rho_{sc}$	Gas density of surface gas at standard conditions	$kg/m^3$
$\delta$	Wellbore roughness	m
$\phi$	Porosity of aquifer	-

## Subscripts

<i>g</i>	Gas
<i>i</i>	Initial conditions
<i>n</i>	The number of compartment
<i>o</i>	Oil
<i>r</i>	Rock
<i>t</i>	Time index
<i>w</i>	Water

# Table of Contents

<b>ABSTRACT</b> .....	<b>i</b>
<b>ACKNOWLEDGEMENTS</b> .....	<b>iii</b>
<b>Nomenclature</b> .....	<b>iv</b>
<b>Table of Contents</b> .....	<b>x</b>
<b>List of Tables</b> .....	<b>xii</b>
<b>List of Figures</b> .....	<b>xiii</b>
<b>Chapter 1 Introduction</b> .....	<b>1</b>
1.1 Reservoir Simulation .....	1
1.2 Compartmentalized Reservoir Modeling.....	3
1.3 Project Definition.....	5
1.4 Thesis Outline .....	7
<b>Chapter 2 Literature Review</b> .....	<b>9</b>
2.1 Material Balance Analysis .....	9
2.2 Compartmentalized Reservoir Modeling.....	16
2.2.1 Compressibility .....	17
2.2.2 Transmissibility.....	20
2.3 Wellbore Modeling .....	31
2.3.1 Friction Factor .....	32
2.3.2 Multiphase flow.....	34
<b>Chapter 3 Methodology</b> .....	<b>42</b>
3.1 Introduction.....	42
3.2 Mathematical Model of a Single Inflow Reservoir Compartment.....	47
3.3 Mathematical Model of Multiple Reservoir Compartments with Aquifer Support....	52
3.4 Mathematical Model of Dry Gas Reservoir with Aquifer Support Modelling .....	64
3.4.1 Water Influx Only (Model 1) .....	66
3.4.2 Including Expansion of Connate Water and Pore Volume Reduction (Model 2)	70
<b>Chapter 4 Results and Discussions</b> .....	<b>73</b>
4.1 Multiple Communicating Reservoir Compartments Coupled with Wellbore .....	73
4.1.1 Numerical Simulation and Analysis.....	76
4.1.2 CPU Time Consumption .....	83

4.2 Multiple Compartmentalized Reservoirs with a Common Aquifer .....	84
4.2.1 Numerical Simulation and Analysis.....	89
4.2.2 CPU Time Consumption .....	93
4.3 Dry Gas Reservoir with Aquifer Support Modeling.....	94
4.3.1 Case Studies Descriptions .....	95
4.3.2 Numerical Simulation and Analysis.....	96
4.3.3 Sensitivity Analysis.....	99
<b>Chapter 5 Conclusions &amp; Recommendations.....</b>	<b>101</b>
5.1 Conclusions.....	101
5.2 Recommendations.....	103
<b>Bibliography .....</b>	<b>104</b>
<b>Appendix.....</b>	<b>113</b>
A    Pseudo Pressure Function.....	113
B    Numerical Method Approach.....	117
C.1  Source Code for Dry Gas Reservoir Simulator.....	120
C.2  Source Code for Multiple Compartmentalized Reservoir Simulators .....	124
D    Case Study Results from Section 4.1.....	132

## List of Tables

Table 3.1: Generalized Governing Equations .....	62
Table 4.1: Reservoir Properties .....	75
Table 4.2: Wellbore Properties .....	75
Table 4.3: Fluid Properties .....	75
Table 4.4: Control Conditions .....	75
Table 4.5: Summary of Changing Parameters in Sensitivity Analysis .....	76
Table 4.6: CPU Time Consumption for Matlab and Eclipse Model .....	83
Table 4.7: Reservoir Properties .....	86
Table 4.8: Compartment Lengths for Multiple Compartmentalized Reservoir with Common Aquifer (from Bottom Hole to Toe) .....	86
Table 4.9: Wellbore Properties Multiple Compartmentalized Reservoir with Common Aquifer .....	86
Table 4.10: Fluid Properties .....	88
Table 4.11: Aquifer Properties .....	88
Table 4.12: Control Conditions .....	88
Table 4.14 Input Data .....	95
Table 4.15: Results Comparison between Two Models .....	96
Table 4.15: Summary of Changing Parameters in Sensitive Analysis .....	99
Table 4.16: Results from Sensitive Analysis .....	100

## List of Figures

Figure 1.1: Reservoir Simulation Stages .....	2
Figure 1.2: Research Map .....	8
Figure 2.1: Material Balance Analysis Schematics (Johansen, 2008) .....	10
Figure 2.2: Aquifer Influx Model Validation.....	13
Figure 2.3: Aquifer Models (Retrieved from AAPG wiki).....	22
Figure 2.4: Inter-Compartment Flow Sketch .....	27
Figure 2.5: Joshi’s Horizontal Well Model (Joshi, 1988).....	29
Figure 2.6: Flow Regimes (Guo et al., 2007) .....	35
Figure 2.7: Flow-pattern Map for Horizontal Pipeline (from Beggs and Brill, 1973).....	37
Figure 3.1: Research Map .....	43
Figure 3.2: Schematic Drawing of Single Inflow Reservoir Compartment.....	44
Figure 3.3: Schematic Drawing of Multiple Communicating Compartmentalized Reservoir Model .....	44
Figure 3.4: Schematic Drawing of Multiple Non-Communicating Compartmentalized Reservoir Model .....	45
Figure 3.5: Dry Gas Reservoir with Bottom Aquifer Support Scheme .....	45
Figure 3.6: Schematic of Multiple Non-Communicating Compartments.....	53
Figure 3.7: Schematic of Multiple Communicating Compartments .....	54
Figure 3.8: Schematic of Total Compressibility for Compartment $i$ .....	55
Figure 3.9: Description of the Flow Process in the Reservoir System .....	56
Figure 3.10: Dry Gas Reservoir with Bottom Aquifer Support Scheme .....	64
Figure 4.1: Schematic of Multiple Compartmentalized Reservoir Model.....	74
Figure 4.2a: Reservoir Pressure (50 Communicating Compartments) .....	78
Figure 4.2b: Cumulative Oil Production (50 Communicating Compartments).....	78
Figure 4.2c: Oil Flowrate (50 Communicating Compartments).....	79
Figure 4.2d: Oil Flowrate between Compartments.....	79
Figure 4.3a: Reservoir Pressure (50 Communicating Compartments) .....	81
Figure 4.3b: Cumulative Oil Production (50 Communicating Compartments).....	81
Figure 4.3c: Oil Flowrate (50 Communicating Compartments).....	82
Figure 4.4: Refined Eclipse (50 Communicating Compartments).....	83
Figure 4.5: Schematic of Multiple Non-Communicating Compartmentalized Reservoir Model .....	85
Figure 4.6: Schematic of Multiple Communicating Compartmentalized Reservoir Model .....	85
Figure 4.7a: Pressure Distribution, Multiple Non-Communicating and Communicating Compartmentalized Reservoir Model .....	90
Figure 4.7b: Pressure Distribution, Multiple Non-Communicating and Communicating Compartmentalized Reservoir Model .....	91
Figure 4.8a: Cumulative Oil Production, Multiple Non-Communicating and Communicating Compartmentalized Reservoir Model .....	91

Figure 4.8b: Cumulative Oil Production at RC1 and RC50, Multiple Communicating Compartmentalized Reservoir Model .....	92
Figure 4.9: Oil Production Flow Rate, Multiple Non-Communicating and Communicating Compartmentalized Reservoir Model .....	92
Figure 4.10: CPU Time Consumptions, Multiple Non-Communicating and Communicating Compartmentalized Reservoir Model .....	94
Figure 4.11: Pressure Distribution .....	97
Figure 4.12: Gas Production Profile .....	98
Figure 4.13: Water Encroachment Profile .....	98
Figure A.1: Reciprocal of Product $\mu B$ versus Pressure (from Hagoort, 1988) .....	113
Figure A.2: Pseudo-Pressure versus Pressure for Gas (from Hagoort, 1988) .....	114
Figure D.1: Reservoir Pressure, Friction Factor Ignored.....	132
Figure D.2: Cumulative Oil Production, Friction Factor Ignored .....	132
Figure D.3: Oil Flowrate, Friction Factor Ignored.....	133
Figure D.4: Reservoir Pressure, Oil FVF Increased .....	133
Figure D.5: Cumulative Oil Production, Oil FVF Increased .....	134
Figure D.6: Oil Flowrate, Oil FVF Increased .....	134
Figure D.7: Reservoir Pressure, Oil Viscosity Increased .....	135
Figure D.8: Cumulative Oil Production, Oil Viscosity Increased .....	135
Figure D.9: Oil Flowrate, Oil Viscosity Increased .....	136
Figure D.10: Cumulative Oil Production Profile, Eclipse .....	136

# **Chapter 1 Introduction**

## **1.1 Reservoir Simulation**

Reservoir engineers predict the future performance of oil and gas reservoirs in order to optimize recovery from the reservoir. Reservoir engineering involves the flow of oil, gas, and water through a porous medium and the associated recovery efficiencies of the contained hydrocarbons under various operating conditions. Reservoir simulation has become a fundamental tool for reservoir engineers. Reservoir simulation combines geoscience, mathematics, physics, computer programming, and reservoir engineering into a tool for forecasting hydrocarbon reservoir performance as well as history match (Abou-Kassem, 2008). The major goal of reservoir simulation is to optimize the management and production of hydrocarbon resources with respect to economies and efficiency.

Reservoir simulation can be divided into four major stages. First, a reservoir parameter model is required to capture the main features of the underlying physical phenomena. Second, a set of time-dependent nonlinear partial differential equations expressing the mass conservation of individual fluid components are formulated and analyzed. Third, a discrete numerical analog is set up by employing the formulated properties of both the parameter model and the mathematical model. Finally, computer algorithms and codes are established to solve the discrete system. These stages are illustrated in Figure 1.1.

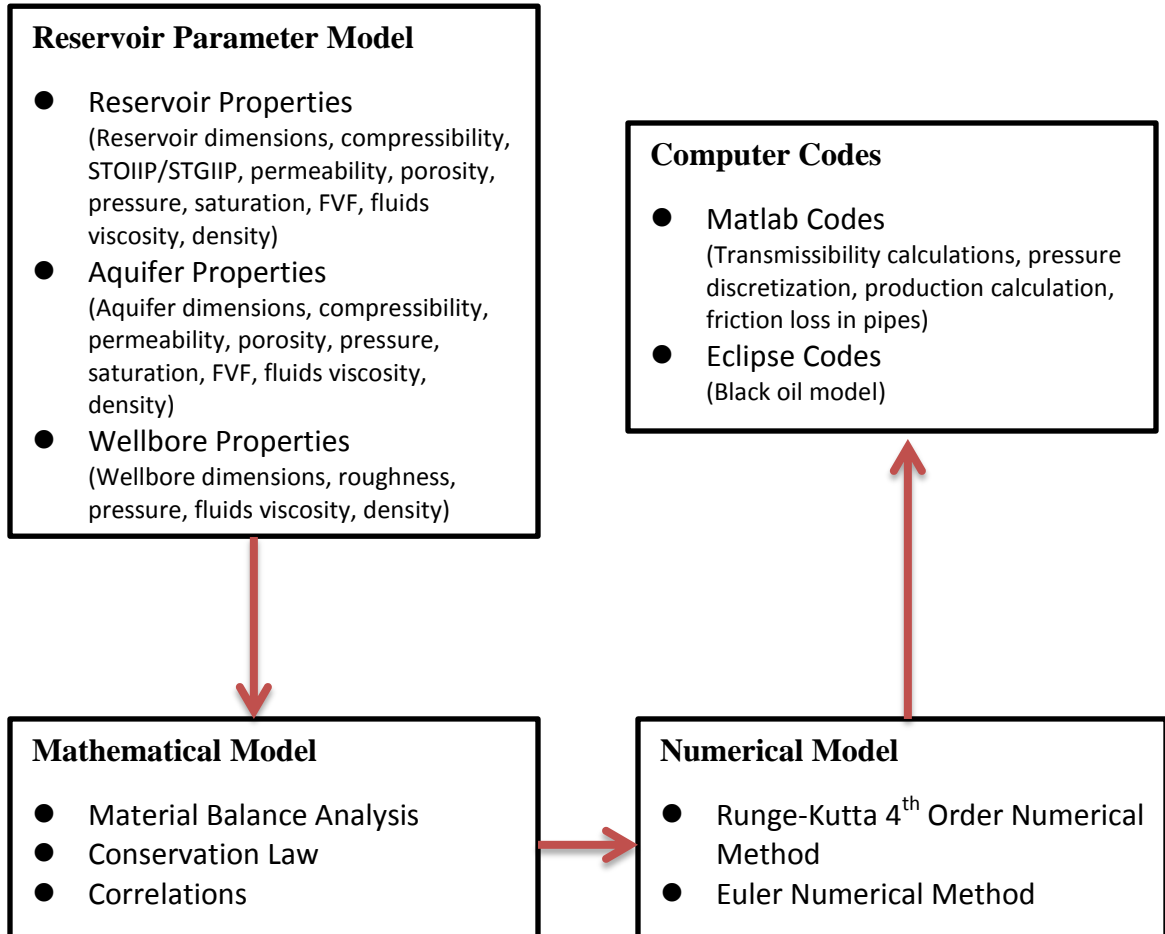


**Figure 1.1: Reservoir Simulation Stages**

A reservoir simulator is usually classified on the basis of different formulations. The model selection for a particular case is based on reservoir fluid characterizations and the type of recovery processes being used. Based on the type of reservoir fluids, reservoir simulators are classified as gas, black oil, or compositional models. Reservoir simulators can also be classified by the number of dimensions, number of phases and components, or the coordinate system applied in the simulator (Chen, 2007). In this thesis, reservoir

simulators are created for two categories, black oil reservoir simulators and gas reservoir simulators.

Recovery processes consist of primary recovery (gas cap expansion, solution gas drive, rock compaction, water drive, and gravity drainage), secondary recovery (water injection and gas injection), and tertiary recovery (water alternating gas injection, solvent displacement, thermal recovery, and chemical flood). Primary recovery and secondary recovery can usually be evaluated by black oil model, and the tertiary recovery such as thermal recovery and chemical recovery need to be evaluated by thermal recovery and chemical flood simulators. The different recovery methods require different simulators.

These recovery processes are evaluated by the use of a simulator selected for the case at hand, which include black oil, thermal recovery, miscible displacement, and chemical flood simulators (Chen et al. 2006).

Reservoir simulation is conducted according to the following steps: defining simulation objectives, reservoir data collection, reservoir simulator design, history matching (tuning of parameters using production data), and prediction making (Ertekin et al. 2001).

## **1.2 Compartmentalized Reservoir Modeling**

A compartmentalized reservoir system is made up of a series of hydraulically communicating or non-communicating compartments. The presence of faults or low permeable barriers may result in poor hydraulic communication between adjacent compartments. Distinct rock and fluid properties may be present in each compartment due

to stratigraphic changes, and partially penetrating wells may pass through several reservoir compartments, based on the production strategy (Rahman and Ambastha, 2000). The concept of reservoir compartments is very useful in many applications, including: faulted reservoirs, a stratified reservoir with variable reservoir properties, a reservoir with multiple well completion technologies, etc.

Compartmentalized reservoirs exist in many fields such as the Raslie and Avondale fields in Roma Area, and North Sea fields (Cervantes, 1996). The giant Hibernia Oilfield developed in the Jeanne d'Arc Basin on the Grand Banks of Newfoundland also exhibits compartmentalized reservoirs, e.g. more than 30 fault blocks have been identified at one of the major oil and gas reservoir, the fluvial-deltaic Hibernia Formation (Sinclair et al, 1999). Reservoir compartmentalization is one of the major challenges in petroleum exploitation, since each compartment may not be economical to develop as stand-alone and may exhibit variable reservoir characteristics. Compartmentalized reservoirs also introduce many difficulties for reservoir simulation. Compartmentalization is also regarded as a significant risk factor that has to be considered in exploitation design, especially for economic development strategies, due to a larger number of wells and surface facilities required. Therefore, a comprehensive understanding of production behaviour, such as pressure behaviour and flow behaviour, of compartmentalized reservoirs can increase the accuracy and efficiency of production forecasting. Compartmentalized reservoir models have been established and applied to for real oil and gas fields in the world.

### **1.3 Project Definition**

Based on first principles for material and momentum balance, an integrated mathematical methodology is formulated and used to represent the behaviour of each compartment over time, including future field production, water encroachment and the pressure decline in a reliable and efficient manner.

In this thesis, each individual reservoir block or aquifer in a compartmentalized reservoir is referred to as a ‘Reservoir Compartment’ (RC). Each compartment comprises a finite volume system with a set of known initial conditions (initial volume, initial pressure, and total compressibility) for which the evolution over a time interval is determined analytically. Each RC will be connected with other RCs in the model with inter-compartment transmissibility and penetrated by the wellbore with a given well transmissibility (See Chapter 2.2), resulting in a coupled set of ODEs.

The objective of this work is to create a quicker and simpler forecasting method for compartmentalized reservoirs. In this thesis, a new method is proposed to simulate compartmentalized reservoirs. This research focuses on a dynamic compartmentalized reservoir model coupled with a wellbore model to provide the most realistic production prediction in an efficient manner. This compartmentalized model builds upon the industry standard formulations, correlations, and methodologies. A series of ordinary differential equations of initial value problems are generated. With the increasing numbers of compartments, systems of ordinary differential equations become complex and are impossible to integrate using analytical solutions. In order to obtain a high degree of

accuracy, the Fourth-Order Runge-Kutta Method is chosen to discretize aquifer, reservoir and wellbore pressure equations in this work. This research also employs two time-stepping levels to allow slowly changing parameters to be solved less frequently than fast transients in order to enhance the performance. Another advantage of this new method, in addition to the speed of simulations, is the added flexibility in the definition of the discrete reservoir blocks (compartments) and the well trajectory.

This thesis generalizes and improves previous work (Thomas, 2012) by incorporating a gas reservoir model and allowing any number of compartments. This is demonstrated for fifty compartments with single aquifer support, a fully perforated wellbore in compartments and blank pipe segments in between compartments. Gas reservoir performance estimates are always difficult to obtain compared to the black oil reservoir performance due to the high compressibility of gas. The special application for a dry gas reservoir system and an oil reservoir system are described, which demonstrate the benefits of the new model.

Eclipse<sup>TM</sup> reservoir simulation software represents the industry standard for complete and robust prediction of dynamic behavior, for all types of reservoirs and complexity in geology, fluids, and development schemes. To validate the solutions from the new model, Eclipse<sup>TM</sup> software is used to simulate the same reservoir cases. The results from the case studies are compared and a sensitivity analysis is performed. The results (e.g. the time consumptions, numbers of compartments, and pressure/flowrate solutions) demonstrate a

higher efficiency and flexibility with the new method when applied to compartmentalized reservoirs.

This new model can be used to simulate oil/gas reservoirs with heterogeneous properties including the presence of faults or baffles, different effective reservoir compartment volumes, and the support of connected aquifers, etc. Wellbore segments with both perforated and blank pipe sections are considered and calculated in the new model. Therefore, this model can also be used to efficiently investigate pre-drill scenarios involving well length compared to well cost.

#### **1.4 Thesis Outline**

The body of work will present an overview of building the general compartmentalized reservoir model for a dry gas reservoir, as well as the multiple oil reservoirs with common bottom aquifer support. The research map is shown in Figure (1.2). Material balance analysis, aquifer models, wellbore models, and compartmentalized models are reviewed in Chapter 2. This chapter starts with the fundamental material balance approach and basic correlations for aquifer and wellbore models. The definition of transmissibility and compressibility are presented in the section on compartmentalized modeling. In Chapter 3, the mathematical model for multiple compartmentalized reservoir models is formulated. Chapter 3 outlines the procedures for a single oil reservoir compartment with aquifer and multiple compartments with an aquifer support.

A series of demonstration cases are presented in Chapter 4 to evaluate the effect of variables and the increasing level of complexity and stability. The data corresponding to all of the cases is used in Eclipse<sup>TM</sup> and MATLAB program for the new model to generate predictions. In order to verify the model and evaluate impact of the changing parameters on the pressure and recovery, a comparison of the results from all cases is also provided in this chapter. Due to the large compressibility and complexity of gas reservoirs, a single compartment, dry gas reservoir with aquifer support model is presented in the last section, including the development of the governing equations, numerical simulation results of the case studies, and a discussion of sensitivity analysis. Finally, Chapter 5 presents the conclusions and recommendations for a further study.

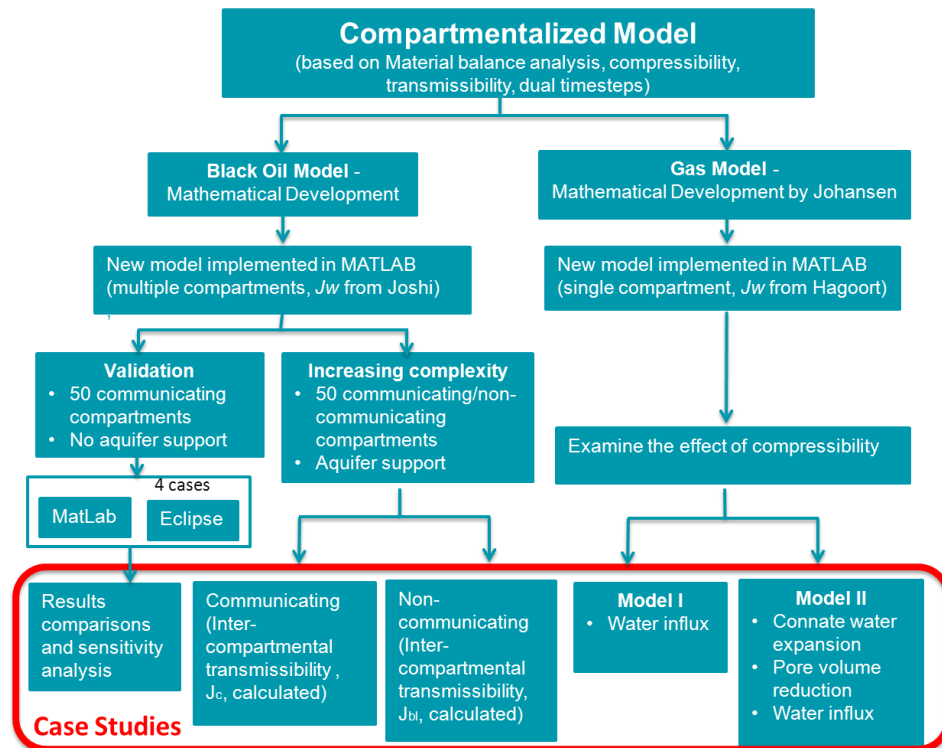


**Figure 1.2: Research Map**

## **Chapter 2 Literature Review**

This chapter consists of four sections, which review material balance analysis, compartmentalized reservoir models, aquifer models, and multiphase flow in wellbore modeling and well friction. Based on the theory and correlations provided in the literature, the coupled compartmentalized reservoir model is developed to predict the long-term reservoir performance (oil/gas production, water encroachment, and reservoir/aquifer pressure, etc.), as well as wellbore flow behaviour, as the fluids are withdrawn.

### **2.1 Material Balance Analysis**

Reservoir simulation techniques have been under development for decades; however, obtaining highly accurate results in an efficient manner for complex petroleum systems remains a challenge for reservoir engineers. The general performance of a reservoir is essentially governed by the nature of energy (i.e. driving mechanism) moving the fluid toward the wellbore. There are four natural driving mechanisms to recover oil and gas from reservoirs: gas cap drive, solution gas drive, natural water drive (aquifer support), and compaction drive. (Muskat, 1949)

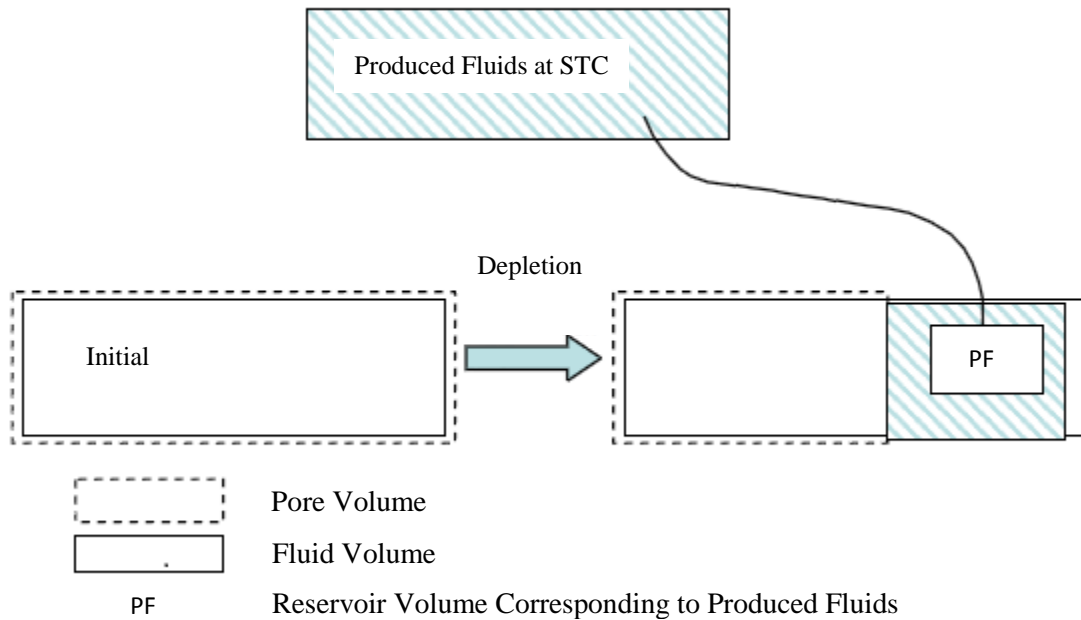


**Figure 2.1: Material Balance Analysis Schematics (Johansen, 2008)**

The Material Balance Analysis (MBA), illustrated in Figure 2.1, is one of the most popular approaches used in reservoir engineering. It is applied to estimate the stock tank oil/gas initially in place (STOIIP/STGIIP). Conventional MBA comprises numerous simplifications that result from a number of assumptions. However, the assumption that rock and fluid properties are constant is inadequate for reservoir problems. As real fluids and rocks are pressure-dependent, removing this assumption is imperative. MBA can take variable compressibilities into account, which allows for pressure-dependent parameters; as a result, it can also be used for calculating the average reservoir pressure and aquifer pressure as a function of time (e.g. Equation 3.46). Thus, more complex and flexible phenomena can be described and simulated in a real reservoir. Recognizing the appropriate driving mechanisms that control the fluid behaviors within reservoirs allows us to

accurately perceive reservoir behaviour and efficiently forecast future production performance. Still, the resulting formulation is not without uncertainties.

Schilthuis (1936) invented the basic analytical MBA technique commonly employed in the modern petroleum industry. Based on the data obtained and technique of measurement developed in the years between 1929 and 1935, Schilthuis modified the equation given by Coleman, Wilde and Moore (1929) in a derivation form and introduced the approach by utilizing so called “active oil”, “active free gas”, aquifer influx, and the experimental fluid properties to interpret the relationship between reservoir pressure and production behaviours. He proposed a framework that would couple theoretical analysis of the oil and gas reservoir with measured pressure and production information so that the effectiveness of primary drive mechanisms and predictions of reservoir pressure could be determined under a variety of operating conditions including gas reinjection and water drive. This was valuable as a procedure to evaluate fields and optimize production strategies. However, some limitations and restrictions were imposed in his analysis. First, this method was only for hand calculation, resulting in a low efficiency computation, especially for complex and heterogeneous reservoirs. Second, although most terms in these equations were selected directly from laboratory data, the derivation of these equations was based on the laws for ideal gases and ideal solutions. Therefore, this may cause severe errors in high pressure or high temperature reservoirs with non-ideal fluids. Moreover, heterogeneity invariably exists in real reservoirs, thus, the oil and gas content of a reservoir may be under- or overestimated due to the discrepancy involved in the actual and theoretical quantities of oil

and gas/liberated gas volume. Finally, the basic material balance expressions did not contain a time variable within the equations.

Carter and Tracy (1960) applied the Schilthuis MBA iteratively over time to predict pressure and water influx behaviour based on the assumption of constant water influx rates, resulting in a faster computation of the solutions.

Havlena and Odeh (1963) employed a straight line method to evaluate the results generated from an analytical aquifer model based on MBA. The authors illustrated different material balance equations depending on reservoir category: saturated reservoirs, undersaturated reservoirs, and gas reservoirs. This approach involves the plotting over time, as production progresses, of one group of variables against another group for a specific production mechanism. The shape of this curve is essential. When an aquifer model is assumed, water influx can be calculated. Then, a plot of the  $\frac{\text{net production in RC}}{\text{oil expansion}}$  vs.  $\frac{\text{water influx}}{\text{oil expansion}}$  over

time will result in a curve. If the assumed aquifer model is correct, the plot must be in a straight line. Figure 2.2 shows the aquifer influx model validation in the saturated oil reservoir with water drive and no original gas cap. If the curve is concave, the aquifer model is under-estimated, and if the plot is convex, the aquifer model is over-estimated. This straight line technique is also applicable for other types of reservoirs with corresponding group of variables on the axes. The straight line method can be used to analyze the drive mechanisms and the volumetrics of a connected reservoir.

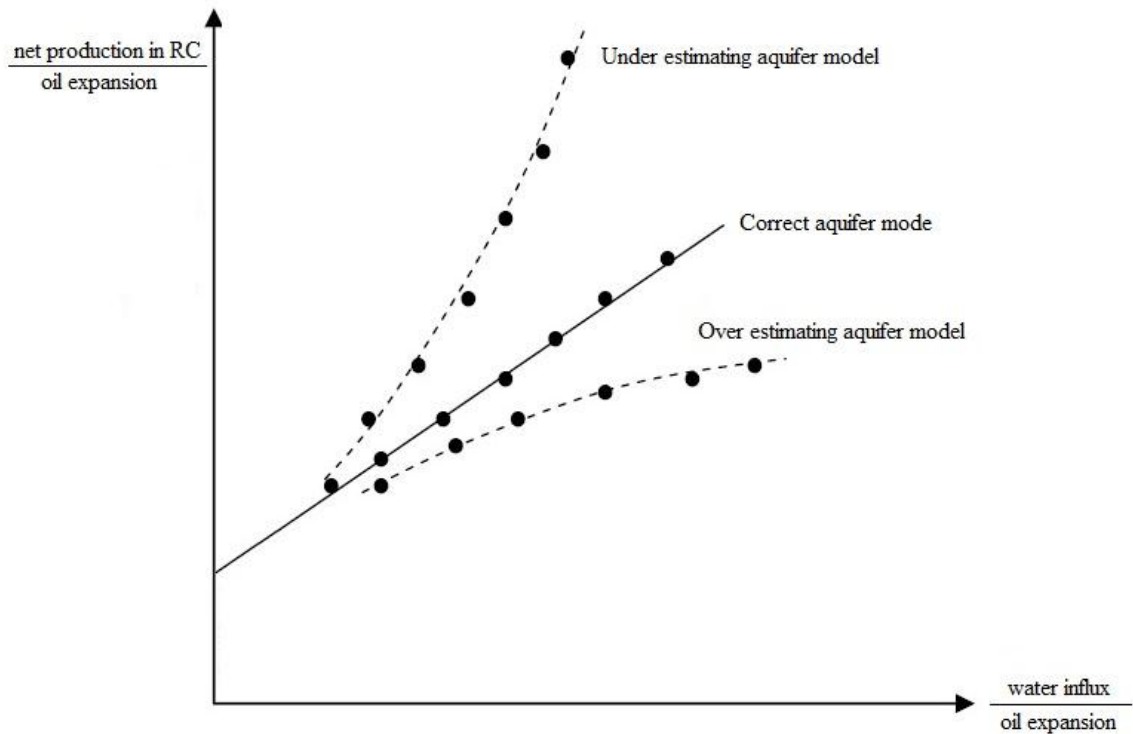


**Figure 2.2: Aquifer Influx Model Validation**

Dake (1978) proposed the zero dimensional MBA to determine underground recovery as a result of the expansion of oil, initially dissolved gases in oil phase, expansion of liberated gases and expansion of gas cap gases. In this, hydrocarbon pore volume (HCPV) reduction due to the swelling of connate water and shrinking of HCPV is incorporated. This common MBA is based on the definition of compressibility of hydrocarbon fluids, connate water and pore volume. When the initial reservoir pressure is higher than its bubble-point pressure and it remains above the bubble-point pressure during the production period, there are only three driving mechanisms present in the formation including oil, water, and rock compressibility. This method is used in the Section 4.1 and 4.2.

Fetkovich et al. (1998) introduced the MBA for high pressured gas reservoirs. They described a cumulative effective compressibility concept to demonstrate the expansion drive mechanisms. The form of the material balance equation is  $(P/Z)[1 - c(P)(P_i - P)] = (P/Z)_i(1 - G_p/G)$ , which took pressure-dependent variables into account, including rock and water compressibility and total water and rock volumes associated with the reservoir and the existing finite aquifer. In Section 3.3, the time-dependent reservoir pressure solution is derived under the same driving mechanisms, which gives a simpler arithmetic.

Ramagost and Farshad (1981) improved the conventional MBA (Havlena and Odeh, 1963; Dake, 1978) by identifying a new plotting group of variables. Based on a modified version of the traditional MBA, the Ramagost and Farshad MBA (1981) provides a more accurate estimate of the average reservoir pressure when abnormally pressured reservoirs with pressure gradients of 0.85 psi/ft are taken into account. This was also presented and verified by Rahman et al. (2006a) and Fetkovich et al. (1998). Rahman et al. (2006a) modified Ramagost and Farshad (1981) by taking the residual fluid saturation into account such as residual oil saturation and connate water saturation in the MBA, while, Ramagost and Farshad (1981) only considered the connate water saturation effects. Both papers stated that formation compressibility, water compressibility and gas compressibility are distinguishable effects and ignore the water influx effects. All these previous researchers characterized the expansion drive mechanism in generating MBA for a gas reservoir. In this thesis, a new dry gas reservoir model with only a water influx term is developed. A second dry gas reservoir model is also presented, which accounts for:

formation compressibility, water compressibility and gas compressibility, in addition to water influx effects. The accuracy of the two models and the importance of the formation (pore volume) compressibility, water compressibility, and gas compressibility are quantitatively demonstrated in the gas case studies (Section 4.3).

Petroleum Experts Ltd. (2009) has successfully incorporated analytical MBA techniques in their Integrated Production Modeling software package to create a simple reservoir simulator, allowing for time dependency. This software package provides the capability to integrate multiple zero-dimensional tanks by applying the inter-compartment transmissibility concept. The major drawbacks of this approach are the reservoir steady-state assumption and finite difference calculation, where some of the time dependent changes, such as aquifer encroachment and aquifer pressure, are not updated with the new pressure-related solutions within each numerical time step. Thus, this approach allows for only a rather rough estimate. The most popular and acknowledged software is a standard reservoir simulation launcher (Eclipse<sup>TM</sup>), so it is chosen instead of the Integrated Production Modeling software package to validate the solutions from the new model. The Eclipse<sup>TM</sup> models are also using finite different method which only offers a low order time discretization in solving governing equations. The pressure solutions in the Eclipse<sup>TM</sup> models are picked up at two ends within one time step. One of the contributions is that a dual time step method is used to solve the system of equations. Well transmissibility and aquifer sizes are kept constant during small time steps in which pressures and flow rates are solved. The new pressure is then used to update the well indices and aquifer size over larger time steps. Another major contributions in this work

is using a high order numerical method to solve the governing equations, which makes the model more accurate than the Eclipse<sup>TM</sup> models as well as Integrated Production Modeling software. Comparing to the Thomas' work (Thomas 2012), the gas reservoir model is another novelty since it is not included in his work. This model is transient during a single large time step calculation and hence represents an enhancement over standard finite difference method formulations. The model could be applied to any system with appreciable pressure gradient, such as faulted reservoirs or a single wellbore draining multiple reservoirs with variable characteristics. This type of model can be efficiently used to predict production behavior from new fields to identify reservoir properties involving transmissibility, the presence of faults or baffles, the effective reservoir volume, and the support supplied by connected aquifers, or to optimize pre-drill scenarios involving well length and perforation length.

## **2.2 Compartmentalized Reservoir Modeling**

Previous researchers presented conventional material balance approaches to evaluate reservoir performance (e.g. pressure behaviour, etc.) and quantify communication between compartmentalized reservoirs (Fox et al., 1988; Stewart and Whaballa, 1989). Fox et al., (1988) presented a simple method to quantify the 'interblock' communication using material balance and steady-state pressure drop concept, and this is also quantified for multiple communicating blocks in steady state pressure condition. An analytical solution of a system of linear ordinary differential and algebraic equations are developed by Stewart and Whaballa (1989). These equations are derived for a complex reservoir comprised of an arbitrary configuration of rectangular compartments separated by partially

communicating barriers. These conventional approaches are governed by the concepts of compressibility and transmissibility. However, the blank pipe section and aquifer support are also not coupled in both Fox et al., (1988) and Stewart and Whaballa (1989) models. The complex reservoir material balance equations are developed for oil reservoir under steady-state conditions, while, pure gas reservoir is not taken into account. A previous researcher, Thomas (2012), contributed to the topic of dynamic reservoir tank modeling. He demonstrated the concept for up to three black oil reservoir tanks with a coupled wellbore model and one common aquifer support with constant aquifer pressure in the simulation. The tank model is developed based on the same concepts as the compartmentalized model. The model presented in Thomas (2012) kept the properties for each individual reservoir tank constant during the time step. The contribution of this work is that the model presented varies the properties of each compartment in the larger time step due to two time steps employed in the compartmentalized reservoir model. In this work, the aquifer, reservoir blocks and wellbore performance are fully integrated into one system. The results show a good agreement with the commercial software. The gas reservoir with aquifer support model is also developed in this thesis, which is not included in any literatures above.

### **2.2.1 Compressibility**

Compressibility is one of the most important properties used in a reservoir simulation model for pure substances: gas, liquid and solid, such as gas compressibility, oil compressibility, and rock compressibility. This concept can also be defined for mixtures, including aquifer compressibility, and total compressibility of a reservoir saturated with oil,

gas, and water. For example, Fox et al. (1988) and Thomas (2012) used the total compressibility in the material balance equations. However, the total compressibility calculation method is not mentioned in Fox et al. (1988).

In this thesis, the system is assumed to be in the isothermal condition. Since the rock, water, and oil compressibility are not changed significantly in this model, the CPU time and storage space will be more costly based on variable compressibilities without a better estimation. For the sake of simplicity, in oil case, the rock, water, and oil compressibility are assumed constant. For gas, compressibilities are not constant. The definition of compressibility is described in the Equation (2.1),

$$c = -\frac{1}{V_i} \frac{dV}{dP} \Big|_T, \quad (2.1)$$

where  $c$  can be either the compressibility of a pure substance (oil  $c_o$ , water  $c_w$ , or gas  $c_g$ ), the compressibility of rocks ( $c_r$ ), or the total compressibility ( $c_t$ ), with units  $\text{Pa}^{-1}$ ,  $V_i$  is the in-situ volume saturated in the reservoir, and  $\frac{dV}{dP} \Big|_T$  represents the partial change in fluid volume with respect to the pressure change under isothermal conditions. A negative sign represents a common convention in order to make a positive compressibility quantity.

Compressibility plays an important role in oil reservoir production drive mechanisms, especially in the primary recovery process. Four drive mechanisms are related to compressibility: reservoir fluid expansion, formation compaction, water influx, and free and dissolved gas expansion (Johansen, 2013). In essence, the four basic compressibilities

associated with a porous medium are defined for the four primary drive mechanisms: rock compressibility, water compressibility, oil compressibility, and gas compressibility.

Rock compressibility is also called pore volume compressibility, and can be expressed as the pore volume change per unit pore volume per unit pressure change. The pore volume compressibility is usually in the range of 0.29 to  $5.075 \times 10^{-6} \text{ kPa}^{-1}$  depending on the net overburden pressure (Fatt, 1958). This range of values will be used to evaluate the impact of compressibility in the gas model.

Water compressibility is commonly assumed to be constant with values in the range 3.4 to  $5.0 \times 10^{-7} \text{ kPa}^{-1}$ . Many authors, e.g. Randolph (1977) and Swanson (1979), use different values according to different conditions. One of the well-known values of water compressibility of  $4.35 \times 10^{-7} \text{ kPa}^{-1}$  is reported to be overestimated by approximately 20% due to gas in the solution (Randolph, 1977). Swanson (1979) calculated the water compressibility as  $3.6 \times 10^{-7} \text{ kPa}^{-1}$  in the geopressed reservoir condition. In this work, water compressibility of  $4 \times 10^{-7} \text{ kPa}^{-1}$  is used.

Oil compressibility is also formulated by the basic compressibility concept, which reflects the oil volume change with respect to the pressure change per unit oil volume. Oil compressibility is usually in the range of 2.9 to  $184.8 \times 10^{-7} \text{ kPa}^{-1}$  over a range of testing temperatures (Retrieved from Petrowiki). This work assumes the isothermal oil compressibility of an undersaturated oil reservoir is a constant value. Here, the value of  $40 \times 10^{-7} \text{ kPa}^{-1}$  is chosen for the oil compressibility.

Many researchers have shown that it is reasonable to assume constant oil and water compressibility; however, this is not a valid assumption for gas.

### **2.2.2 Transmissibility**

Three transmissibilities are used in this work: aquifer transmissibility, inter-compartment transmissibility, and well transmissibility. The transmissibility is a term reflecting the average compartment (aquifer/rock/well) properties and the potential gradient between the regions. The transmissibility refers to the ability of the fluid to flow between two compartments, for example, between the aquifer and reservoir, from one reservoir block to another reservoir block, or from the reservoir to the wellbore. All the transmissibilities used have the same form as given in Equation (2.2) (Schilthuis, 1936),

$$q = J(P_1(t) - P_2(t)), \quad (2.2)$$

Where  $q$  is the flow rate between compartment 1 and compartment 2,  $J$  can be the aquifer transmissibility, the inter-compartment transmissibility, or the well transmissibility, and  $P_1(t)$  and  $P_2(t)$  are the pressures in compartment 1 and compartment 2 at any time  $t$ .

#### **1. Aquifer Transmissibility**

The aquifer transmissibility ( $J_a$ ), also called the aquifer productivity index, is a function of aquifer geometry and rock and fluid properties of the aquifer. The aquifer transmissibility is used to determine the flow rate from the aquifer to the reservoir. Aquifer transmissibility can be determined by different aquifer properties, such as aquifer geometry, fluid mobility, and aquifer connectivity. In order to obtain the aquifer transmissibility, we need to first

define the aquifer model. The main objective of aquifer models is to estimate the cumulative water influx by a material balance analysis, since water drive is one of the primary recovery process mechanisms. In fact, the shape and size of the aquifer is usually unidentified in reservoir engineering. The data obtained from an aquifer is often quite limited and may only have an estimated bulk volume available on the basis of seismic interpretation. Information, such as aquifer geometry, the pore volume and the water mobility, is usually unknown, at least initially. Therefore, the direct calculation of aquifer properties, even though it is possible, is inaccurate due to the many uncertainties which exist in the model. Reservoir simulators are generally employed to characterize aquifer models based on production history matching with previous reservoir performance. The best fit aquifer model is commonly accepted as a valid model for the reservoir.

There are numerous aquifer models commonly used in reservoir engineering studies. Based on the available aquifer models, the performance of aquifers is essentially controlled by aquifer/reservoir geometry, aquifer/reservoir size ratio, flow regime, and petrophysical properties of aquifers. Based on the location of the aquifer and reservoir, two scenarios (Figure 2.3) are commonly cited in petroleum engineering literature: Edge Water Drive Aquifer (EWDA) models and Bottom Water Drive Aquifer (BWDA) models. The Edge Water Drive Aquifer Model describes a model where water influx takes place only from the edges of the reservoir, such as at the downdip edges of an anticlinal structure. The vertical water flow is not considered to be significant. The Bottom Water Drive Aquifer Model is characterized by vertical water flow.

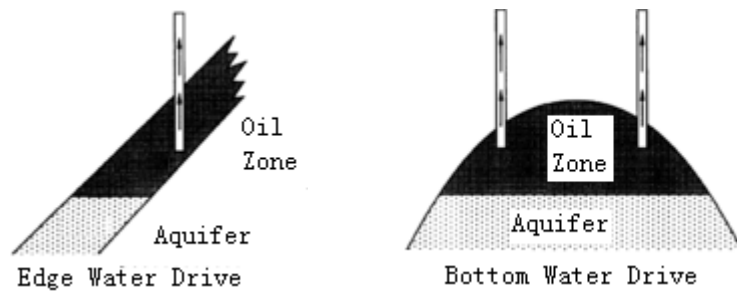


**Figure 2.3: Aquifer Models (Retrieved from AAPG wiki)**

There are several aquifer rate equations widely used to describe different aquifer models. Many authors have published analytical approaches to estimate aquifer inflow model including Van Everdingen and Hurst (1949), Hurst (1958), Carter-Tracy (1960), Coats (1962), Fetkovich (1971), Vogt and Wang (1987), and Allard and Chen (1988).

Van Everdingen and Hurst (1949) provided a simple solution expressed in a dimensionless form for both infinite and finite Edge Water Drive Aquifers. The Van Everdingen and Hurst Aquifer Model is used to describe the inflow from radial and linear aquifers under infinite, pseudo steady-state, and steady-state conditions. This model summates the individual water influx obtained from each subsequent pressure drop, and all the results computed from previous time steps have to be recalculated at a later time, which requires rapid computation effort.

Hurst (1958) presented a mathematical simplification of the material balance equation by the Laplace transformation and superposition and incorporated both a linear and radial aquifer system with undersaturated and saturated oil reservoirs. This model was accomplished by assuming constant oil production rates.

Based on the material balance equation of Schilthuis (1936), Carter and Tracy (1960) provide a simplified approach to approximate the aquifer influx behavior by eliminating superposition calculations. This is achieved by assuming water influx rates are constant over a finite time interval. The Carter-Tracy Aquifer Model improved the Hurst(1958) water influx model by the assumption of constant water influx rates over finite intervals of time, which resulted in a considerable reduction in computing time without the superposition calculations, and illustrated a good agreement with the Hurst(1958) model. This model can cover any flow geometry based on the dimensionless pressure solutions with time.

Coats (1962) created a semi-analytical model that considered an infinitely large Bottom Water Drive Aquifer. This method takes into account the pressure gradients for water flow and permeability heterogeneity due to rock compaction. The solution of the pressure profile as a function of time was also presented in a dimensionless form. This model was integrated with gas MBA to analyze the stock tank gas initial in place (STGIIP) in gas fields.

By using the same physical Van Everdingen and Hurst aquifer model, Fetkovich (1971) presented a simpler solution for a pseudo steady-state flow condition. Fetkovich(1971) provided a common method for different aquifer geometries, which has been shown to be useful for long term predictions.

Vogt and Wang (1987) developed the linear pressure formula, considered to be more accurate than step pressure formula presented by Van Everdingen and Hurst (1949). This linear pressure formula presents an efficient computation time and is readily applicable to

a wide range of systems. This method evaluates the water influx superposition integral more precisely, is able to determine the original gas or oil in place and aquifer parameters, and can predict the reservoir pressure more accurately with the known aquifer parameters as well as the original gas or oil in place. This method can also determine these parameters under variable reservoir driving mechanisms including rock compressibility and water influx, and it does not require the actual drive mechanism to be confirmed or known.

Allard and Chen (1988) demonstrated an implicit numerical model for a finite Bottom Water Drive Aquifer. This model includes the effects of vertical flow at the interface between reservoir and aquifer, which differs from the previous aquifer models. The results calculated from this model are shown in dimensionless groups, which make it readily applicable to predict the reservoir and aquifer behavior. The authors also applied this model to a sample calculation to predict water influx, and distinguished the results from conventional radial flow models derived from the Van Everdingen and Hurst (1949).

Yildiz and Khosravi (2007) derived a new analytical finite Bottom Water Drive Aquifer model by using material balance analysis. This model was a fast explicit transient flow aquifer model. The accuracy of this model was verified by comparing the results, such as cumulative water influx and reserve forecasts, from the Coats (1962) and Allard and Chen (1988) models.

As the Fetkovich aquifer model is the most popular model used in current reservoir simulation field as well as the commercial software package. And it is critical to compare

the results by using the same aquifer model. In this thesis, we use an aquifer that is located under the reservoir, so the pseudo-steady state bottom drive model from Fetkovich aquifer model is chosen and used for the demonstrated cases in Eclipse and Matlab software.

The basic Fetkovich Aquifer Model (1971) is generalized by combining Darcy's Law, Equation 2.3, and material balance for constant compressibility, Equation 2.4,

$$q_w = J_a (\bar{P} - P_{wf}), \quad (2.3)$$

where,  $q_w$  is the average water influx rate,  $J_a$  is the transmissibility from aquifer to reservoir,  $\bar{P}$  is the average initial aquifer pressure, and  $P_{wf}$  is the average pressure at the aquifer/reservoir interface, and

$$\bar{P} = -\left(\frac{P_i}{W_{ei}}\right)W_e + P_i. \quad (2.4)$$

Fetkovich provided a simple step-wise solution to calculate the time dependent water influx and average aquifer pressure function at the boundary. This yields Equation 2.5 and Equation 2.6, as shown

$$\Delta W_{e_n} = \frac{W_e}{P_i} (\bar{P}_{(n-1)} - \bar{P}_{wfn}) \left(1 - e^{-\frac{(q_{wi})_{\max} \Delta t_n}{W_{ei}}}\right), \quad (2.5)$$

where the average pressure at time n is

$$\bar{P}_{wfn} = \frac{P_{wf(n-1)} + P_{wf(n)}}{2}. \quad (2.6)$$

In this work, the aquifer transmissibility is

$$J_a = \frac{0.00127k_a \pi r_w^2}{\mu_w L_a}, \quad (2.7)$$

where,  $k_a$  is aquifer permeability,  $r_w$  is reservoir radius,  $\mu_w$  is water viscosity,  $L_a$  is defined as

$$L_a = \frac{10^6 V_a}{\pi r_w^2 \phi}, \quad (2.8)$$

where,  $V_a$  = aquifer volume, and  $\phi$  is aquifer porosity.

## 2. Inter-Compartment Transmissibility

There are two different the inter-compartmental transmissibilities defined in this thesis depending on the communication of the reservoir compartments. For the non-communicating reservoir compartment model, the inter-compartment transmissibility  $J_{bl}$  is solved to fulfil the same model as the communicating reservoir compartment model, which is derived as the Equation (3.35). For communicating reservoir compartment model, the inter-compartment transmissibility ( $J_c$ ) is determined by using the average properties between two communicating compartments, see Equation (4.36). The flow between two compartments is shown graphically in Figure 2.4.

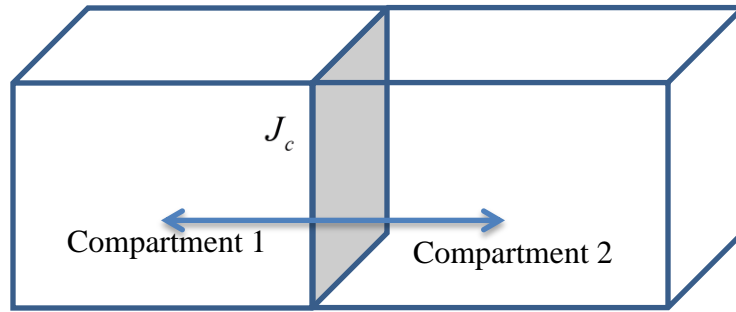


**Figure 2.4: Inter-Compartment Flow Sketch**

### 3. Well Transmissibility

Well transmissibility ( $J_w$ ) or the well productivity index, represents the ease of flow from the reservoir into the wellbore. Joshi (1998) presented the equation of well transmissibility based on Darcy's law for horizontal wells in undersaturated oil reservoir (this equation is used to calculate the well transmissibility for the base case in Chapter 4). However, it is not applicable for a dry gas reservoir. Compared with an undersaturated oil reservoir, a dry gas reservoir model is more complicated. Two significant differences are present: first, higher gas flow velocities cause significant inertial forces, (in other words, Darcy's Law may not be applicable for near-well gas flow in porous media), and secondly, some gas properties (compressibility and viscosity) are highly pressure-dependent. This results in a non-linear pressure differential equation for dry gas. In order to simplify the complexity of the calculation, a concept of 'pseudo-potential pressure' is introduced in Chapter 5, thus allowing for a similar model for both an undersaturated oil reservoir and a dry gas reservoir. Many approaches have been suggested to calculate well transmissibility for variable reservoir situations. Well transmissibility is usually used to show the relationship between the inflow into a well and the pressure drawdowns, which can be calculated from a

knowledge of the reservoir conditions. It is commonly assumed that well transmissibility is constant for the steady-state radial flow of a single incompressible fluid system.

Evinger and Muskat (1942) developed several experiments to compare the well transmissibility from experiments with theoretical values in both homogenous and heterogeneous systems. They pointed out the well transmissibility are not only constant in heterogeneous fluid systems, but also in homogenous fluid systems with both gas and oil present. The experimental results showed the variation in well transmissibility depended on the different pressure discrepancies, oil/gas saturation, permeability, oil and gas properties (e.g. oil/gas viscosity, gas solubility, gas oil ratio, non-ideal gas behavior), etc. Because the well transmissibility varies in oil and gas system, Gilbert (1954) termed an inflow performance relationship instead of the single well transmissibility, which is the whole curve of inflow rates plotted against bottom-hole well pressure.

Vogel (1968) presented the inflow performance relationship for solution-gas drive wells that covers a wide range of fluid PVT properties and reservoir characteristics. Hydraulic fractures in the well are also taken into account. This can provide more accurate calculations for oil well productivity rather than the constant well transmissibility methods.

Joshi (1988) presented an equation to determine the transmissibility of slanted and horizontal wells draining from an elliptical cylinder reservoir in the steady state flow condition. The reservoir anisotropy and well eccentricity are also taken into account in this equation. The effective wellbore radius and the effective skin factors of horizontal wells

can also be calculated based on the theoretical equations proposed by Joshi (1988). Experiments were also conducted to verify the accuracy. His paper compares the vertical, slanted, and horizontal well transmissibility with the assumption of the equal drainage area and the equal reservoir contact area.

The derivation of Joshi's formula (see Equation 3.6) assumes the drainage area in the horizontal plan where the horizontal well is located takes the shape of an ellipse (Figure 2.4). The half major axis in the ellipse is  $a$  and the horizontal well length is  $L$ . The ellipse is a constant pressure boundary with pressure equal to  $P_r(t)$ .

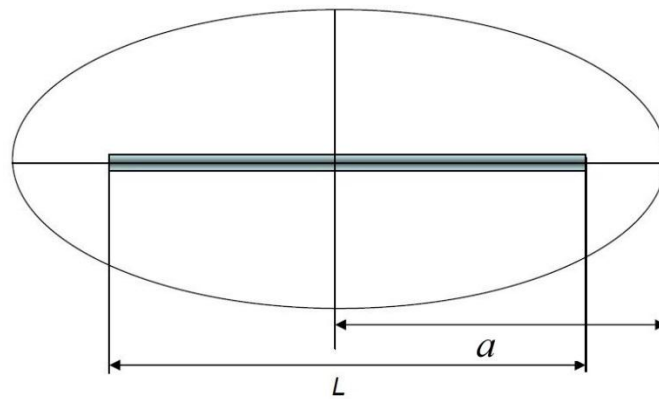


**Figure 2.5: Joshi's Horizontal Well Model (Joshi, 1988)**

Gas is more compressible than oil and water. In order to obtain a similar equation as for liquid flow ( $q = J\Delta P$ ), gas compressibility, gas compressibility factor, and gas viscosity must be considered in the calculations. The concept of gas pseudo-pressure function was developed for flow of gas to account for the variable viscosity and compressibility of gas with respect to pressure by Al-Hussainy et al. (1966). Hagoort (1988) derived a new gas pseudo-pressure function (see Equation 3.43) to simplify the gas model calculation. The detailed derivation is in Appendix A.

Babu and Odeh (1989) presented a method to calculate the productivity of a horizontal well draining from a rectangular reservoir in the pseudo steady state flow condition. This can be used to analyze the effects of some critical parameters on well productivity, including well length, well location, degree of penetration, vertical and horizontal permeability, and length of drainage volume.

Peaceman (1993) derived an equation for the equivalent well block radius of a well in an anisotropic medium under the assumptions of uniform grid if the well is far away from the grid boundaries. This assumption may not be valid for horizontal wells. The validation of Peaceman's equation is examined by using the work in Babu and Odeh (1989). Peaceman (1993) shows that the equations from neither Peaceman (1983) nor Babu and Odeh (1989) are valid if the grid is not uniform or the reservoir is stratified. As Peaceman (1993) mainly focused on single wells and ignored the interaction between wells, Peaceman (1995) represented a new equation to calculate the equivalent well block radius for all wells in the reservoir that fully accounts for the time-dependent well inflow rates and the interaction between wells.

Furui et al. (2002) developed a new analytical model for formation damage skin factor and reservoir inflow model for a horizontal well that fully accounts for the effect of reservoir anisotropy and damage heterogeneity. Any distribution of damage along the well can be simulated in the new skin factor model which can be readily incorporate with any existing reservoir inflow model. A reservoir inflow model for a damaged parallelepiped-shape reservoir draining by a horizontal well is also developed in this paper.

Johansen et al. (2015) developed a new analytical coupled axial and radial productivity model for steady-state flow that can be applied to calculate horizontal well productivity. The new equations can also be used to predict the flowrate and pressure distribution in damaged horizontal wells. The frictional losses in the well productivity calculations are considered and presented in this model.

These models presented above can be used to determine well transmissibility for different situations.

In this thesis, this variable is changed in the black oil case studies to evaluate the reservoir behaviour. As the Joshi (1998) model is the most popular model used in current black oil reservoir simulation field as well as the commercial software package. And it is critical to compare the results by using the reservoir model. The well transmissibilities for the undersaturated oil reservoir (Section 4.1&4.2 base case) and dry gas reservoir model (Section 4.3) are calculated based on Joshi (1998) and Hagoort (1988) respectively.

### **2.3 Wellbore Modeling**

Estimating the pressure loss along the wellbore is a problem frequently encountered by petroleum engineers. The friction factor is an important parameter to calculate the pressure loss in either single phase flow or multiphase flow calculations. As the multiphase flow needs more field data and equations to be integrated in the model, for this work, steady-state single phase flow is assumed.

### 2.3.1 Friction Factor

For single phase flow, the friction factor  $f$  for a pipe segment is a very important parameter, which depends on the pipe properties and the flow regimes within the pipe segment.

More specifically,

- i) If the flow is steady state, laminar and single phase, the Darcy-Weisbach friction factor is inversely proportional to the Reynolds number (Guo et al., 2007)

$$f = \frac{\alpha}{\text{Re}} = \frac{\alpha\mu}{\rho v_m D}, \quad (2.9)$$

where,  $\alpha$  is the Poiseuille number (constant). This constant is characteristic for the shape of the cross section, for example, for a circular cross section is 64. Reynolds Number  $\text{Re}$ , (dimensionless), is defined as

$$\text{Re} = \frac{\rho v_m D}{\mu}, \quad (2.10)$$

where  $\rho$  is fluid density, [ $\text{kg}/\text{m}^3$ ],  $D$  is the pipe diameter, [m], and  $\mu$  is fluid viscosity, [mPa.s].

The volumetric flux of a mixture of fluids in the pipe  $v_m$  is written by

$$v_m = \frac{q}{A}, \quad (2.11)$$

where,  $q$  is the volumetric flow rate in the pipe segment and  $A$  is the cross sectional area of the pipe.

- ii) If the flow is steady state, turbulent and single phase flow in a smooth circular pipe, the friction factor refers to Blasius equation as follows (Blasius,1913),

$$f = \frac{0.3164}{\sqrt{Re}}. \quad (2.12)$$

Because the Blasius correlations do not have term for pipe roughness, it is only valid for smooth pipes. However, sometimes it is used in rough pipes due to its simplicity, and it is valid up to the Reynolds number of  $10^6$ .

- iii) For rough pipes, the Haaland friction factor is used to calculate pressure loss for a full-flowing circular pipe (Haaland, 1983),

$$f = \frac{1}{\left( -1.8 \log \left( \frac{6.9}{Re} + \left( \frac{\delta / D}{3.7} \right)^{1.11} \right) \right)^2}, \quad (2.13)$$

where,  $\delta$  is the pipe wall roughness, [m].

- iv) For non-circular ducts in the turbulent regime, this approach may also be a good approximation with the hydraulic diameter  $D_h$  instead of pipe diameter,

$$D_h = \frac{A}{\text{wetted perimeter}}. \quad (2.14)$$

There are a few equations for solving the friction factor in the rough pipes such as Haaland Equation (Haaland, 1983), Swamee-Jain Equation (Swami and Jain, 1976),

Serghides's Equation (Serghides, 1984), Goudar-Sonnad Equation (Goudar and Sonnad, 2008), etc. As Haaland Equation (Haaland, 1983) shows an explicit solution for the rough pipe friction factor, a fast speed of computation as well as a good precision, in this work, Haaland (1983) is chosen to calculate the pressure loss in the horizontal well.

### **2.3.2 Multiphase flow**

The pressure-gradient equations for multiphase flow in pipes at all angles for many flow patterns have been developed by the use of experiments and the principles of conservation of mass and linear momentum over the last 65 years. To obtain the most realistic prediction results, methods for predicting multiphase flow pressure gradients are required. Currently, many researches have concentrated on predicting either horizontal or inclined flow in pipes.

As a result of gravity impacts and density diversity, multiphase flow in pipes tends to exhibit different flow patterns, which behave in a much more complex way than single phase systems or homogenized multiphase flow. Some theoretical mechanistic models and many empirical correlations have been published to predict slippage between phases, flow regimes (Figure 2.6), **liquid hold-up** (in-situ liquid volume fraction), pressure loss in pipes, and other parameters (Guo et al., 2007).

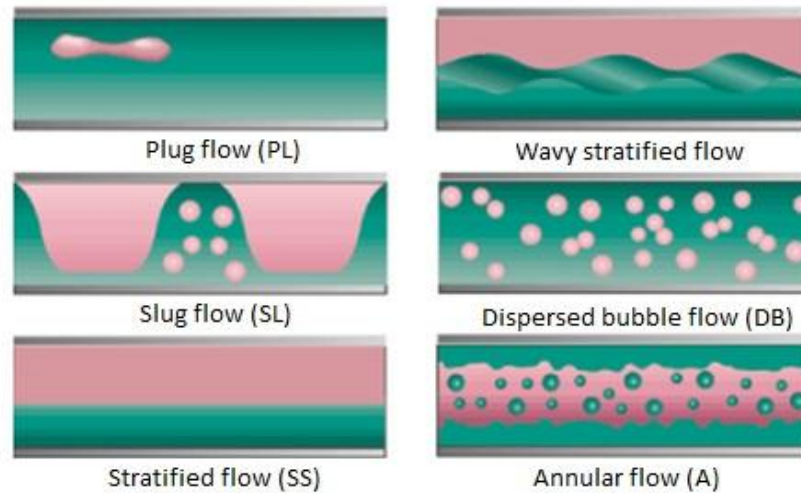


**Figure 2.6: Flow Regimes (Guo et al., 2007)**

Based on the principle of conservation of mass, momentum and energy, the pressure-gradient equation for wellbore flow is derived by considering the fluids to be a homogeneous mixture. This indicates that the steady-state pressure gradient consists of three components, as shown in Equation (2.15), (Lyons and Plisga, 2011),

$$\left(\frac{dp}{dL}\right)_{total} = \left(\frac{dp}{dL}\right)_{friction} + \left(\frac{dp}{dL}\right)_{elevation} + \left(\frac{dp}{dL}\right)_{acceleration} \quad (2.15)$$

Multiphase flow correlations are based on different assumptions made by different investigators.

In general, three types of assumptions are usually used:

- No slippage between phases, only evaluated friction factor empirically;
- Both liquid hold-up and friction factor calculated;
- Slippage considered, flow pattern considered.

The third set of assumptions predicts more realistic results as they are based on more considerations. All the correlations belonging to this group first predict the flow pattern in the pipeline at the specified physical conditions, depending on a flow pattern map (e.g. Figure 2.7). The Froude number is a dimensionless quantity used in fluid mechanics to indicate the flow regimes of open channel flow. The Froude number is defined as a ratio of inertial and gravitational forces on an element of fluid. This is expressed as Equation (2.16),

$$N_{FR} = \frac{V}{\sqrt{gD}}, \quad (2.16)$$

where,  $V$  is water velocity, (m/s),  $g$  is gravity, ( $\text{m/s}^2$ ), and  $D$  is hydraulic depth (cross sectional area of flow/top width), (m).

The input liquid content is defined as a ratio of liquid flow rate to the total flow rate of gas and liquid in Equation (2.17),

$$\lambda = \frac{q_L}{q_L + q_g}, \quad (2.17)$$

where,  $q_L$  is liquid flow rate, ( $\text{m}^3/\text{s}$ ),  $q_g$  is gas flow rate, ( $\text{m}^3/\text{s}$ ).

The Froude number and input liquid content are very important correlating parameters in distinguishing the flow patterns (e.g. segregated flow, distributed flow, or intermittent flow) in horizontal pipe flow.

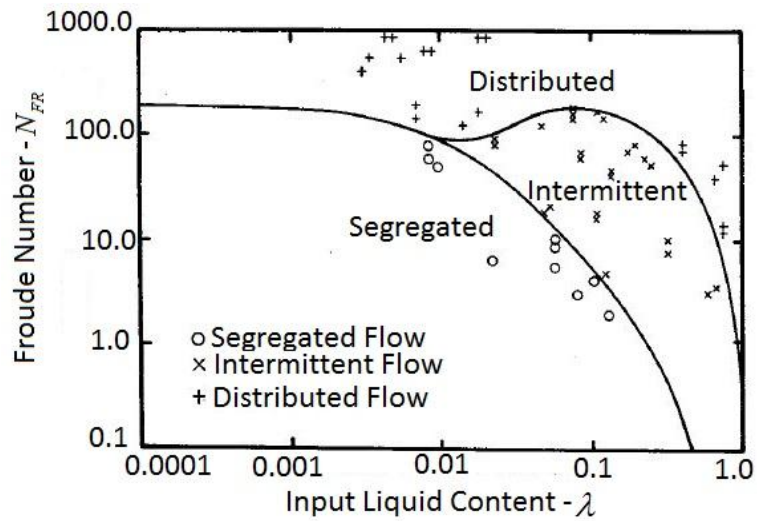


**Figure 2.7: Flow-pattern Map for Horizontal Pipeline (from Beggs and Brill, 1973)**

Some of the correlations use the same map for all inclined pipes as well as the horizontal pipeline, while others take advantage of different maps for different inclinations. Once the flow pattern is determined, the correlations evaluate **liquid hold-up** and friction factor from which the pressure drop can be calculated.

Many correlations have been established for estimating the pressure loss in pipes. The most commonly used correlations that considers both slippage and flow pattern are: Hughmark and Pressburg (1961), Duns and Ros (1963), Hagedorn and Brown (1965), Eaton et al. (1967), Aziz and Govier (1972), Beggs and Brill (1973), Griffith et al. (1973), Brill et al. (1981), Mukherjee and Brill (1983), revised Hagedorn and Brown (1989), and Ral et al. (1989).

Hughmark and Pressburg (1961) proposed an experimental study on vertical upward concurrent air-liquid flow under isothermal conditions. They found the experimental results such as **liquid hold-up** and two phase pressure drop data did not agree with the

Lockhart-Martinelli type of correlation for horizontal flow. Therefore, they developed a statistical correlation for holdup including fluid physical properties, total mass velocity, and the air-liquid ratio entering the pipe. The new twophase pressure drop correlations were developed based on a one inch diameter pipe for vertical uphill flow, and the pipe was filled of water, air, oils with different viscosities. The correlations showed a good agreement with the experimental observed data.

Duns and Ros (1963) presented correlations, including friction correlation, slip correlation, **liquid hold-up** correlation, acceleration, wall friction, and pressure gradient for gas and liquid mixtures in vertical flow. This can be applied to a full range of field operating conditions such as tubing and annular flow with variable water cuts. In this paper, the correlation was developed and applied to mist flow regimes for oil and gas mixtures, and this can also be used in gas or condensate wells or those wells with a water cut presented and without formed emulsion.

Hagedorn and Brown (1965) conducted two phase flow experiments in a continuous vertical well that was 1,500 ft long with 1 in., 1.25 in., and 1.5 in. nominal size tubing. The experiments were done to study the pressure gradients for a wide variety of liquid flow rates, gas liquid ratios, and liquid viscosities. Based on the results obtained from the experiments, correlations were developed in the dimensionless form and examined for a wide range of tubing size, fluid properties, and flow conditions, which allows for the accuracy in both single phase and two phase flow.

Eaton et al. (1967) conducted experimental studies on two phase, gas-liquid flow in three field-size horizontal pipelines with 2 and 4 in. in diameter. The water and crude oil are used as the liquid phase and natural gas is the gas phase. They presented a new reliable flow pattern map that does not require the pressure loss calculations. They developed the liquid-holdup correlations and an energy-loss factor correlation, as well as a two phase flow power balance, to predict the pressure losses during two phase flow in horizontal pipelines.

Aziz and Govier (1972) developed the methodology to predict the in-situ volume fraction of gas phase, flow patterns, and pressure gradient for two phase flow in vertical wells based on mechanistic considerations. This work shows a better prediction result compared with the results from previous work developed by Duns and Ros (1963) and Hagedorn and Brown (1965).

Beggs and Brill (1973) predicted the pressure drop and liquid hold-up that occur during twophase flow in inclined pipelines. The experiments were conducted to measure liquid hold-up and pressure drop by using transparent acrylic pipes filling with water and air. The liquid hold-up and friction factor correlation were developed to predict pressure loss occurring in two phase, air/water flow in 1 or 1.5 inch smooth, circular pipes at any inclination angles from 0 to  $\pm 90^\circ$ . Based on the general mechanical energy balance, the Beggs and Brill Method (1973) uses the average in-situ density to calculate the pressure gradient. This method works for either horizontal or inclined angle flows. It also takes into account the different flow regimes. Payne et al. (1979) found that using the Beggs and Brill (1973) correlation over-predicted liquid hold-up for both uphill and downhill flow.

For this reason, Payne et al. (1979) proposed an effectiveness factor to correct the prediction.

Griffith et al. (1973) took care of the inclination effect in predicting the pressure drop with two phase flow in the wells, without considering the effects of three variables: pipe roughness, liquid and gas viscosities, and entrainment effects. The accuracy of the pressure drop prediction is about  $\pm 10\%$ . In this paper, they found an optimum pipe diameter allowing for a minimum pressure loss in any gas and oil flowrate.

Brill et al. (1981) conducted 29 two phase flow experiments in two 3-mile long flow lines in Prudhoe Bay field in Alaska. The flow rate, inlet and outlet pressures, and temperatures were monitored and measured for each test. They compared the results with the correlations in Beggs and Brill (1973) and found very little scatter appeared in the comparison.

Mukherjee and Brill (1983) developed the liquid hold-up correlations for both uphill and downhill inclined flow, no matter what the inclination angle and flow directions are. They found that four dimensionless parameters (dimensionless liquid & gas velocity numbers, liquid viscosity number, and inclination angle) control the set of holdup correlations. The flow pattern transitions can also be determined by the same parameters in two phase inclined flow.

Hagedorn and Brown (1989) modified the liquid hold-up correlations in Hagedorn and Brown (1965) by using 51 pressure profiles with 540 pressure loss measurements. This modified Hagedorn and Brown correlation gave a higher liquid hold-up value than the

result from previous work. The calculated pressure drop in the revised method was determined to be superior to the old one when comparing the results with field data.

Ral et al. (1989) presented a composite model to estimate the pressure drop for multiphase flow in inclined and deviated wells. This model covers a wide range of liquid flow rate, gas oil ratio, API gravity, and water cut. On the basis of field data comparison, the correlations from Hagedorn and Brown (1965), Aziz and Govier (1972), and Beggs and Brill (1973) and Ral et al. (1989) had a good performance.

In this thesis, the multiphase flow is not considered in the model; however, it is suggested for the future work.

## **Chapter 3 Methodology**

### **3.1 Introduction**

The compartmentalized reservoir model not only simulates realistic behavior of multiple compartments but also integrates the complexity of a wellbore inflow model including blank pipe segments and perforated segments. Obviously, the fundamental building blocks of compartmentalized modeling are the compartments themselves. Each compartment represents any homogeneous section of the entire system such as the aquifer, a reservoir simulator grid block or a fault block, penetrated by a completed wellbore or a blank pipe section. The method integrates three separate flow models: one for the wellbore, one for the reservoir and one for the aquifer influx. The reservoir statics and flow properties have to be reasonably estimated in order to achieve an accurate approximation for the reservoir dynamic behavior.

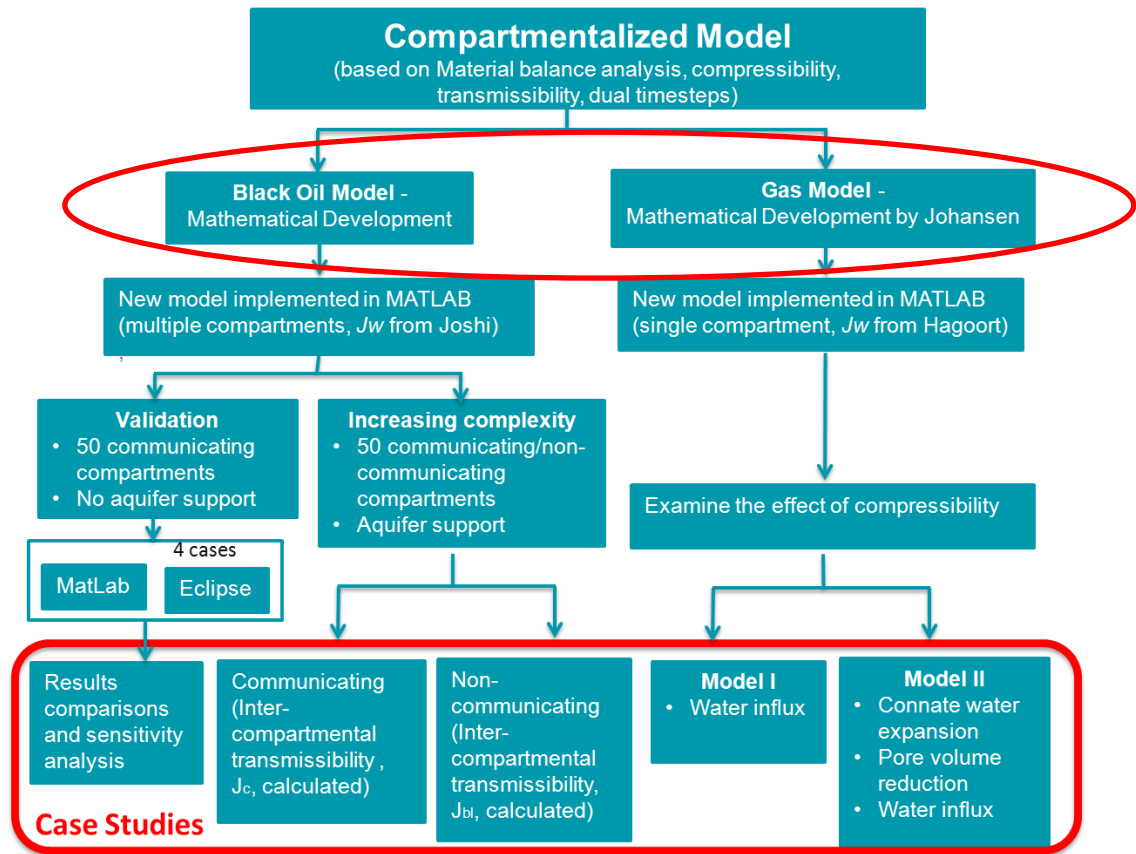


**Figure 3.1: Research Map**

This chapter presents the methodology of the multiple compartmentalized reservoir models (Figure 3.1) under consideration in this thesis:

- i) Single inflow reservoir compartment (Figure 3.2, Section 3.2),
- ii) Generalized formulas for multiple compartmentalized reservoirs with one common aquifer (Figure 3.3 & 3.4, Section 3.3).
- iii) Dry gas reservoir with bottom aquifer support model (Figure 3.5, Section 3.4).

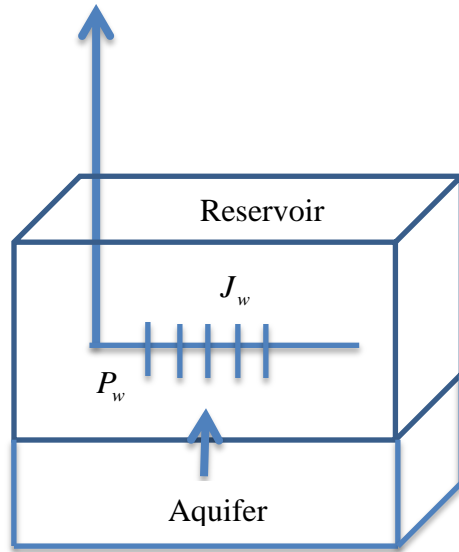


Figure 3.2: Schematic Drawing of Single Inflow Reservoir Compartment

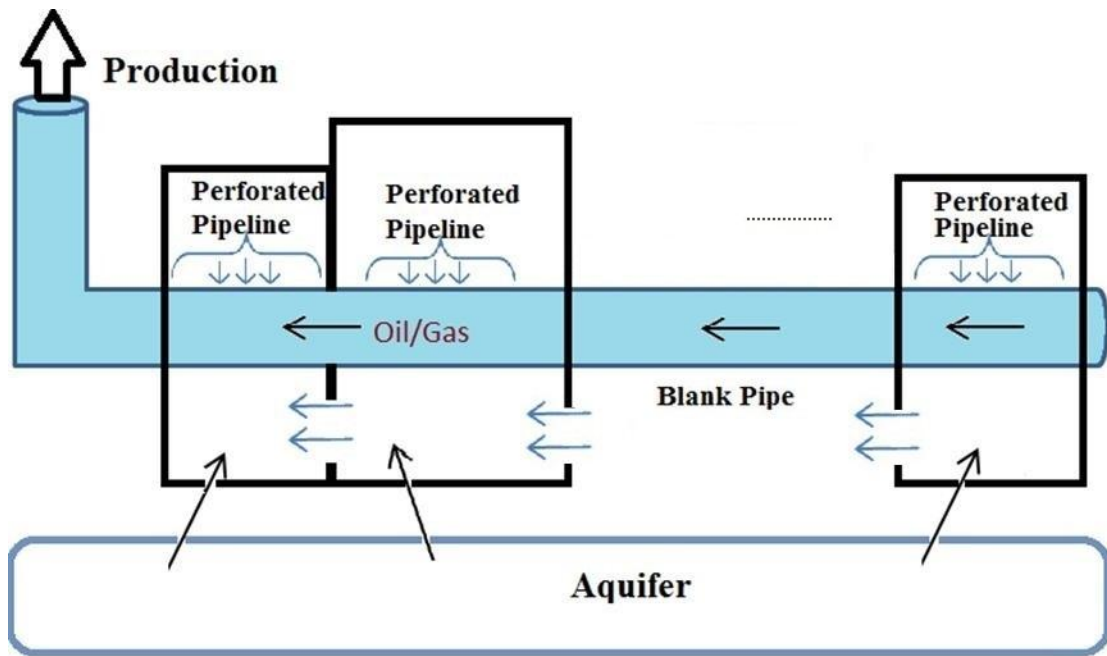
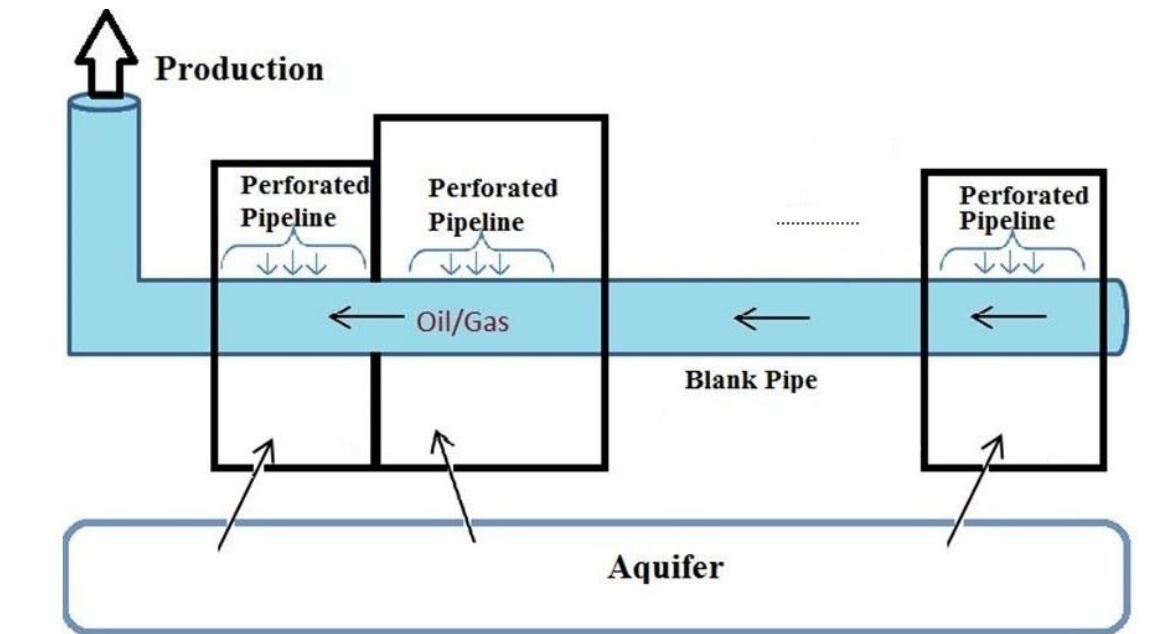
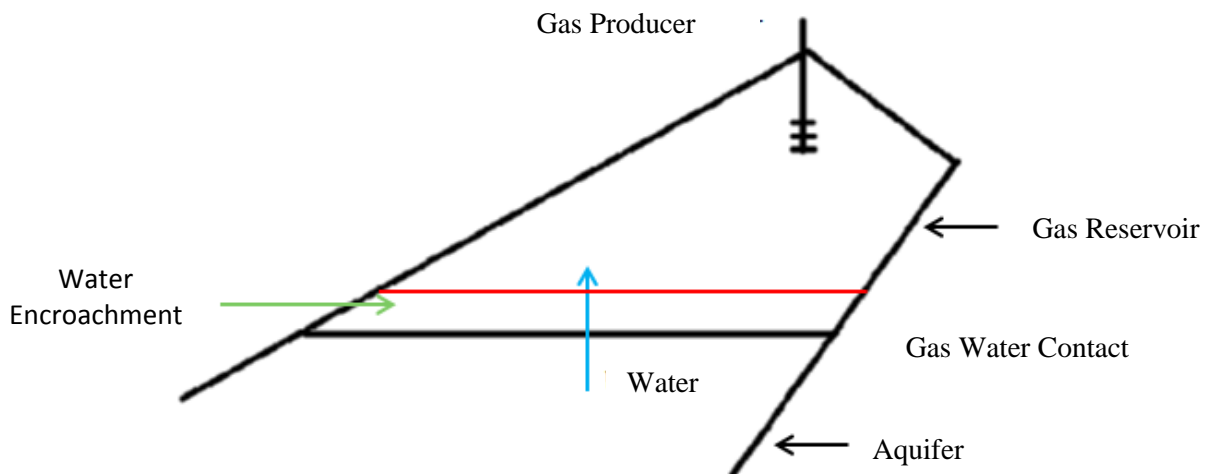


Figure 3.3: Schematic Drawing of Multiple Communicating Compartmentalized Reservoir Model



**Figure 3.4: Schematic Drawing of Multiple Non-Communicating Compartmentalized Reservoir Model**



**Figure 3.5: Dry Gas Reservoir with Bottom Aquifer Support Scheme**

Figure 3.2 shows a single inflow reservoir compartment. Figure 3.3 and Figure 3.4 show a bottom drive common aquifer compartment, and a number of reservoir compartments, which may or may not be in communication. The figures also show the wellbore with

several perforated and/or blank pipe segments. Figure 3.5 shows a dry gas reservoir with a bottom aquifer support.

The data corresponding to the reservoir and well were used in the Matlab program based on the theory described in Chapter 3 to predict future reservoir performance (all related Matlab code is in Appendix C). In order to evaluate the accuracy of this model, a second model was built using the industrial standard Eclipse<sup>TM</sup> software using the same reservoir geometry and parameters. A sensitivity analysis was completed to better understand the relationships between input variables and output results in both models. There are four cases illustrated in the Chapter 4. Three input parameters of interest were changed simultaneously in the Matlab and Eclipse<sup>TM</sup> models, while all other properties remained fixed in order to verify the model and investigate their effect on the production and recovery factor. The changing parameters for the sensitive analysis are:

- 1) Friction Factor
- 2) Oil Formation Volume Factor
- 3) Oil Viscosity

Unless otherwise described, for the sake of simplicity and limiting the scope to the compartmentalized reservoir model, the following assumptions were made for oil reservoirs:

- 1) The fluid properties (density, viscosity) are constant,
- 2) The bulk, pore and water compressibilities are constant over the pressure range we are considering,

- 3) The water formation volume factor and oil formation volume factor will be constant,
- 4) Initial wellbore pressure is less than initial reservoir pressure,
- 5) The average pressure for a segment of wellbore through a reservoir compartment is calculated as the average pressure at two ends of each wellbore segment,
- 6) The reservoir is an undersaturated oil reservoir during production, which means the reservoir pressure is larger than bubble point pressure,
- 7) Ignoring acceleration for the simplification purpose, only the friction component is taken into account to calculate the pressure loss in the pipe.

Unless otherwise described, for the sake of simplicity and limiting the scope to the compartmentalized reservoir model, the following assumptions were made in the dry gas reservoir model:

- 1) Initially the aquifer and reservoir pressure are equal.
- 2) The system is isothermal.
- 3) Only dry gas is present, no liquid drop-out.
- 4) The flowing wellbore pressure is assumed constant.

The mathematical models are described in following Sections.

### **3.2 Mathematical Model of a Single Inflow Reservoir Compartment**

As discussed in Chapter 2, the dynamic behavior of a reservoir compartment is controlled by two parameters, compressibility and transmissibility.

These are defined by the following equations:

$$c = -\frac{1}{V_i} \frac{dV}{dP}, \text{ units} = \text{Pa}^{-1}, \quad (3.1)$$

where,  $c$  can be either the compressibility of a pure substance (oil  $c_o$ , water  $c_w$ , or gas  $c_g$ ), the compressibility of rock ( $c_r$ ), or the total compressibility ( $c_t$ ) formulated by

$$c_t = S_o c_o + S_w c_w + S_g c_g + c_r. \quad (3.2)$$

Here,  $V_i$  is the initial saturated volume of oil or water, and  $S_o$ ,  $S_w$  and  $S_g$  represents the oil, water, and gas saturation within the pore volume, respectively, and  $\frac{dV}{dP}$  is the change in volume per change in pressure. For oil, water, gas systems

$$S_o + S_w + S_g = 1, \quad (3.3)$$

Aquifer compressibility is also an important term in the calculations of aquifer drive reservoirs, which is defined from (3.2) as

$$c_a = c_w + c_r, \text{ since } S_w = 1. \quad (3.4)$$

In this work, we consider isothermal systems; hence, the volume of a substance is a unique function of pressure,  $V = V(P)$ . Water compressibility of  $4 \times 10^{-7} \text{ kPa}^{-1}$  is used. The value of  $40 \times 10^{-7} \text{ kPa}^{-1}$  is chosen for the oil compressibility.

In addition, transmissibility is another important parameter defined in Section 2.2; the basic equation is defined in Equation (2.2). For the well inflow model, the flow rate into the well is presented as the same formulation in Equation (3.5),

$$q_{wf} = J_w (P_r(t) - P_{wf}(t)), \quad (3.5)$$

where,  $q_{wf}$  is the volumetric flow rate from the reservoir to the wellbore in stock tank condition,  $J_w$  is the well transmissibility measured in  $\text{Sm}^3/(\text{kPa}\cdot\text{day})$ ,  $P_r$  is the reservoir pressure at time  $t$ , and  $P_{wf}$  is the flowing wellbore pressure at time  $t$ .

In this thesis, we use the well transmissibility ( $J_w$ ) given in Joshi (1988) as

$$J_w = \frac{2\pi K_H h}{\mu B \left[ \ln \left( \frac{a + \sqrt{a^2 - (L/2)^2}}{L/2} \right) + \left( \frac{I_{ani} h}{L} \right) \ln \left( \frac{I_{ani} h}{r_w (I_{ani} + 1)} \right) + S \right]}, \quad (3.6)$$

where,  $K_H$  and  $K_V$  are the horizontal and vertical permeability, respectively,  $h$  is the reservoir thickness,  $\mu$  is the fluid viscosity in the well,  $B$  is the formation volume factor,  $a$  is the half major axis in the ellipse,  $L$  is the horizontal well length,  $r_w$  is the well radius,  $S$  is skin factor, and,

$$I_{ani} = \sqrt{\frac{K_H}{K_V}}. \quad (3.7)$$

Compressibility given in Equation (3.1) can be reformulated as

$$c = -\frac{1}{V_i} \frac{dV}{dt} \frac{dt}{dP} = -\frac{1}{V_i} q_{wf} \frac{dt}{dP}, \quad (3.8)$$

where,  $c$  is the total compressibility,  $V_i = V(t)$  is the total fluid volume saturated in the reservoir condition, which is changing when the production starts,  $\frac{dV}{dt}$  is the partial change in fluid volume with respect to time, which is equal to the flow rate into the well ( $q_{wf}$ ) in reservoir condition, and  $P = P_r(t)$  is the reservoir pressure at any time  $t$ .

Moving the term  $\frac{dt}{dP}$  to the left side of Equation (3.8), we get

$$\frac{dP_r(t)}{dt} = -\frac{q_{wf}}{cV(t)}. \quad (3.9)$$

Equation (3.5) gives the flow rate in the stock tank condition; therefore, the formation volume factor  $B$  ( $\text{Rm}^3/\text{Sm}^3$ ) has to be added into this equation.

$$q_{wf} = BJ_w(P_r(t) - P_{wf}(t)). \quad (3.10)$$

Here,  $q_{wf}$  is the fluid flow rate in reservoir condition, if the well is producing oil,  $B$  is the oil formation volume factor  $B_o$ ; if the well is producing gas,  $B$  is the gas formation volume factor  $B_g$ . However, this linear pressure function is not valid for gas, and has to be changed to a pseudo-pressure function. The special derivations for gas reservoir are shown in Section 3.4.

Inserting Equation (3.10) into Equation (3.9), we get the reservoir pressure equation,

$$\frac{dP_r}{dt} = -\frac{BJ_w}{cV(t)}(P_r(t) - P_{wf}(t)). \quad (3.11)$$

The flow rate in the stock tank condition is

$$\frac{dV}{dt} = J_w(P_r(t) - P_{wf}(t)). \quad (3.12)$$

Equations (3.11) and (3.12) can be integrated to determine  $P_r(t)$  and  $V(t)$  if given the initial conditions  $P_r(0)$  and  $V(0)$ .

For the special case when  $P_r(t)$  is constant, Equation (3.11) is equal to 0.

$$\frac{dP_r}{dt} = -\frac{BJ_w}{cV(t)}(P_r(t) - P_{wf}(t)) = 0, \quad (3.13)$$

- If the pressure  $P_r(t) - P_{wf}(t) = 0$ , the oil cannot be produced since there are no driving forces existing between the reservoir and the well. In this case, the flow rate is zero. From Equation (3.12) we can get the same result  $\frac{dV}{dt} = J_w(P_r(t) - P_{wf}(t)) = 0$ . From a physical point of view, if the reservoir pressure keeps constant and it is same as wellbore pressure, the fluid cannot be produced, as there are no driven forces.
- If the pressure  $P_r(t) - P_{wf}(t) \neq 0$ , the term  $\frac{BJ_w}{cV(t)}$  in Equation (3.13) has to be zero.

As  $B$  and  $c$  are not zero, we can have three assumptions of (i)  $J_w = 0$ , (ii)  $V(t) = 0$ , and (iii)  $J_w = V(t) = 0$ . Inserting the three assumptions into Equation (3.12), we can get an identical result of  $\frac{dV}{dt} = J_w(P_r(t) - P_{wf}(t)) = 0$ , and  $J_w = V(t) = 0$ . From a physical point of view, if the reservoir pressure keeps constant, and the reservoir pressure and wellbore pressure are not the same, the fluid cannot be produced due to the low permeability of the reservoir. In this case, the transmissibility  $J_w$  is zero.

In this work, the 4th Order Runge-Kutta method is used to determine the pressure and cumulative production at any time  $t$ , (See Appendix B). In mathematics, the Courant-Friedrichs-Lewy condition (CFL condition) is a necessary condition for convergence for solving differential equations by the numerical method. For one dimensional case, the CFL has the form of  $dt \leq C_{\max} * dx/v$ ,  $dt$  is the time step,  $C_{\max}$

changes with the method used to solve the discretized equation,  $\Delta x$  is the length interval, and  $v$  is the velocity. If an explicit solver is used then  $C_{\max}=1$ . For more details on this, see (Courant et. al, 1928). In this model, when  $\Delta t \leq Vc/(BJ)$ , where  $V$  is the fluid volume in compartment,  $c$  is the compressibility,  $B$  is the formation volume factor,  $J$  is the transmissibility, the numerical method is stable.

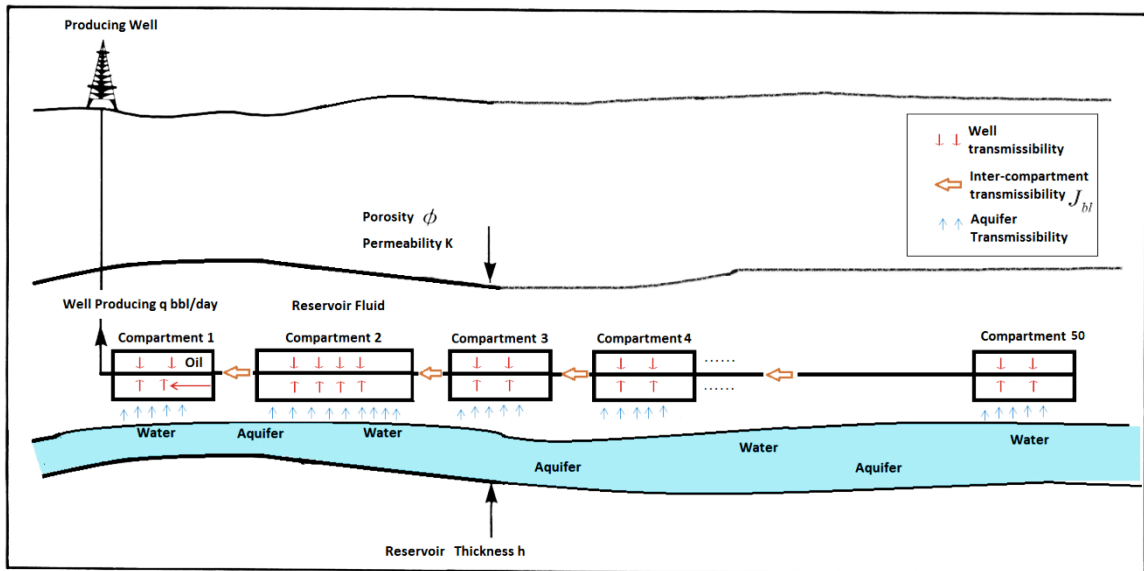
These two equations (3.11) and (3.12) can also be expanded to encompass more reservoir compartments by using the concept of inter-compartment transmissibility.

### **3.3 Mathematical Model of Multiple Reservoir Compartments with Aquifer Support**

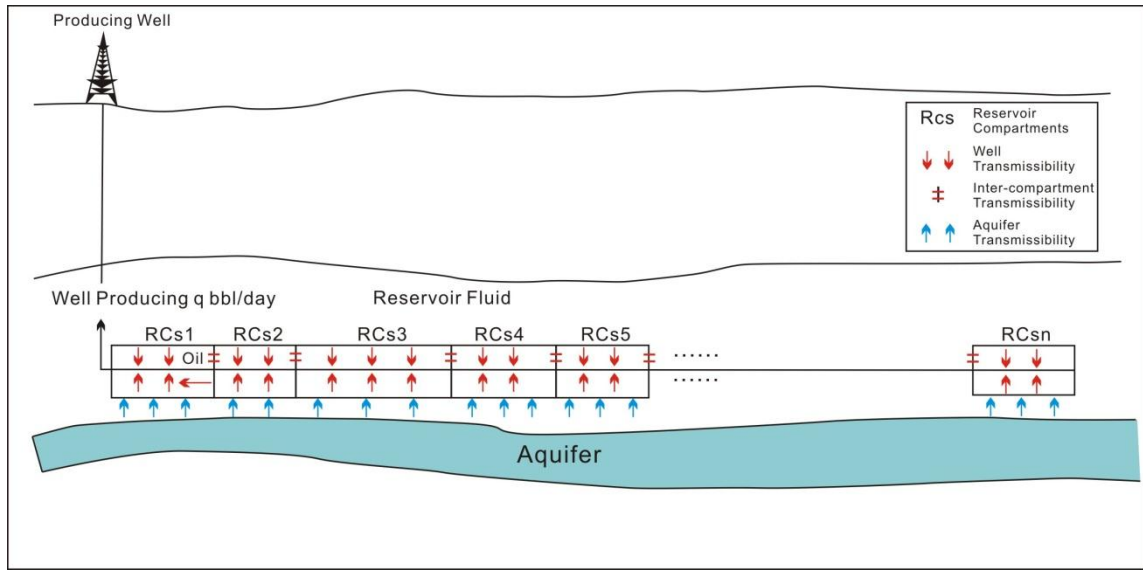
Many complex reservoirs exhibit significant flow barriers between different regions in terms of faults or stratigraphic changes. Therefore, a multiple reservoir compartment model for both non-communicating and communicating compartments is developed to describe these complex reservoirs more accurately. This allows us to recognise and understand reservoir behaviour and optimize production behaviour in such complex fields.

Figure 3.6 illustrates a reservoir with multiple non-communicating compartments supported by a common bottom aquifer. A horizontal well is draining through  $n$  reservoir compartments with completely impermeable rock between the reservoir compartments. The pipeline segments penetrated within the reservoir compartments are fully perforated. The blank pipe segments within the sealed portions are connecting any two neighboring reservoir compartments with no influx from the reservoir. In order to integrate the blank pipe segments into the model, an inter-compartment transmissibility of the blank pipe

segment  $J_{bl}$  is defined in this section. Figure 3.7 illustrates a reservoir model with multiple communicating compartments with a horizontal wellbore. The compartments are also supported by one common aquifer. The only difference for this case is that there is no blank pipe or impermeable rock between compartments. For this scenario, the inter-compartment transmissibility  $J_c$  is used in the model instead of the inter-compartment transmissibility of the blank pipe segment  $J_{bl}$ .



**Figure 3.6: Schematic of Multiple Non-Communicating Compartments**



**Figure 3.7: Schematic of Multiple Communicating Compartments**

It is assumed for both scenarios that all the reservoir compartments contain compressible fluids such as oil and water. In this section, the following system of governing equations for reservoir compartments and aquifer compartments are derived from the basic compressibility definition and transmissibility concept.

For any reservoir compartment (RC)  $i$ , the total compressibility ( $c_{t,i}$ ) is

$$c_{t,i} = -\frac{1}{V_{ir,i} - W} \frac{dV_{r,i}}{dP_{r,i}}, \quad (3.14)$$

where  $V_{ir,i}$  is the oil initially in place for RC  $i$  at time  $t$ ,  $W$  is the influx from the aquifer during  $dt$ ,  $\frac{dV_{r,i}}{dP_{r,i}}$  is the change of the saturated fluid volume in compartment  $i$  per change in average reservoir pressure in RC  $i$  (Figure 3.8).

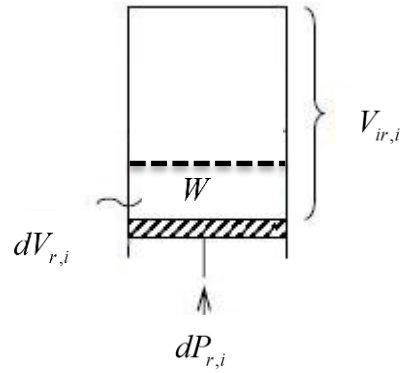


**Figure 3.8: Schematic of Total Compressibility for Compartment  $i$**

This formula can be mathematical re-written as

$$c_{t,i} = -\frac{1}{V_{ir,i} - W} \frac{dV_{r,i}}{dt} \frac{dt}{dP_{r,i}}. \quad (3.15)$$

For each reservoir compartment  $i$ , there are four types of flow taking place in the process, i) fluids in RC  $i$  flow into the wellbore, ii) fluids flow from RC  $i$  to RC  $i-1$ , iii) fluids flow from RC  $i+1$  to RC  $i$ , and iv) the water flows into RC  $i$  from the aquifer. This is illustrated in Figure 3.9.

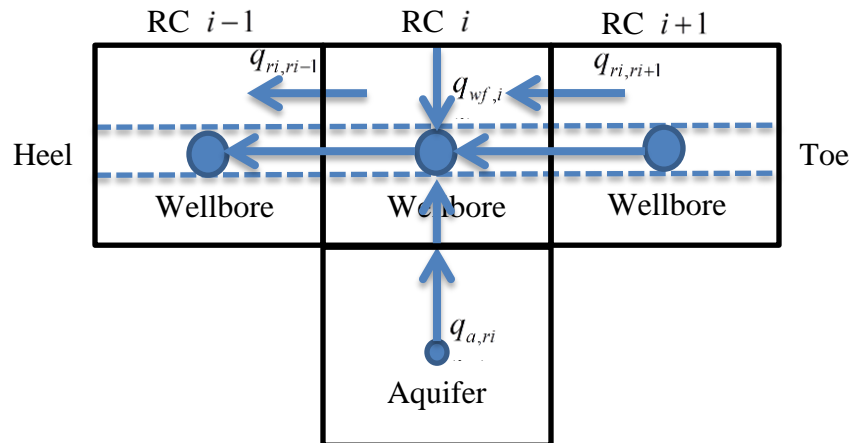


### Figure 3.9: Description of the Flow Process in the Reservoir System

Therefore, the change in volume of compartment  $i$   $\frac{dV_{r,i}}{dt}$  in reservoir condition is given by

$$\frac{dV_{r,i}}{dt} = q_{wf,i} + q_{ri,ri-1} - q_{ri,ri+1} - q_{a,ri}, \quad (3.16)$$

where

$$q_{wf,i} = B_o J_{w,i} (P_{r,i}(t) - P_{wf,i}(t)). \quad (3.17)$$

Here,  $B_o$  is the oil the formation volume factor,  $J_{w,i}$  is well transmissibility in reservoir compartment  $i$ , see Joshi Equation (3.6),  $P_{r,i}$  is the average reservoir pressure in reservoir compartment  $i$  at time  $t$ ,  $P_{wf,i}$  is the flowing bottom hole pressure in reservoir compartment  $i$  at time  $t$ ,  $q_{ri,ri+1}$  is the flow rate from RC  $i+1$  to RC  $i$  at time  $t$ , and  $q_{a,ri}$  is the flow rate from the aquifer to the RC  $i$ .

The flow rate ( $q_{ri,ri+1}$ ) from RC  $i+1$  to RC  $i$  in the reservoir condition is given by

$$q_{ri,ri+1} = B_o J_{i,i+1} (P_{r,i+1}(t) - P_{r,i}(t)), \quad (3.18)$$

where,  $J_{i,i+1}$  is the inter-compartment transmissibility between RC  $i$  and RC  $i+1$ .

The inter-compartment transmissibility is divided into two categories depending on the communication of the two neighbouring compartments,

- i) For the communicating compartment reservoir model, inter-compartment transmissibility is

$$J_{i,i+1} = J_{ci,i+1}, \text{ and} \quad (3.19)$$

- ii) For the non-communicating compartment reservoir model, the blank pipe transmissibility is

$$J_{i,i+1} = J_{bli,i+1}. \quad (3.20)$$

The flow rate ( $q_{ri,ri-1}$ ) from RC  $i$  to RC  $i-1$  in reservoir condition can be obtained from

$$q_{ri,ri-1} = B_o J_{i,i-1} (P_{r,i}(t) - P_{r,i-1}(t)). \quad (3.21)$$

The water influx rate from the aquifer to RC  $i$  in reservoir condition is given by

$$q_{a,ri} = B_w J_a (P_a(t) - P_{r,i}(t)), \quad (3.22)$$

where,  $J_a$  is the aquifer transmissibility to RC  $i$ ,  $B_w$  is the water formation volume factor, and  $P_a$  is the average aquifer pressure.

We obtain a differential equation for the reservoir pressure in RC  $i$  by rewriting Equation (3.15) as

$$\frac{dP_{r,i}}{dt} = -\frac{1}{c_{t,i}(V_{ir,i} - W)} \frac{dV_{r,i}}{dt}. \quad (3.23)$$

Using Equation (3.16), Equation (3.23) becomes

$$\frac{dP_{r,i}}{dt} = -\frac{1}{c_{t,i}(V_{ir,i} - W)} (q_{wf,i} + q_{ri,ri-1} - q_{ri,ri+1} - q_{a,ri}), \quad (3.24)$$

Finally, inserting Equations (3.17), (3.18), (3.21), and (3.22) into Equation (3.24) yields the reservoir pressure for RC  $i$  given by

$$\begin{aligned} \frac{dP_{r,i}}{dt} = & -\frac{B_o J_{w,i}}{c_{t,i}(V_{ir,i} - W)} (P_{r,i}(t) - P_{wf,i}(t)) - \frac{B_o J_{i,i-1}}{c_{t,i}(V_{ir,i} - W)} (P_{r,i}(t) - P_{r,i-1}(t)) - \\ & \frac{B_o J_{i,i+1}}{c_{t,i}(V_{ir,i} - W)} (P_{r,i}(t) - P_{r,i+1}(t)) - \frac{B_w J_a}{c_{t,i}(V_{ir,i} - W)} (P_{r,i}(t) - P_a(t)), \end{aligned} \quad (3.25)$$

At the two boundaries,  $i=1$  at heel location and  $i=n$  at toe location, the term

$$\frac{B_o J_{i,i-1}}{c_{t,i}(V_{ir,i} - W)} (P_{r,i}(t) - P_{r,i-1}(t)) \quad \text{and} \quad \frac{B_o J_{i,i+1}}{c_{t,i}(V_{ir,i} - W)} (P_{r,i}(t) - P_{r,i+1}(t))$$

both zero.

Aquifer compressibility, introduced in Section 2.2.1, is essential in determining the aquifer pressure solution. This parameter is given by Equation (3.4). It can also be written as

$$c_a = -\frac{1}{W_i} \frac{dW}{dt} \frac{dt}{dP_a}, \quad (3.26)$$

where,  $\frac{dW}{dt}$  is the change of the volume of water in the aquifer over the time step, so it can

be solved by

$$\frac{dW}{dt} = \sum_{i=1}^n q_{a,ri}. \quad (3.27)$$

The water influx ( $q_{a,ri}$ ) from the aquifer to RC  $i$  refers to Equation (3.22).

Rewriting Equation (3.26) by inserting Equation (3.22) and (3.27), the average aquifer pressure is given by

$$\frac{dP_a}{dt} = -\frac{1}{c_a W_i} \sum_{i=1}^n B_w J_a (P_a(t) - P_{r,i}(t)). \quad (3.28)$$

For a better prediction of production behaviour, the wellbore pressure loss during both the perforated pipeline segments and blank pipe segments must be taken into account in the model.

For perforated pipeline segments, the pressure gradient in a horizontal well in differential form is

$$\frac{dP_{wf,i}}{dL} = \frac{f_{per} \rho v_{m,i}^2}{2D}, \quad (3.29)$$

where

$L$  is the length of the pipeline segment,  $f_{per}$  is friction factor, which can be chosen from Equation (2.9), (2.12) and (2.13) based on different flow regime and pipeline properties, and

$$v_{m,i} = \frac{q_{wf,i}}{A}, \quad (3.30)$$

For blank pipe segments, the pressure loss ( $P_{wfi,i+1}$ ) due to friction in the blank pipe segment between RC  $i$  and  $i+1$  is given by

$$\frac{dP_{wfi,i+1}}{dL} = \frac{f_{bl} \rho v_{mi,i+1}^2}{2D}, \quad (3.31)$$

where,

$L$  is the length of blank pipe segments between RC  $i$  and  $i+1$ ,  $f_{bl}$  is the friction factor, which can also be chosen from Equation(2.9), (2.12) and (2.13),  $v_{mi,i+1}$  is the volumetric flux of mixture fluids in the blank pipe between RC  $i$  and  $i+1$ ,

$$v_{mi,i+1} = \frac{q_{wfi,i+1}}{A}, \quad (3.32)$$

$D$  is the blank pipe diameter [m], which is same as perforated pipeline diameter.

When the wellbore pressure function for the blank pipe segment is calculated, the inter-compartment transmissibility of the blank pipe segment  $J_{bli,i+1}$  between compartments  $i$  and  $i+1$  can also be determined. In this work, Haaland (1983) is chosen to calculate the pressure loss in the horizontal well.

For two non-communicating reservoir compartments, the inter-transmissibility  $J_{bli,i+1}$  is solved to fulfil the same model as the communicating reservoir compartment model. It is derived as follows.

Substituting Equation (3.32) into (3.31), the flow rate in a horizontal blank pipe is formulated as

$$q = \sqrt{\frac{2DA^2}{f_{bl}\rho L} \frac{dP_{wfi,i+1}^2}{dP_{wfi,i+1}}}. \quad (3.33)$$

Therefore, we get the relationship between flow rate and wellbore pressure as

$$q = \sqrt{\frac{2DA^2}{f_{bl}\rho L} dP_{wfi,i+1}}. \quad (3.34)$$

Hence, the inter-compartment transmissibility  $J_{bl}$  for the blank pipe segment is defined by

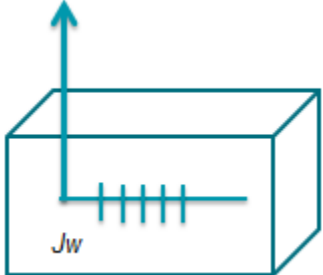
$$J_{bli,i+1} = \sqrt{\frac{2DA^2}{f_{bl}\rho LdP_{wfi,i+1}}}, \quad (3.35)$$

where,  $J_{bli,i+1}$  is a pressure dependent variable.

The inter-transmissibility for the communicating reservoir compartment model  $J_{ci,i+1}$  in the stock tank condition is given by

$$J_{ci,i+1} = \frac{(Kk_r)_{i,i+1} A_{ci,i+1}}{\mu L_{i,i+1} B}, \quad (3.36)$$

where,  $K$  is absolute permeability of each compartment,  $k_r$  is relative permeability of oil,  $A_{ci,i+1}$  is the area of contact between compartments  $i$  and  $i+1$ ,  $\mu$  is the viscosity of fluid,  $L_{i,i+1}$  is the distance between the center of the compartments  $i$  and  $i+1$ , and  $B$  is the formation volume factor.

Single Compartment	
	$\frac{dP_r}{dt} = -\frac{J_w}{cV_i} (P_r(t) - P_{wf}(t)) \quad (3.11)$ $\frac{dV}{dt} = J_w (P_r(t) - P_{wf}(t)) \quad (3.12)$

Complex Compartments with Aquifer	
	$\frac{dP_{r,i}}{dt} = -\frac{B_o J_{w,i}}{c_{t,i}(V_{ir,i} - W)} (P_{r,i}(t) - P_{wf,i}(t)) - \frac{B_o J_{i,i-1}}{c_{t,i}(V_{ir,i} - W)} (P_{r,i}(t) - P_{r,i-1}(t)) - \frac{B_o J_{i,i+1}}{c_{t,i}(V_{ir,i} - W)} (P_{r,i}(t) - P_{r,i+1}(t)) + \frac{B_w J_a}{c_{t,i}(V_{ir,i} - W)} (P_{ri}(t) - P_a(t)) \quad (3.25)$ $\frac{dW}{dt} = \sum_{i=1}^n q_{a,ri} \quad (3.27)$ $\frac{dP_a}{dt} = -\frac{1}{c_a W_i} \sum_{i=1}^n B_w J_a (P_a(t) - P_{r,i}(t)) \quad (3.28)$ $\frac{dP_{wf,i}}{dL} = \frac{f_{per} \rho v_{m,i}^2}{2D} \quad (3.29)$

**Table 3.1: Generalized Governing Equations**

From the Table 3.1, considering Equation (3.25), (3.27), (3.28), and (3.29), we have a system of first order ordinary differential equations with the unknowns  $P_r$ ,  $W$ ,  $P_a$  and  $P_{wf}$ , which can be solved simultaneously by a numerical method e.g. the 4<sup>th</sup> order Runge-Kutta method, once we have specified the initial conditions such as: initial reservoir pressure, initial aquifer pressure, initial wellbore pressure, and initial water encroachment (zero) in the Equation (3.37):

$$\begin{aligned} P_r(0) &= P_0 \\ P_a(0) &= P_0 \\ P_{wf}(0) &= P_{wf0} \\ W(0) &= 0, \end{aligned} \quad (3.37)$$

Once the model is solved over time interval  $[0, t]$ , the cumulative oil flow rate into RC  $i$  in stock tank condition can be found by integrating Equation (3.17),

$$q_{wf,i} = \int_0^t J_{w,i}(P_{r,i}(t) - P_{wf,i}(t))dt. \quad (3.38)$$

The cumulative stock tank condition oil production is the summation of Equation (3.38), i.e.

$$q_{bh} = \sum_{i=1}^n \int_0^t J_{w,i}(P_{r,i}(t) - P_{wf,i}(t))dt. \quad (3.39)$$

For example, the governing pressure equations for the fifty reservoir compartments case (Section 4.1) are given by:

When  $n = 1$ ,

$$\frac{dP_{r,n}}{dt} = -\frac{B_o J_{w,n}(P_{r,n} - P_{w,n})}{c_t V_{i,n}} + \frac{B_o J_{c,n}(P_{r,n+1} - P_{r,n})}{c_t V_{i,n}}, \quad (3.40)$$

When  $1 < n < 50$ ,

$$\frac{dP_{r,n}}{dt} = -\frac{B_o J_{w,n}(P_{r,n} - P_{w,n})}{c_t V_{i,n}} + \frac{B_o J_{c,n}(P_{r,n+1} - P_{r,n})}{c_t V_{i,n}} - \frac{B_o J_{c,n-1}(P_{r,n} - P_{r,n-1})}{c_t V_{i,n}}, \quad (3.41)$$

When  $n = 50$ ,

$$\frac{dP_{r,n}}{dt} = -\frac{B_o J_{w,n}(P_{r,n} - P_{w,n})}{c_t V_{i,n}} - \frac{B_o J_{c,n-1}(P_{r,n} - P_{r,n-1})}{c_t V_{i,n}}. \quad (3.42)$$

The cumulative oil production in reservoir condition is

$$q_{o,n} = \sum_{n=1}^{50} B_o J_{w,n} (P_{r,n} - P_{w,n}) dt \quad (3.43)$$

The oil flowrate in reservoir condition is

$$q_{o,n} = B_o J_{w,n} (P_{r,n} - P_{w,n}) \quad (3.44)$$

The above method can also be modified to account for other effects such as pore compressibility, connate water expansion, and oil/gas expansion. It can also be used for a gas reservoir, which will be illustrated in following Section 3.4.

### 3.4 Mathematical Model of Dry Gas Reservoir with Aquifer Support Modelling

This section will consider a pure gas reservoir as a compressible fluid in a tank. The gas will be extracted from this reservoir without considering the flow of the gas through a permeable medium except for well inflow. Only volumetric quantities such as porosity, compressibility, and connate water will come into play in the system. (Johansen, 2013)

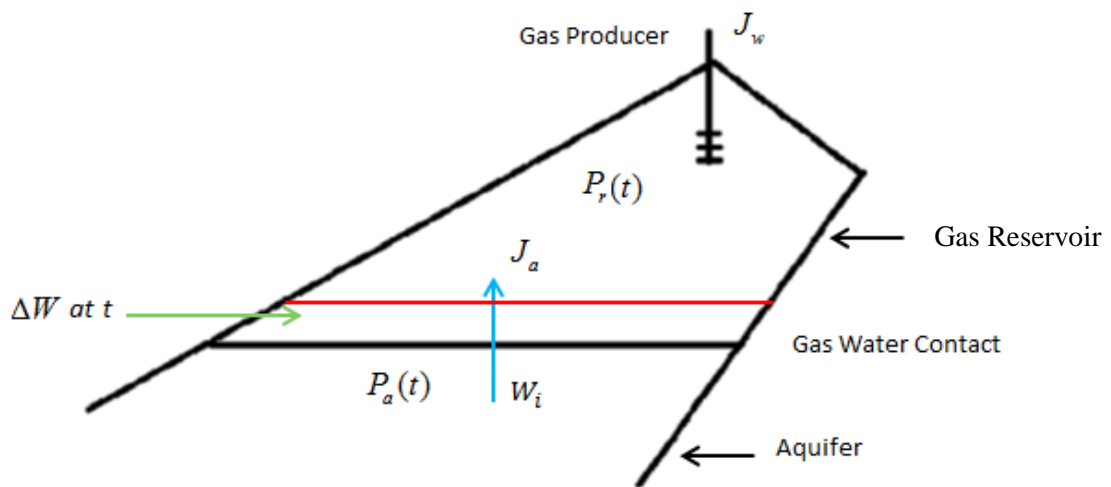


Figure 3.10: Dry Gas Reservoir with Bottom Aquifer Support Scheme

With reference to Figure 3.10, the corresponding parameters are:

$W_i$  is initial water aquifer volume, ( $\text{Rm}^3$ ),  $J_a$  is aquifer transmissibility, ( $\text{Sm}^3/\text{Day-kPa}$ ),

$J_w$  is well transmissibility, ( $\text{Sm}^3/\text{Day-kPa}$ ),  $P_a(t)$  is average aquifer pressure at time  $t$ ,

(kPa),  $P_r(t)$  is average reservoir pressure at time  $t$ , (kPa),  $\Delta W$  is cumulative water

encroachment at reservoir condition at time  $t$ , ( $\text{Rm}^3$ ).

In the defined gas reservoir, hydrocarbon pore volume (HCPV) at reservoir condition (RC) at time  $t$  is given by

$$HCPV = B_g (G - G_p), \quad (3.45)$$

where,  $B_g$  is gas formation volume factor at reservoir pressure  $P_r(t)$ , ( $\text{Rm}^3/\text{Sm}^3$ ),  $G_p$  is

cumulative gas produced at stock tank condition (STC) from time  $t = 0$  to  $t$ , ( $\text{Sm}^3$ ),  $G$  is

stock tank gas initially in place, ( $\text{Sm}^3$ ).

When gas is produced, the reservoir pressure depletion will lead to:

- 1) Influx of water from the aquifer ( $\Delta W$ ),
- 2) Expansion of connate water in the gas zone ( $\Delta V_{cw}$ ),
- 3) Reduction of pore volume ( $\Delta PV$ ) in the reservoir.

The HCPV can also be calculated by,

$$HCPV = HCPV_i - \Delta W - \Delta V_{cw} - \Delta PV. \quad (3.46)$$

### 3.4.1 Water Influx Only (Model 1)

The gas is more compressible than oil and water, thus, in order to obtain an equation similar to liquid flow, some changing gas properties have to be dealt with in the calculations, such as gas compressibility, gas compressibility factor (Z-factor), and gas viscosity ( $\mu$ ). The concept of gas pseudo-pressure function ( $m$ ) is developed by Al-Hussainy et al. (1966) for the flow of gas to account for the variable viscosity and compressibility of gas with respect to pressure.

$$m(P) = 2 \int_0^P \frac{PdP}{\mu Z}, \quad (3.47)$$

Twenty two years later, Hagoort derived a new gas pseudo-pressure function (1988, Appendix A),

$$m(P) = (\mu B)_{ref} \int_{P_{ref}}^P \frac{1}{\mu B} dP, \quad (3.48)$$

where,  $P_{ref}$  stands for reference pressure.

In this particular case, when is  $P = P_r$  (reservoir pressure), Equation (3.48) becomes

$$m(P_r) = (\mu B)_{ref} \int_{P_{ref}}^{P_r} \frac{1}{(\mu B)_r} dP. \quad (3.49)$$

When  $P = P_w$  (wellbore pressure is constant in this case), Equation (3.48) becomes

$$m(P_w) = (\mu B)_{ref} \int_{P_{ref}}^{P_w} \frac{1}{(\mu B)_w} dP. \quad (3.50)$$

Combining Equation (3.49) and (3.50) gives

$$\frac{m(P_r) - m(P_w)}{(\mu B)_{ref}} = \frac{1}{\mu B} (P_r - P_w), \quad (3.51)$$

where,

$$\overline{\mu B} = \frac{2(\mu B)_r (\mu B)_w}{(\mu B)_r + (\mu B)_w}. \quad (3.52)$$

Here, the subscript  $r$  means reservoir condition, and  $w$  means wellbore condition. The complete derivation is provided in Appendix A.

If we ignore the effects of connate water swelling and the change in the pore volume, Equation (3.51) can be written as

$$HCPV = B_{gi} G - \Delta W. \quad (3.53)$$

Therefore, Equation (3.45) becomes,

$$B_g [G - G_p] = B_{gi} G - \Delta W. \quad (3.54)$$

Applying Equation (3.53) to an arbitrary time interval  $dt$ , when change in reservoir pressure is  $dP_r$  and gas produced is  $dG_p$ ,

$$[B_g (P_r + dP_r) - B_g (P_r)] G = B_g dG_p - dW, \quad (3.55)$$

where,  $dW$  is water encroachment during  $dt$ .

The net influx of water from the aquifer at reservoir conditions is given by

$$dW = B_w J_a (P_a - P_r) dt. \quad (3.56)$$

The net gas production from the reservoir at stock tank condition is given by

$$dG_p = J_w(m(P_r) - m(P_w))dt. \quad (3.57)$$

Substitution of Equation (3.56) and (3.57) into Equation (3.58) gives

$$[B_g(P_r + dP_r) - B_g(P_r)]G = B_g J_w(m(P_r) - m(P_w))dt - B_w J_a(P_a - P_r)dt. \quad (3.58)$$

Re-writing Equation (3.58) in terms of time derivatives gives:

$$GB'_g(P_r) \frac{dP_r}{dt} = B_g J_w(m(P_r) - m(P_w)) - B_w J_a(P_a - P_r). \quad (3.59)$$

Rearranging Equation (3.59), the reservoir pressure function can be represented as

$$\frac{dP_r}{dt} = \frac{1}{GB'_g(P_r)} (B_g J_w(m(P_r) - m(P_w)) - B_w J_a(P_a - P_r)). \quad (3.60)$$

The aquifer pressure function (refers Equation 3.27) is given by

$$\frac{dP_a}{dt} = -\frac{J_a}{c_a W} (P_a - P_r), \quad (3.61)$$

where,  $c_a$  is aquifer compressibility ( $\text{kPa}^{-1}$ ),  $W$  is aquifer size at time  $t$  ( $\text{Rm}^3$ ) which can be written as

$$W = W_i + \int_0^t B_w J_a(P_a - P_r)dt. \quad (3.62)$$

The cumulative gas production  $G_p(t)$  at stock tank condition can be calculated as

$$G_p(t) = \int_0^t J_w(m(P_r(t)) - m(P_w(t)))dt. \quad (3.63)$$

The cumulative influx obtained by integration of flow rate over time from the initial reservoir condition can be written as follows

$$G_{p,RC}(t) = \int_0^t \frac{kA}{\mu BL} (P_r - P_w) dt. \quad (3.64)$$

Equation (3.63) in reservoir conditions is given by

$$G_{p,RC}(t) = \int_0^t B_g J_w (m(P_r(t)) - m(P_w(t))) dt. \quad (3.65)$$

In order to simplify Equation (3.65), we have

$$\frac{kA}{\mu BL} (P_r - P_w) = B_g J_w (m(P_r(t)) - m(P_w(t))) = B_g J_w^* (P_r(t) - P_w(t)), \quad (3.66)$$

where, a new well transmissibility  $J_w^*$  is defined to keep the gas flow equation in a similar format as the flow of liquid. Therefore,  $J_w^*$  can be obtained from the following equation

$$\frac{kA}{\mu BL} = B_g J_w^*. \quad (3.67)$$

Equation (3.63) is simplified as

$$G_p(t) = \int_0^t J_w^* (P_r(t) - P_w(t)) dt, \quad (3.68)$$

$$J_w^* = J_{wi} \frac{(\overline{\mu B}) B_g}{(\mu_i B_i) B_{gi}}. \quad (3.69)$$

Where, subscript  $i$  stands for initial condition.

Substituting Equation (3.66) to Equation (3.60) becomes:

$$\frac{dP_r}{dt} = \frac{1}{GB_g'(P_r)} (B_g J_w^* (P_r(t) - P_w(t)) - B_w J_a (P_a(t) - P_r(t))). \quad (3.70)$$

The recovery factor at any given time is:

$$RF = \frac{G_p}{G}. \quad (3.71)$$

Updating the aquifer size at each time point by substituting Equation (3.62) into Equation (3.61), the reservoir pressure and aquifer pressure can be solved based on numerical approaches (such as the fourth order Runge-Kutta method) in Appendix B.

The model formulated above uses a large time step  $[0, T]$  where aquifer size and well transmissibility are kept constant. Then reservoir pressure and aquifer pressure are solved by the fourth order Runge-Kutta method using a small time step  $dt$  from  $[0, t]$ . The aquifer size and well transmissibility are updated with new values of reservoir pressure ( $P_r$ ) and aquifer pressure ( $P_a$ ) before starting a new large time step.

### 3.4.2 Including Expansion of Connate Water and Pore Volume Reduction (Model 2)

By using the definition of compressibility, the change of volume of connate water in the gas cap at reservoir pressure  $P_r$  is given by

$$\Delta V_{cw} = c_w V_{cwi} \Delta P = c_w PV_i S_{cwi} \Delta P = c_w \frac{GB_{gi} S_{cwi}}{1 - S_{cwi}} \Delta P, \quad (3.72)$$

Change of pore volume is given by

$$\Delta PV = c_r PV_i \Delta P = c_r \frac{GB_{gi}}{1 - S_{cwi}} \Delta P. \quad (3.73)$$

Initial hydrocarbon pore volume is given by

$$HCPV_i = B_{gi} G. \quad (3.74)$$

From Equation (3.45) and (3.46),

$$B_g (G - G_p) = HCPV_i - \Delta W - \Delta V_{cw} - \Delta PV. \quad (3.75)$$

Substituting Equation (3.72), (3.73), (3.74) into Equation (3.75), we get

$$B_g (G - G_p) = B_{gi} G - \Delta W - c_w \frac{GB_{gi} S_{cwi}}{1 - S_{cwi}} \Delta P - c_r \frac{GB_{gi}}{1 - S_{cwi}} \Delta P. \quad (3.76)$$

By rearrangement, Equation (3.76) is:

$$(B_g - B_{gi} - \alpha B_{gi} \Delta P) G = B_g G_p - \Delta W, \quad (3.77)$$

where,

$$\alpha = c_w \frac{S_{cwi}}{1 - S_{cwi}} + c_r \frac{1}{1 - S_{cwi}}. \quad (3.78)$$

The left hand side of Equation (3.77) in differential form becomes

$$\begin{aligned} LHS &= (B_g (P_r + dP_r) - B_g (P_r) - \alpha B_g (P_r) dP_r) G \\ &= \left( \frac{B_g (P_r + dP_r) - B_g (P_r)}{dP_r} - \alpha B_g (P_r) \right) G dP_r \\ &= G (B_g' (P_r) - \alpha B_g (P_r)) dP_r. \end{aligned} \quad (3.79)$$

The right hand side of Equation (3.77) can be written:

$$RHS = B_g J_w (m(P_r) - m(P_w)) dt - B_w J_a (P_a - P_r) dt. \quad (3.80)$$

Combining Equation (3.79) and (3.80),

$$G (B_g' (P_r) - \alpha B_g (P_r)) \frac{dP_r}{dt} = B_g J_w (m(P_r) - m(P_w)) - B_w J_a (P_a - P_r). \quad (3.81)$$

Therefore, the reservoir pressure equation becomes

$$\frac{dP_r}{dt} = \frac{1}{G(B_g(P_r) - \alpha B_g(P_r))} (B_g(P_r)J_w(m(P_r) - m(P_w)) - B_wJ_a(P_a - P_r)). \quad (3.82)$$

By substitution of pseudo pressure Equation (3.66), the Equation (3.82) is given by

$$\frac{dP_r}{dt} = \frac{1}{G(B_g(P_r) - \alpha B_g(P_r))} (B_g(P_r)J_w^*(P_r - P_w) - B_wJ_a(P_a - P_r)). \quad (3.83)$$

Equation (3.83) together with Equation (3.61), (3.62), and (3.68) constitute a complete model for the unknowns  $P_a$ ,  $P_r$ ,  $G_p(t)$  and  $W$ .

## Chapter 4 Results and Discussions

This chapter demonstrates two reservoir models, a model with multiple communicating reservoir compartments coupled with wellbore and multiple compartmentalized reservoirs with a common aquifer model. A series of case studies using the first model are investigated to evaluate the flexibility and accuracy of this work. Both models are simulated to examine the time consumption with the number of compartments. A horizontal production well is draining the reservoir for all of the cases. The first model demonstrates a simple reservoir system coupled with an open well in the center and without aquifer support. This model is controlled by a constant bottom hole pressure, then uses a minimum flow rate for control. The Matlab simulation results from this model are compared to those generated by a standard reservoir simulation launcher (Eclipse™). The second model presents a more complicated case involving communicating and non-communicating compartments with a common bottom aquifer. This model is controlled by a target initial rate, and then also uses a minimum flow rate for control.

### 4.1 Multiple Communicating Reservoir Compartments Coupled with Wellbore

In this section, we describe a horizontal production well draining multiple communicating reservoir compartments (RCs). The physical model is illustrated in the Figure 4.1. The model results are not compared with the real data since the real data is not available.

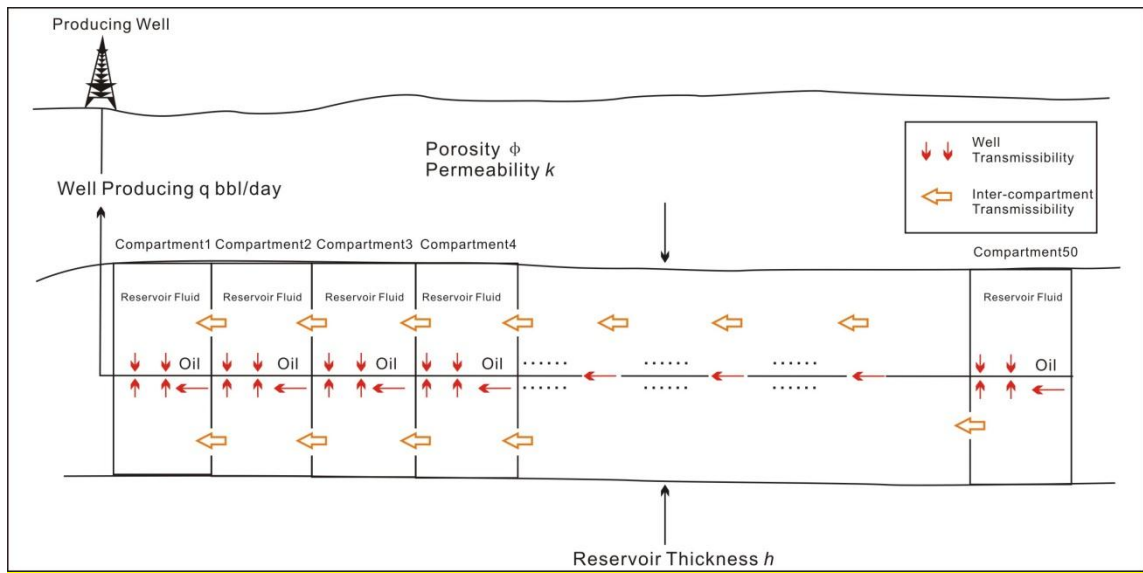


**Figure 4.1: Schematic of Multiple Compartmentalized Reservoir Model**

The model consists of 50 communicating inflow compartments penetrated by a 2000 m long horizontal well of diameter 21.9 cm. This well is producing oil of viscosity of 2 cp from a box shaped oil reservoir. The reservoir is 2000 m x 100 m x 100 m. Datum depth is located at 970 meter. The oil density, in stock tank condition, is  $973 \text{ kg/m}^3$ . The average reservoir pressure is 25,000 kPa, and the bottom hole pressure is 10,000 kPa and is kept constant. The horizontal and vertical permeability of the formation is 10 mD. The porosity of the formation is 0.20. **The time interval needs to be selected based on the model stability and efficiency.**

The data used to build the base model is presented in the following tables, reservoir properties (Table 4.1), wellbore properties (Table 4.2), fluid properties (Table 4.3), and control conditions (Table 4.4).

**Table 4.1: Reservoir Properties**

Variables	Units	Values
Initial Pressure	kPa	25,000
Reservoir Length	m	2,000
Reservoir Width	m	100
Reservoir Height	m	100
Datum	m	970
Connate Water Saturation		25%
Water Compressibility	/kPa	$4 \times 10^{-7}$
Oil Compressibility	/kPa	$40 \times 10^{-7}$
Rock Compressibility	/kPa	$12 \times 10^{-7}$
Total Compressibility	/kPa	$43 \times 10^{-7}$
Horizontal Permeability	mD	10
Vertical Permeability	mD	10

**Table 4.2: Wellbore Properties**

Variables	Units	Values
Initial Pressure	kPa	10,000
Transmissibility	$\text{Sm}^3/(\text{kPa}\cdot\text{day})$	Joshi Formula
Wellbore Diameter	m	0.219
Wellbore Roughness	m	$4.6 \times 10^{-5}$
Wellbore Length	m	2000
Depth	m	1020

**Table 4.3: Fluid Properties**

Variables	Units	Value (Constant)
Water Formation Volume Factor	$\text{Rm}^3/\text{Sm}^3$	1.0
Oil Formation Volume Factor	$\text{Rm}^3/\text{Sm}^3$	1.0
Fluid Viscosity	Pa.s	$0.5 \times 10^{-3}$
Fluid Density	$\text{kg}/\text{m}^3$	973

**Table 4.4: Control Conditions**

Variables	Units	Value
Constant BHP	kPa	10,000
Minimum Rate	$\text{Sm}^3/\text{d}$	100
Max Time Step	days	10
Max Pressure Drop per Step	kPa	50
Minimum Time Step	days	0.5

The changing variables simulated in four different cases are presented in Table 4.5.

**Table 4.5: Summary of Changing Parameters in Sensitivity Analysis**

<b>Sensitivity Analysis</b>	<b>Case 1 (Base Case)</b>	<b>Case 2 (friction ignored)</b>	<b>Case 3 (increased FVF)</b>	<b>Case 4 (increased viscosity)</b>
Friction factor considered	Yes	No	Yes	Yes
Oil FVF	1	1	1.2	1
Viscosity (cP)	2	2	2	5

#### **4.1.1 Numerical Simulation and Analysis**

In this section, the base case (case 1) is developed for a model with fifty communicating compartmentalized reservoirs. The fifty reservoir compartments are identical and penetrated with the horizontal pipeline. The dimensions for each compartment are 40 m x 100 m x 100m. Cases 2, 3, and 4 are also simulated in Matlab model with the changing parameters in Table 4.5. Case 1 is the base case with Case 2 eliminates the effect of friction factor in the pipeline flow to illustrate how the friction loss affects the flow. Case 3 and 4 make oil formation volume factor and oil viscosity higher, respectively, in order to find out how they influence the flow and pressure behavior. All the first four cases are simulated in both Matlab and Eclipse<sup>TM</sup> software and compared for sensitivity analysis and validation purpose.

The well casing is fully perforated within the compartments. The well transmissibility is calculated by using the Joshi model (1998, Equation (3.6) in Section 3.2), and the inter-transmissibility is calculated using Equation (3.36) in the Matlab simulation. The aquifer transmissibility is not applicable as no aquifer support. The initial average reservoir pressure, aquifer pressure, and wellbore pressure for all compartments are in

equilibrium. The numerical solutions and simulation results will be presented graphically and discussed from a physical point of view in the following sub-sections.

Results include average reservoir pressure distribution (Figure 4.2a), cumulative oil production profile (Figure 4.2b), oil flow rate profile (Figure 4.2c), and oil flow rate profile between two compartments (Figure 4.2d).

As can be seen from the figures, when the friction in the pipe is ignored (case 2), we see a reduced reservoir pressure, increased oil production/increased oil flow rate. However, cumulative oil production at the end of production (100 days) is almost equivalent, which means, in this particular case, the friction loss in the pipe does not significantly affect the total oil production very much.

Oil formation volume factor is increased in Case 3(from 1.0 to 1.2), hence, the oil production in standard condition is decreased when the reservoir condition remains the same; therefore, the last point in Case 3 is below the last point in Case 1.

In Case 4, wherein the oil viscosity is increased (from 2cP to 5 cP), we observe an increased reservoir pressure (compared to the base case), a decrease in cumulative oil production in the early stages, and a decreased, but longer-lived, oil flow rate.

The production behaviors simulated in Matlab are physically as expected. This helps provide confidence for both models.

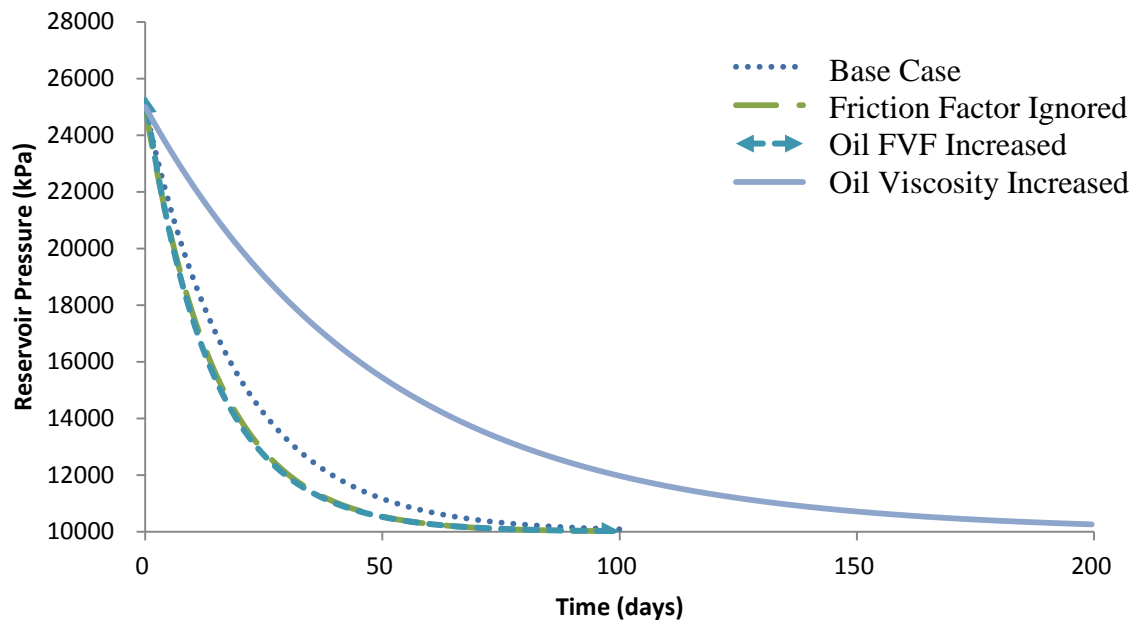


**Figure 4.2a: Reservoir Pressure (50 Communicating Compartments)**

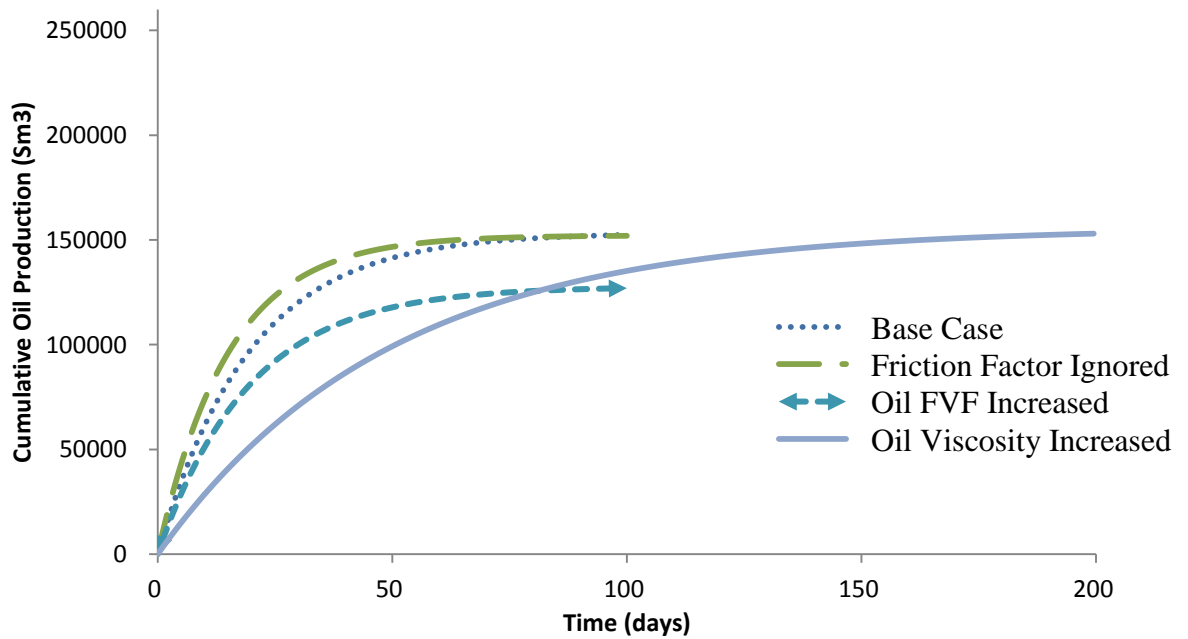


**Figure 4.2b: Cumulative Oil Production (50 Communicating Compartments)**

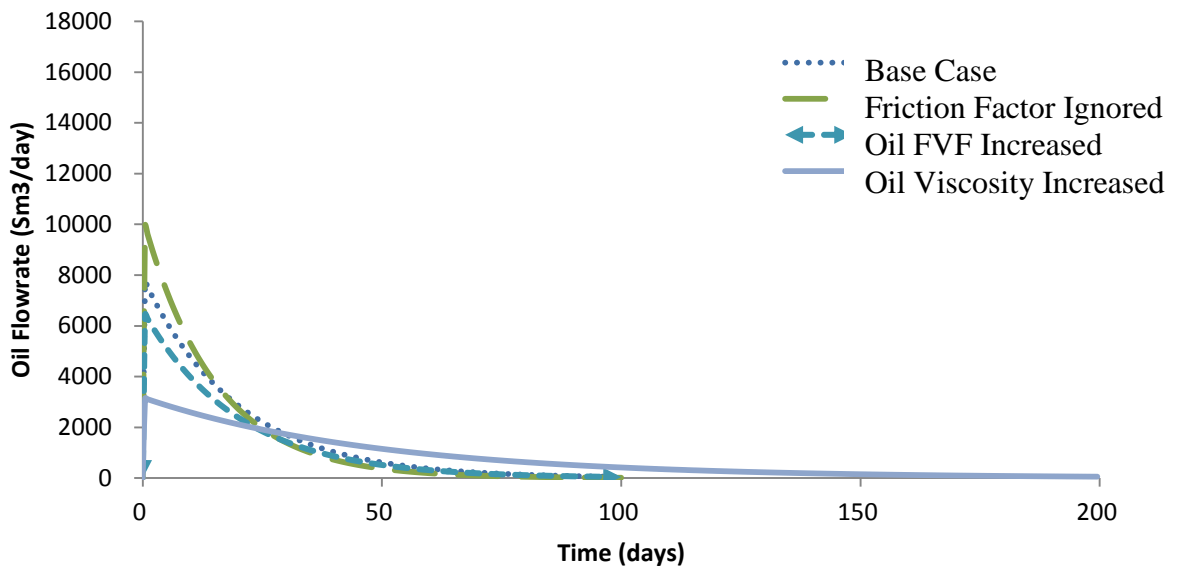


**Figure 4.2c: Oil Flowrate (50 Communicating Compartments)**

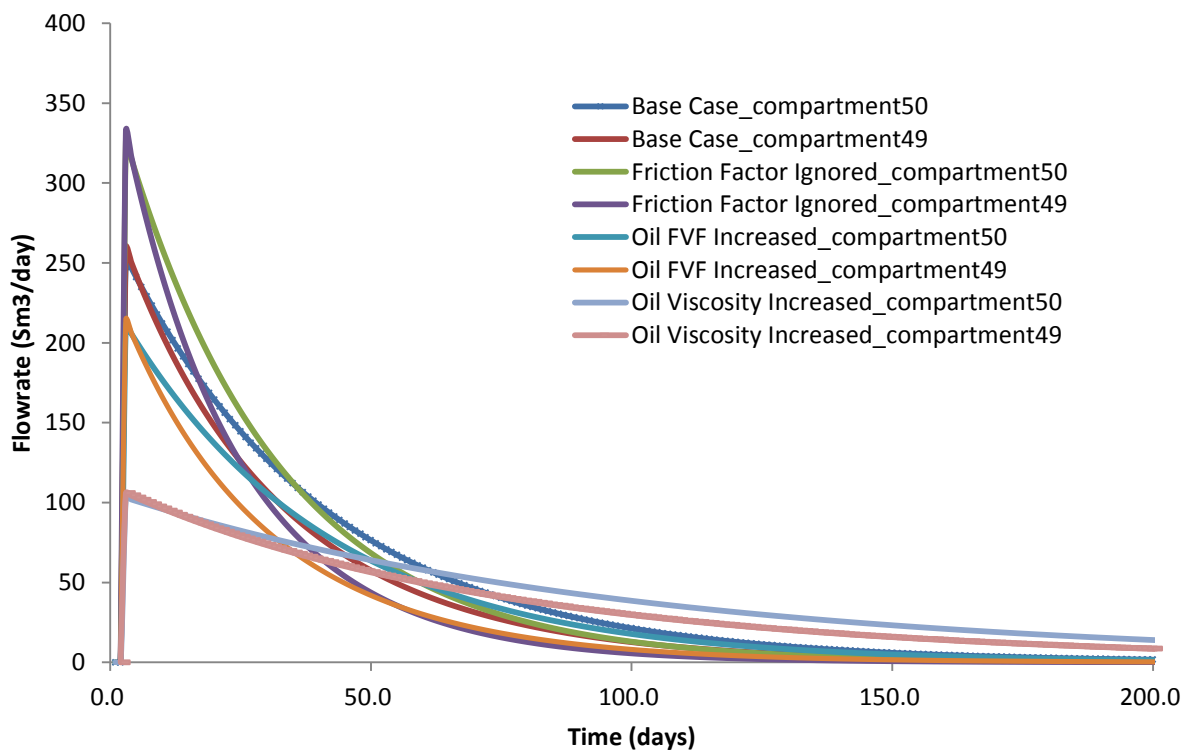


**Figure 4.2d: Oil Flowrate between Compartments**

In an effort to evaluate the performance of the compartmentalized model implemented in Matlab, the same physical model was simulated using a standard reservoir simulation software launcher, Eclipse<sup>TM</sup> and the results of the two were compared. Figure 4.3a-4.3c show the results of reservoir pressure distribution, cumulative oil production profile, and oil flow rate profile from both the Matlab and Eclipse<sup>TM</sup> models for Case 1. Both models showed similar overall trends, albeit with slightly different results. Some of the discrepancy in cumulative oil production between the two methods can be attributed to the different numerical methods. The Eclipse<sup>TM</sup> models are using finite difference method which only offers a low order time discretization in solving governing equations. The pressure solutions in the Eclipse<sup>TM</sup> models are picked up at two ends within one time step. However, the compartmentalized reservoir model is using Runge-Kutta 4<sup>th</sup> order numerical method to solve the governing equations, which allows for an average pressure solution at each time step. Therefore, the results of reservoir pressure distribution, cumulative oil production profile, and oil flow rate profile from both the Matlab and Eclipse<sup>TM</sup> models are presenting a small discrepancy. A comparison was made using each case study with similar results. (All comparison graphs are provided in Appendix D)

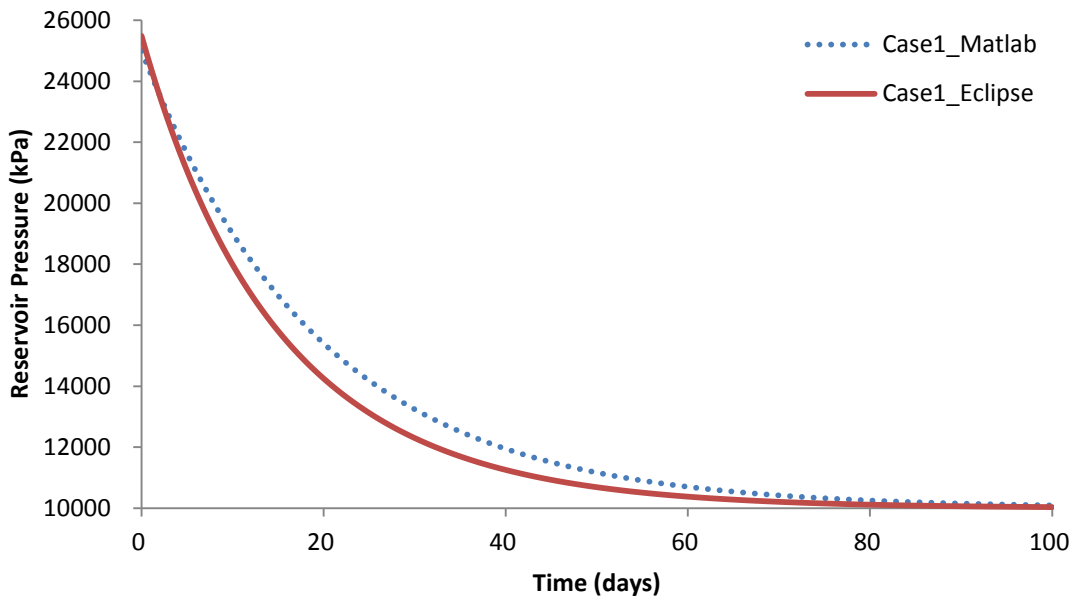


**Figure 4.3a: Reservoir Pressure (50 Communicating Compartments)**

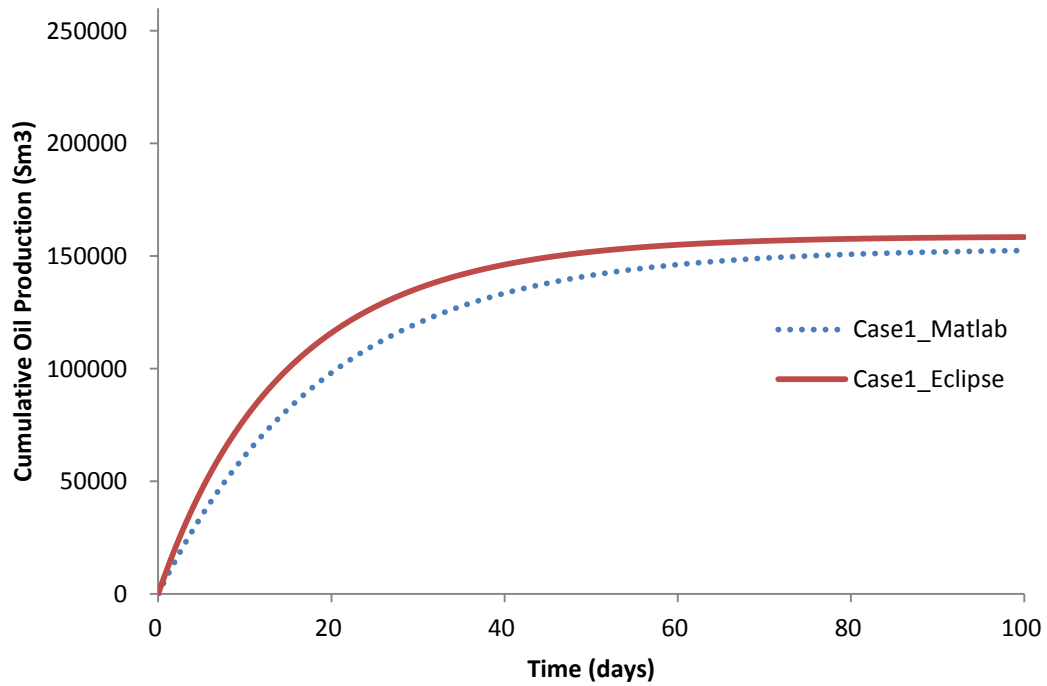


**Figure 4.3b: Cumulative Oil Production (50 Communicating Compartments)**

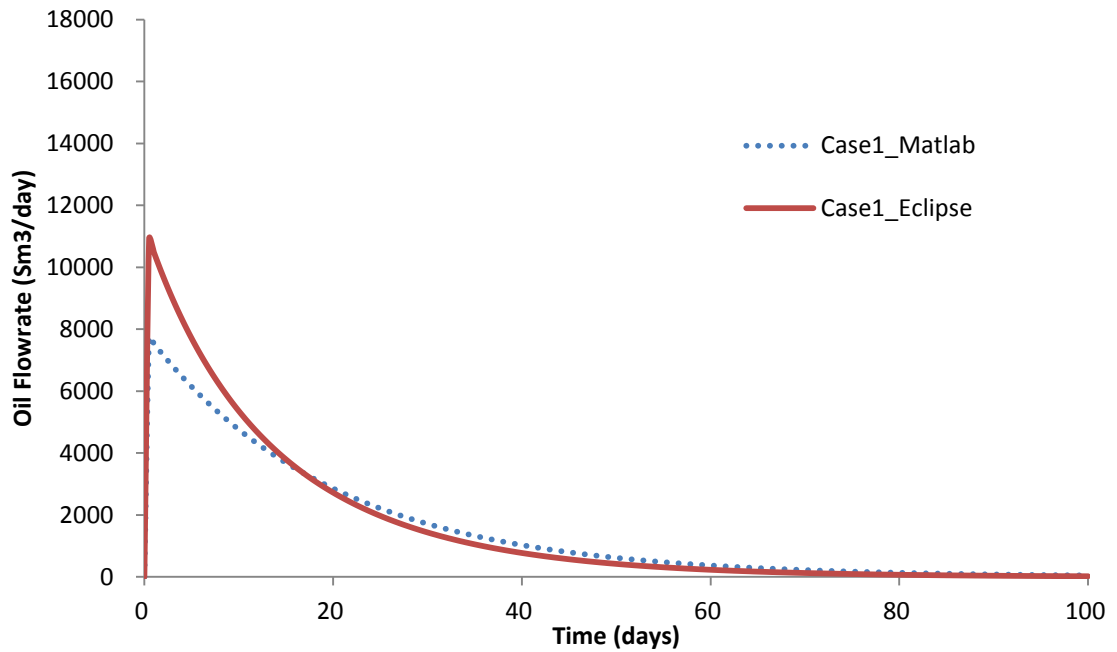


**Figure 4.3c: Oil Flowrate (50 Communicating Compartments)**

At this point we have two representations of a system, but it remains to be seen which is the more accurate. Generally speaking, a more refined grid Eclipse<sup>TM</sup> model is anticipated to be more accurate than a coarse-grid model. For this reason, a refinement of the Eclipse<sup>TM</sup> model was completed by increasing the grid block numbers to 100 x 100 x 10 (Case 5). Therefore, in this case, the dimensions for each compartment in the Eclipse<sup>TM</sup> model are changed to 20 meter long by 1 meter wide by 10 meter high, while, the number of compartment in the Matlab model remains same. The results of this refined model for the base case are shown in Fig. 4.4. As can be seen from the figure, the more refined Eclipse<sup>TM</sup> model is approaching the new model implemented in Matlab. This lends credence to the new model.

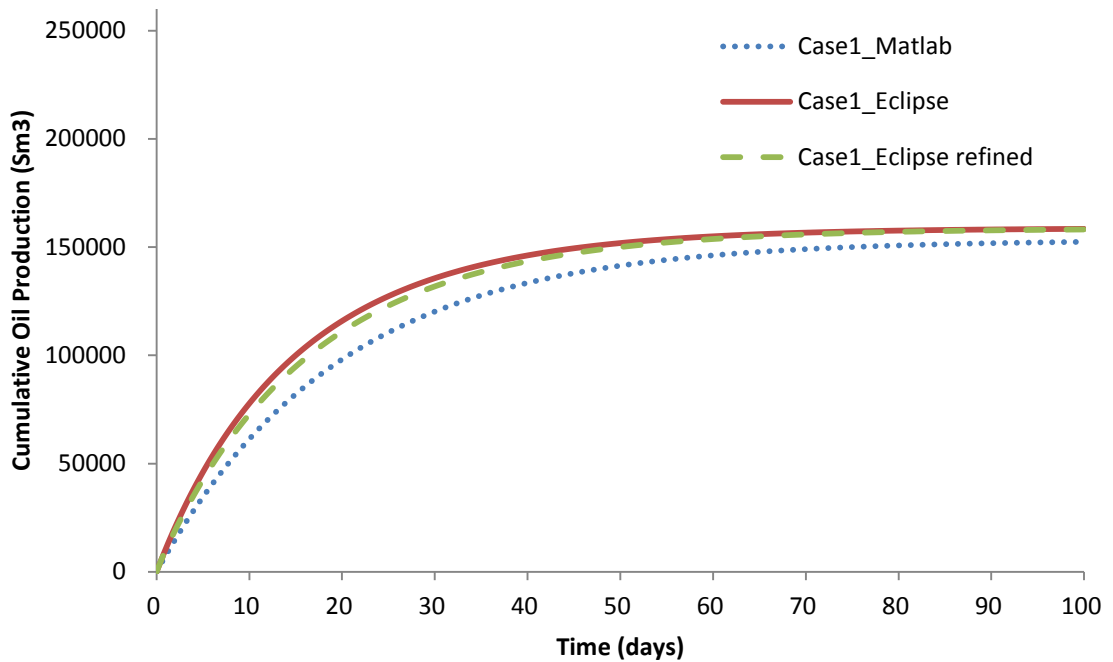


**Figure 4.4: Refined Eclipse (50 Communicating Compartments)**

#### 4.1.2 CPU Time Consumption

The model speed (CPU time) is another important factor in reservoir simulation; therefore, the CPU time consumption for each individual case in both Eclipse and Matlab simulation model were determined and recorded in Table 4.6.

**Table 4.6: CPU Time Consumption for Matlab and Eclipse Model**

Case Study	Changing Variables	CPU Time-Compartmentalized Model - Matlab(s)	CPU Time-Commercial Reservoir Simulator - Eclipse (s)
Case 1	No changes	178	573
Case 2	Friction Factor	176	572
Case 3	Oil FVF	182	580
Case 4	Viscosity	173	577
Refined Case	Grid block number	-	678

The CPU time consumption in the refined case is much higher than the first four cases due to the number of compartment increased. In addition, the Eclipse simulation models

consume almost four hundred extra seconds as compared to the Matlab simulation models in all cases. For the sake of simplicity and limiting the scope to this model, the variable fluid properties (e.g. density and viscosity) and compressibility for rock, water and oil in the oil reservoir model are ignored; multiphase flow in the pipeline is also out of consideration. If these assumptions are not made, more parameters are required and more correlations are coupled in this model, therefore, the CPU time consumption will be much higher than the simplified case with a more accurate result. And these are also the technical challenges with the modeling methodology due to the complexity of the model.

## **4.2 Multiple Compartmentalized Reservoirs with a Common Aquifer**

In this section, we model a horizontal production well penetrating multiple reservoir compartments supported by a common aquifer. The physical model is illustrated in the Figure 4.5 and Figure 4.6 for non-communicating and communicating compartments, respectively. The non-communicating reservoir compartment model (Figure 4.5) consists of 50 compartments with commingled production and 49 blank pipe compartments. The compartments are supported by a bottom aquifer. The communicating reservoir compartment model (Figure 4.6) consists of 50 communicating compartments supported by a bottom aquifer compartment.

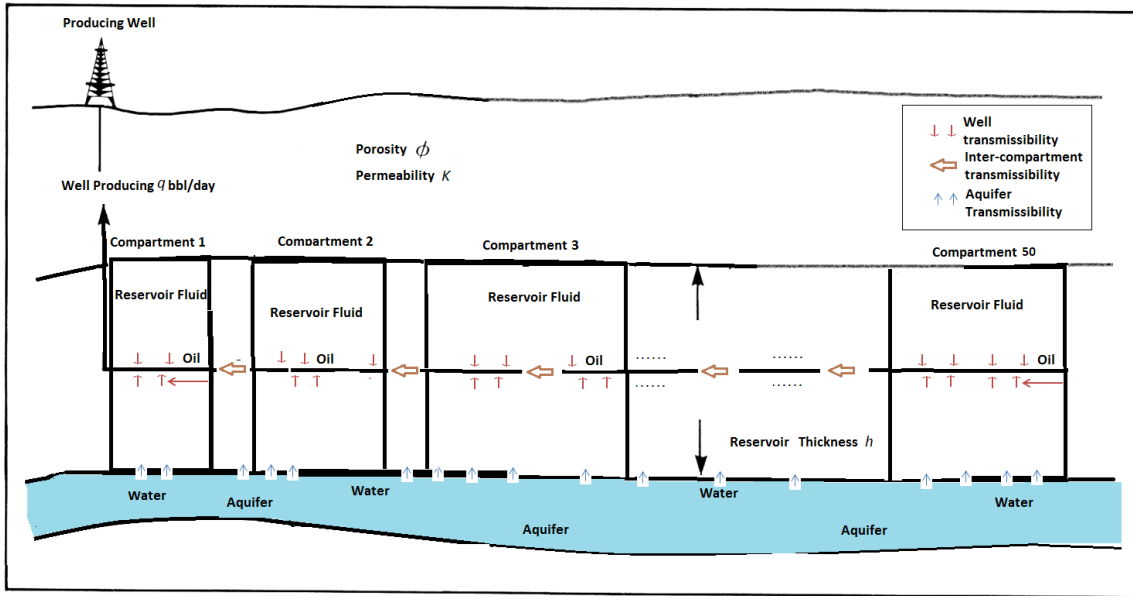


**Figure 4.5: Schematic of Multiple Non-Communicating Compartmentalized Reservoir Model**

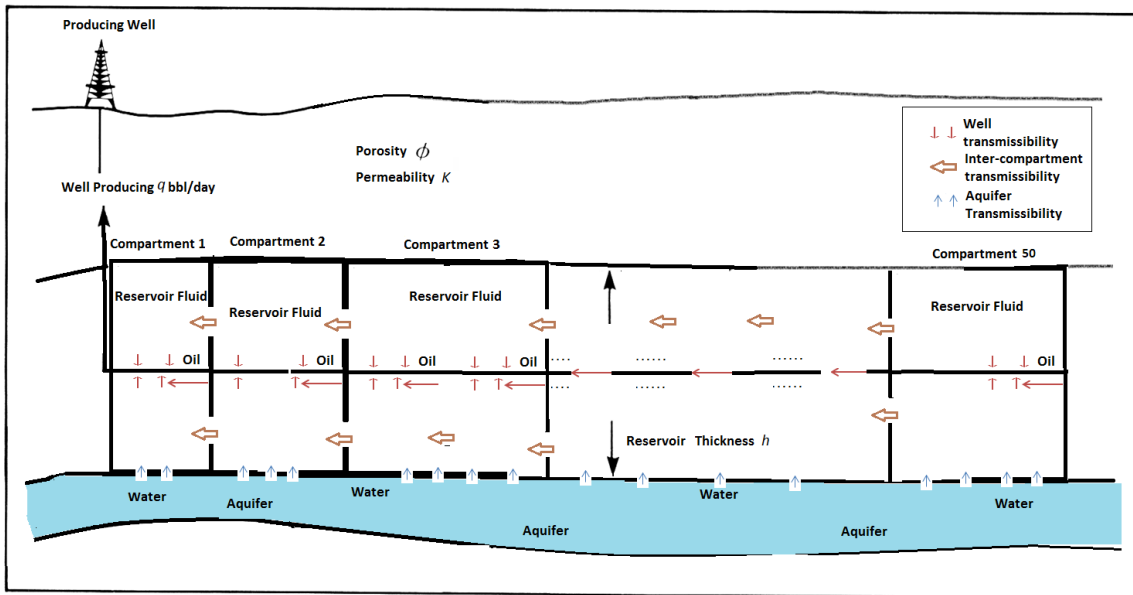


**Figure 4.6: Schematic of Multiple Communicating Compartmentalized Reservoir Model**

The reservoir is 2000 m x 100 m x 100 m, which is divided into 50 compartments with different sizes as shown in Table 4.7. The horizontal wellbore length is 2km and it is

located in the center of the reservoir. The oil density is  $973 \text{ kg/m}^3$ . The average reservoir pressure is 25,000 kPa, and the initial aquifer pressure is also 25,000kPa. The reservoir properties, wellbore properties, fluid properties, and aquifer properties are presented in Table 4.7 to 4.12.

**Table 4.7: Reservoir Properties**

Variables	Units	Values
Initial Pressure	kPa	25,000
Reservoir Length	m	2,000
Reservoir Width	m	100
Reservoir Height	m	100
Datum	m	970
Initial Fluid Saturation		100%
Connate Water Saturation		25%
Water Compressibility	/kPa	$4 \times 10^{-7}$
Oil Compressibility	/kPa	$40 \times 10^{-7}$
Rock Compressibility	/kPa	$12 \times 10^{-7}$
Total Compressibility	/kPa	$43 \times 10^{-7}$
Horizontal Permeability	mD	10
Vertical Permeability	mD	10

**Table 4.8: Compartment Lengths for Multiple Compartmentalized Reservoir with Common Aquifer (from Bottom Hole to Toe)**

RC #	RC Length (m)	RC#	RC Length (m)	RC #	RC Length (m)	RC #	RC Length (m)	RC #	RC Length (m)
1	20	11	20	21	20	31	20	41	20
2	30	12	30	22	30	32	30	42	30
3	40	13	40	23	40	33	40	43	40
4	40	14	40	24	40	34	40	44	40
5	50	15	50	25	50	35	50	45	50
6	40	16	40	26	40	36	40	46	40
7	50	17	50	27	50	37	50	47	50
8	40	18	40	28	40	38	40	48	40
9	50	19	50	29	50	39	50	49	50
10	40	20	40	30	40	40	40	50	40

**Table 4.9: Wellbore Properties Multiple Compartmentalized Reservoir with Common Aquifer**

Variables	Units	Values
-----------	-------	--------

Wellbore Diameter		m		0.219	
Wellbore Roughness				0.046E-3	
Depth				1020	
RC#	Non-Communicating		Communicating		
	Well Length in RC (m)	Blank Pipe Length (m)	Well Length in RC (m)	Blank Pipe Length (m)	
1	20	4	20	0	
2	28	4	30	0	
3	38	2	40	0	
4	36	4	40	0	
5	40	3	50	0	
6	38	4	40	0	
7	44	4	50	0	
8	38	2	40	0	
9	46	4	50	0	
10	38	3	40	0	
11	20	4	20	0	
12	28	4	30	0	
13	38	2	40	0	
14	36	4	40	0	
15	40	3	50	0	
16	38	4	40	0	
17	44	4	50	0	
18	38	2	40	0	
19	46	4	50	0	
20	38	3	40	0	
21	20	4	20	0	
22	28	4	30	0	
23	38	2	40	0	
24	36	4	40	0	
25	40	3	50	0	
26	38	4	40	0	
27	44	4	50	0	
28	38	2	40	0	
29	46	4	50	0	
30	38	3	40	0	
31	20	4	20	0	
32	28	4	30	0	
33	38	2	40	0	
34	36	4	40	0	
RC#	Non-Communicating		Communicating		
	Well Length in RC (m)	Blank Pipe Length (m)	Well Length in RC (m)	Blank Pipe Length (m)	
35	40	3	50	0	

36	38	4	40	0
37	44	4	50	0
38	38	2	40	0
39	46	4	50	0
40	38	3	40	0
41	20	4	20	0
42	28	4	30	0
43	38	2	40	0
44	36	4	40	0
45	40	3	50	0
46	38	4	40	0
47	44	4	50	0
48	38	2	40	0
49	46	4	50	0
50	38	3	40	0

**Table 4.10: Fluid Properties**

Variables	Units	Value
Water Formation Volume Factor	Rm <sup>3</sup> / Sm <sup>3</sup>	1.0
Oil Formation Volume Factor	Rm <sup>3</sup> / Sm <sup>3</sup>	1.0
Fluid Viscosity	Pa.s	0.5×10 <sup>-3</sup>
Fluid Density	kg/m <sup>3</sup>	973

**Table 4.11: Aquifer Properties**

Variables	Units	Value
Initial Pressure	kPa	25,000
Aquifer Size	Rm <sup>3</sup>	4.0×10 <sup>7</sup>
Aquifer Compressibility	/kPa	1.60×10 <sup>-6</sup>
Transmissibility	(Sm <sup>3</sup> /(kPa-day))	0.2

**Table 4.12: Control Conditions**

Variables	Units	Value
Minimum THP	kPa	4,200
Minimum Rate	m <sup>3</sup> /d	100
Target Rate	m <sup>3</sup> /d	5,000
Max Time Step	days	10
Max Pressure Drop per Step	kPa	50
Minimum Time Step	days	0.5

The data corresponding to this reservoir and aquifer was used in the Matlab program to generate prediction results. The assumptions made for this model are the same as those described in Section 4.1.1.

### **4.2.1 Numerical Simulation and Analysis**

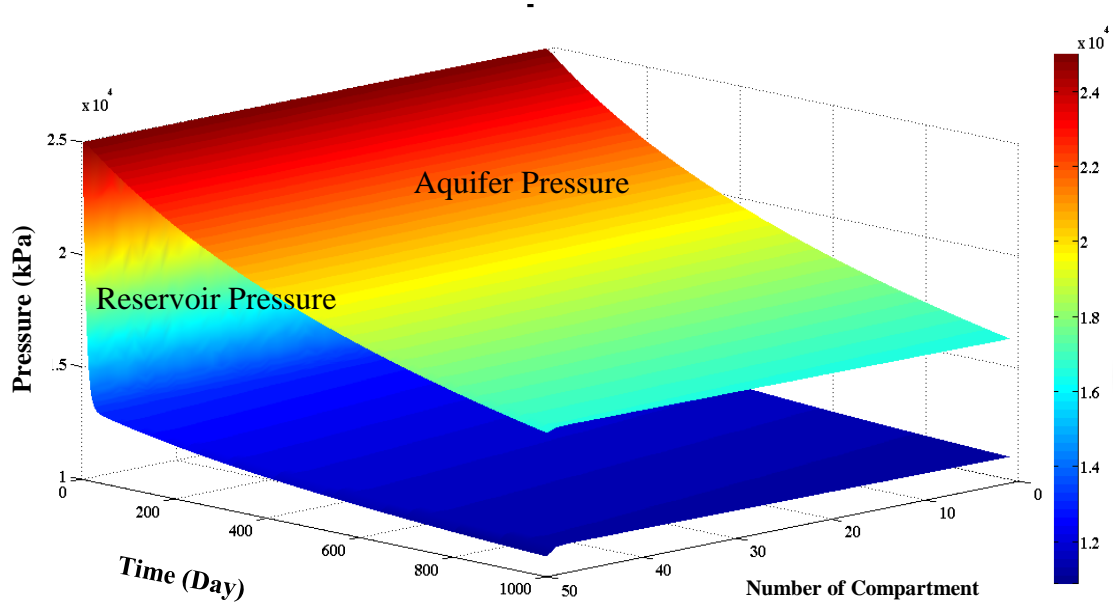
The important observation from this model is the change in reservoir pressure, aquifer pressure, and wellbore production from the communicating and non-communicating reservoir compartments models.

Figure 4.7a shows the pressure profile of 50 communicating compartments with one common aquifer support system during 900 days of production. Figure 4.7b depicts the pressure profile of both 50 communicating compartments and 50 non-communicating compartments during 900 production days. One important observation relates to the pressure decline. It is clear from Figure 4.7a and 4.7b that aquifer pressure declines with the reservoir pressure and the communicating reservoir compartments results in greater reservoir pressure declines as demonstrated by looking at the 50 reservoir compartments.

Figure 4.8a shows the cumulative oil production from both models during the production time of 900 days. As the perforated well lengths are different for both communicating and non-communicating cases, the cumulative oil production from the simulation results shows different. The behaviour indicates that the communicating reservoir compartment model produces roughly extra 20% of oil compared to the non-communicating model. The final recovery factor is around 29% for the communicating compartment reservoir model, while, for the non-communicating compartment reservoir model, the recovery factor is around 23%. When evaluating development strategies, this model could be used to evaluate the benefit of achieving an extended production profile versus the cost of additional well length and perforations. Figure 4.8b presents cumulative oil production at reservoir compartment 1 and 50 in communicating compartment case. As shown in this

figure, the friction loss through the wellbore and the inflow performance result in the difference between two curves.

Figure 4.9 shows that the oil production flow rate of both non-communicating and communicating compartments during the production time of 900 days. The liquid target of  $5000 \text{ m}^3$ , as illustrated in this figure, is achieved for about 20 days. This is a short period as the pressure depletes in the reservoir compartments. The flow rate after 20 days drops dramatically in the first 200 days.



**Figure 4.7 a: Pressure Distribution, Multiple Non-Communicating and Communicating Compartmentalized Reservoir Model**

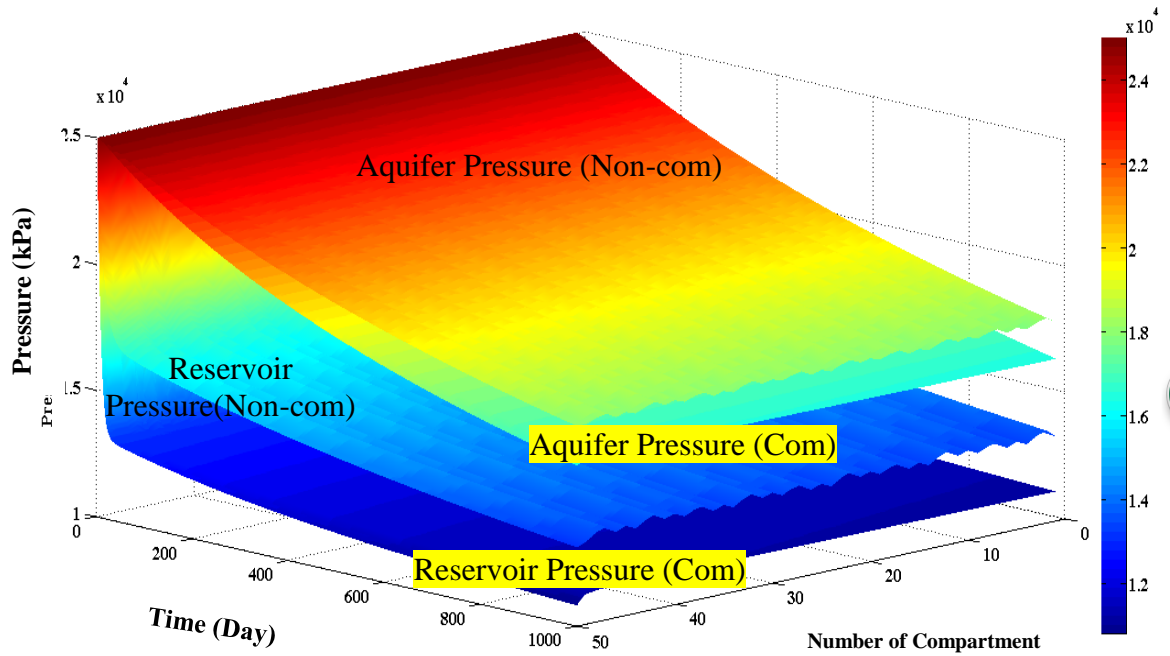


**Figure 4.7 b: Pressure Distribution, Multiple Non-Communicating and Communicating Compartmentalized Reservoir Model**

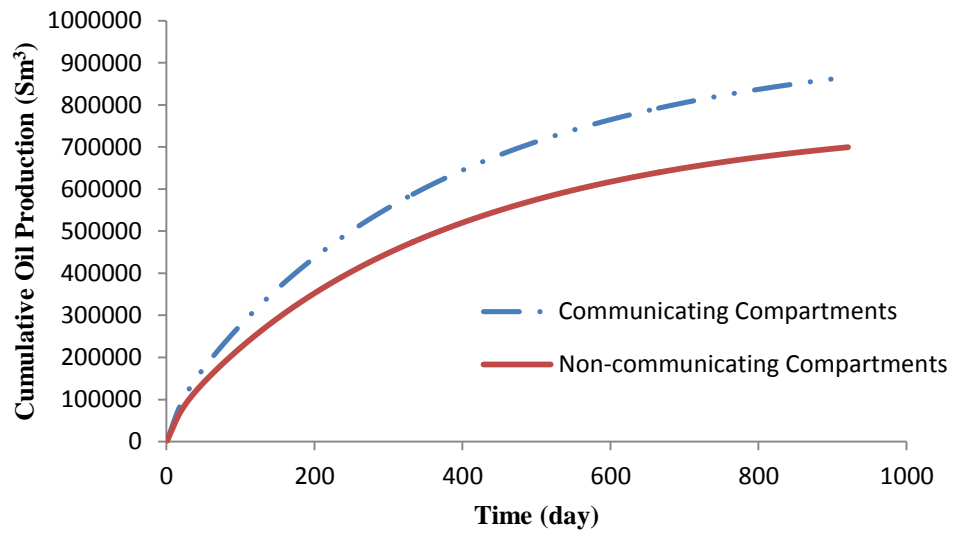


**Figure 4.8 a: Cumulative Oil Production, Multiple Non-Communicating and Communicating Compartmentalized Reservoir Model**

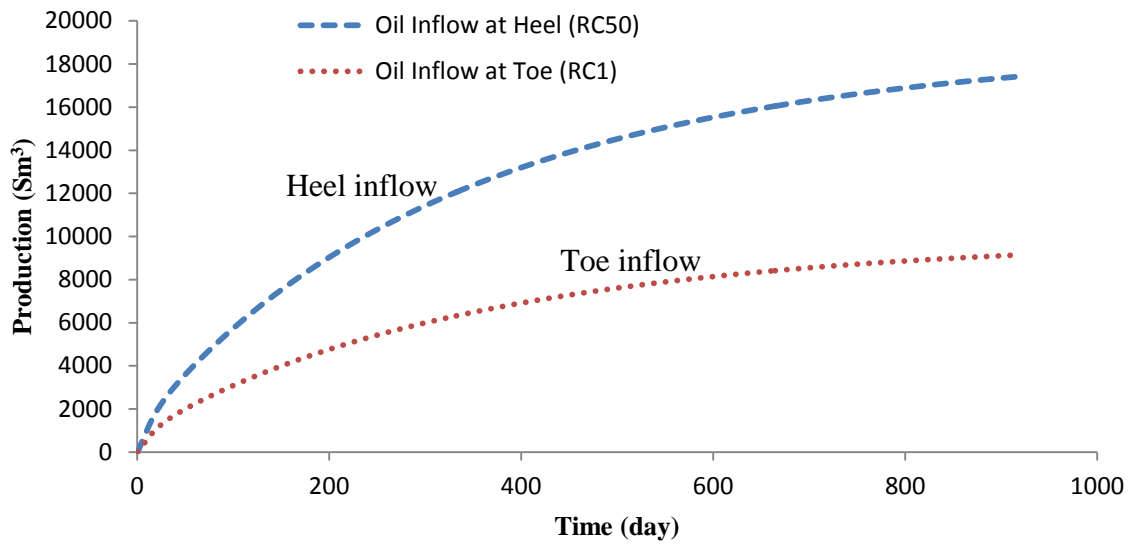


**Figure 4.8 b: Cumulative Oil Production at RC1 and RC50, Multiple Communicating Compartmentalized Reservoir Model**

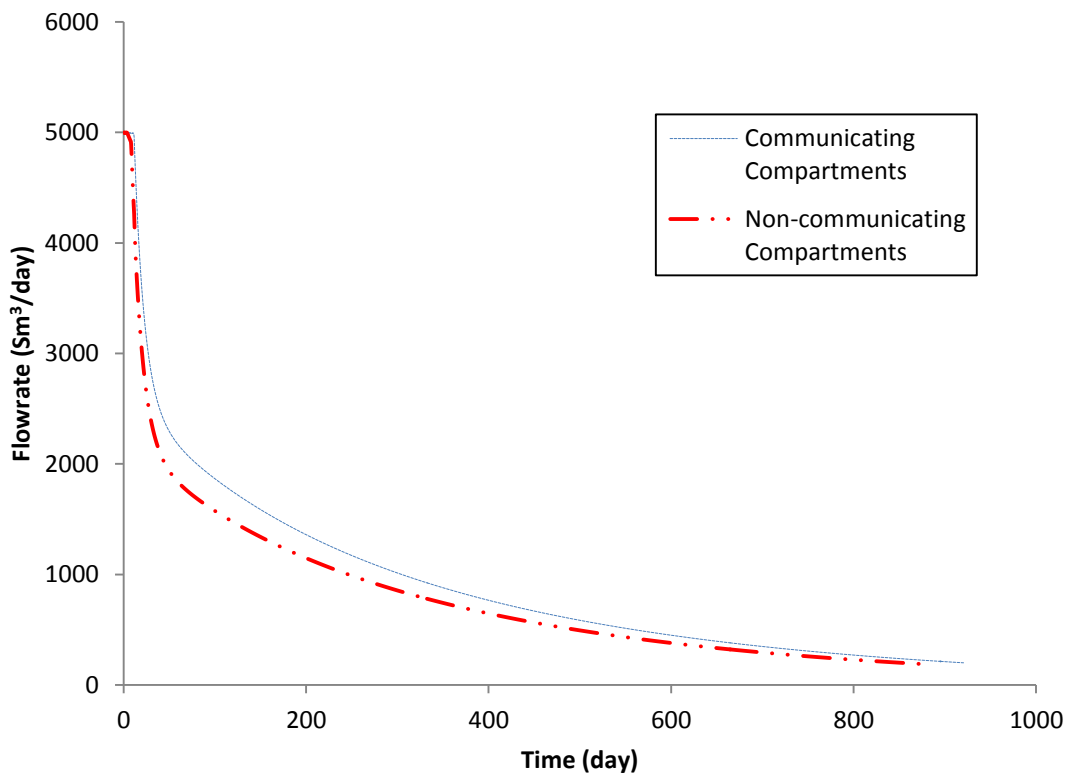


**Figure 4.9: Oil Production Flow Rate, Multiple Non-Communicating and Communicating Compartmentalized Reservoir Model**

### 4.2.2 CPU Time Consumption

The CPU time consumptions respective for both multiple communicating and non-communicating reservoir models are recorded in Table 4.13.

The CPU time increased with an increasing number of compartments due to complexity of system. In order to understand the relationship between the CPU time consumption and the number of compartments, we plot Figure 4.10 by adding the data from both non-communicating and communicating cases. As shown in Figure 4.10, the CPU time consumption increases with the number of compartments, and the trend lines for both multiple communicating compartments and non-communicating compartments are estimated as the quadratic function, which gives a fair result for increasing compartment numbers.

**Table 4.13: Time Consumption for Communicating and Non-communicating Cases**

<b>Number of Compartments</b>	<b>Time Consumption of Communicating Case (s)</b>	<b>Time Consumption of Non-communicating Case (s)</b>
5	199	579
20	204	583
50	211	590
100	228	607
200	282	652
300	352	719
400	445	809
500	564	923

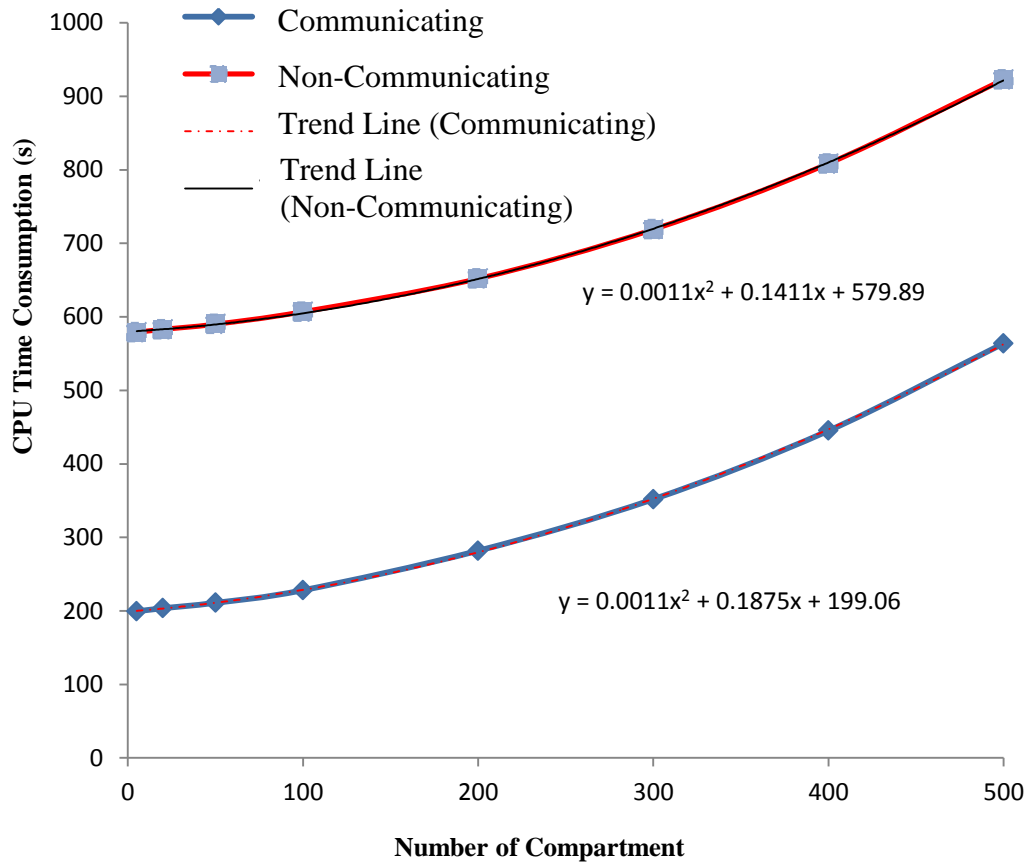


**Figure 4.10: CPU Time Consumptions, Multiple Non-Communicating and Communicating Compartmentalized Reservoir Model**

### 4.3 Dry Gas Reservoir with Aquifer Support Modeling

In this section we build two models developed for a single compartment gas reservoir with an adjacent aquifer in communication with the reservoir. The parameters are presented in Table 4.14. The conditions used to generate the numerical simulations are from the book “Multiphase Flow in Wells” by James P. Brill and Hemanta Mukherjee (1999).

### 4.3.1 Case Studies Descriptions

A small gas reservoir contains  $1.08 \times 10^9 \text{ Sm}^3$  of dry gas. The initial reservoir pressure is 21000 kPa and the reservoir temperature is  $97^\circ \text{C}$ . Beggs and Brill Correlations for the Z-factor are used. The reservoir is supported by an aquifer. The initial size of the aquifer in reservoir conditions is estimated as  $9.0 \times 10^6 \text{ m}^3$ . The initial connate water saturation is 25%. As the stability of the numerical methods can directly affect the accuracy of the numerical solutions, the selection of an appropriate time step for the reservoir simulation becomes a key factor. In the current two models, the time steps are 0.01 days. All values are outlined in Table 4.14.

**Table 4.14 Input Data**

Parameters	Model 1 (Incompressible)	Model 2 (Compressible)
Reservoir Temperature ( $T_r$ )	370 K	
Temperature at Standard Condition ( $T_0$ )	288 K	
Bottom Hole Pressure ( $P_w$ )	15000 kPa	
Pressure at Standard Condition ( $P_0$ )	101 kPa	
Initial Reservoir Pressure ( $P_{ri}$ )	21000 kPa	
Abandonment Reservoir Pressure ( $P_{ra}$ )	16000 kPa	
Initial Aquifer Pressure ( $P_{ai}$ )	21000 kPa	
Water Formation Volume Factor ( $B_w$ )	$1.0 \text{ Rm}^3/\text{Sm}^3$	
Aquifer Compressibility ( $c_a$ )	$1.6 \times 10^{-6} \text{ kPa}^{-1}$	
Rock Compressibility ( $c_r$ )	N/A	$1.2 \times 10^{-6} \text{ kPa}^{-1}$
Water Compressibility ( $c_w$ )	N/A	$0.4 \times 10^{-6} \text{ kPa}^{-1}$
Well Transmissibility ( $J_{wi}$ )	$40 \text{ Sm}^3/(\text{kPa}\cdot\text{day})$	
Aquifer Transmissibility ( $J_a$ )	$30 \text{ Sm}^3/(\text{kPa}\cdot\text{day})$	
Stock Tank Gas Initially in Place ( $G$ )	$1.08 \times 10^9 \text{ Sm}^3$	
Initial Aquifer Size ( $W_i$ )	$9.0 \times 10^6 \text{ Rm}^3$	
Connate Water Saturation ( $S_{cwi}$ )	N/A	0.25
Time Step ( $dt$ )	0.01 day	

- 1) In the Model I, pore volume reduction and connate water expansion are ignored during the reservoir pressure depletion, only water encroachment is considered.
- 2) In the Model II, the volumetric quantities are considered including water influx from the aquifer, reduction of the pore volume and expansion of connate water in the gas zone.

### 4.3.2 Numerical Simulation and Analysis

This section compares the results from Model 1 and Model 2. The numerical solutions will be presented graphically and discussed from a physical point of view.

As shown in the Table 4.15 below, the total gas production in the second model is larger than the first model due to the contributions of the pore volume reduction and the connate water expansion. The water encroachment in the two models is identical, which means the water influx from the aquifer will not be affected by the assumption of ignoring the pore volume and connate water change. The simplified model requires a shorter simulation time.

**Table 4.15: Results Comparison between Two Models**

Simulation Results	Model 1	Model 2
Gas Production ( $\text{Sm}^3$ )	$3.05 \times 10^8$	$3.14 \times 10^8$
Water Encroachment ( $\text{Rm}^3$ )	$9.071 \times 10^6$	$9.072 \times 10^6$
Recovery Factor	28%	29%
CPU time (s)	1.4	1.5

From the Figure 4.11, the reservoir pressure and aquifer pressure in both models drop to the abandonment pressure (16000 kPa). The simulated aquifer pressure is always larger than reservoir pressure, as it should be. Due to the contribution of the swelling connate water and the reduced pore volume, the pressure in the second model decreases with a slower rate

compared to the first model and it yields a longer production. The gas production profile is presented in the Figure 4.12. Clearly, the connate water and pore volume change make a positive contribution to the gas recovery. From a physical point of view, the initial aquifer size and the aquifer transmissibility are identical in the two models, which suggests an equal water encroachment that is matched in Figure 4.12.

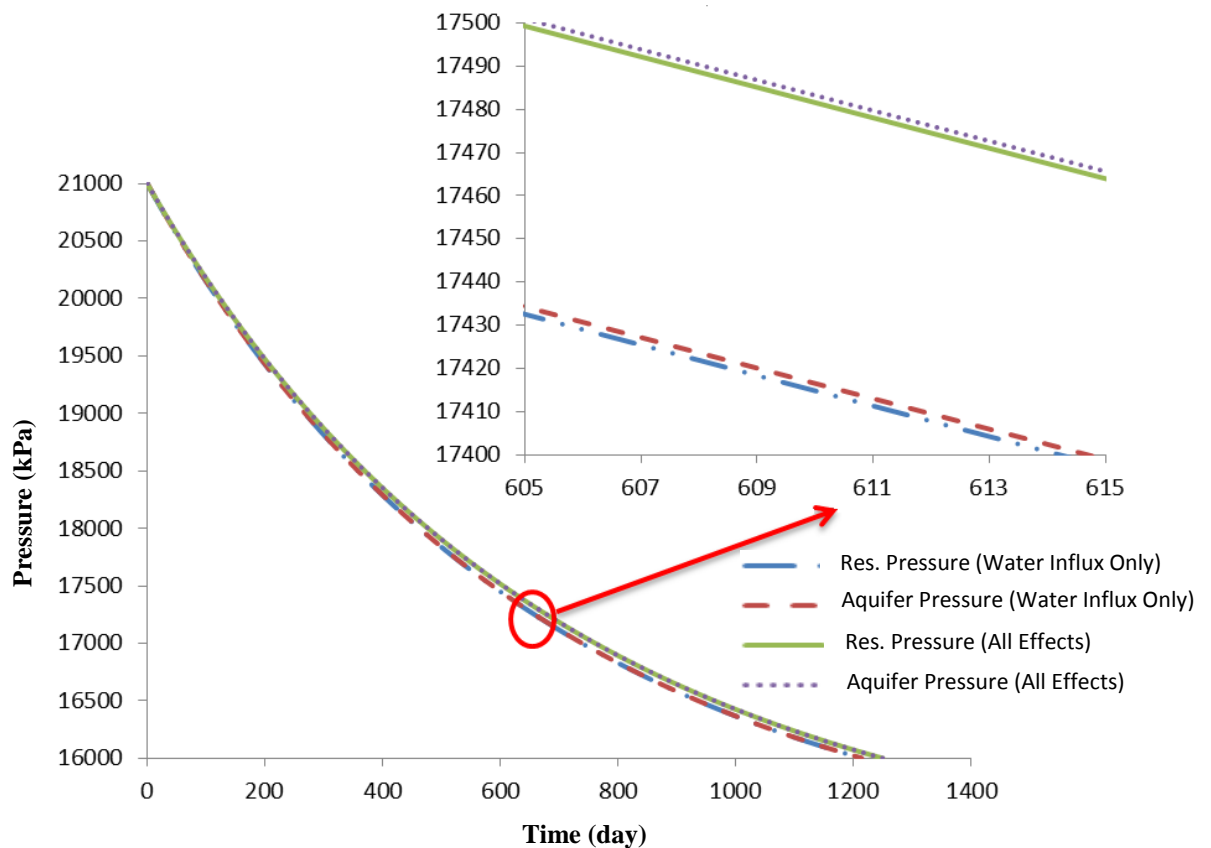


**Figure 4.11: Pressure Distribution**

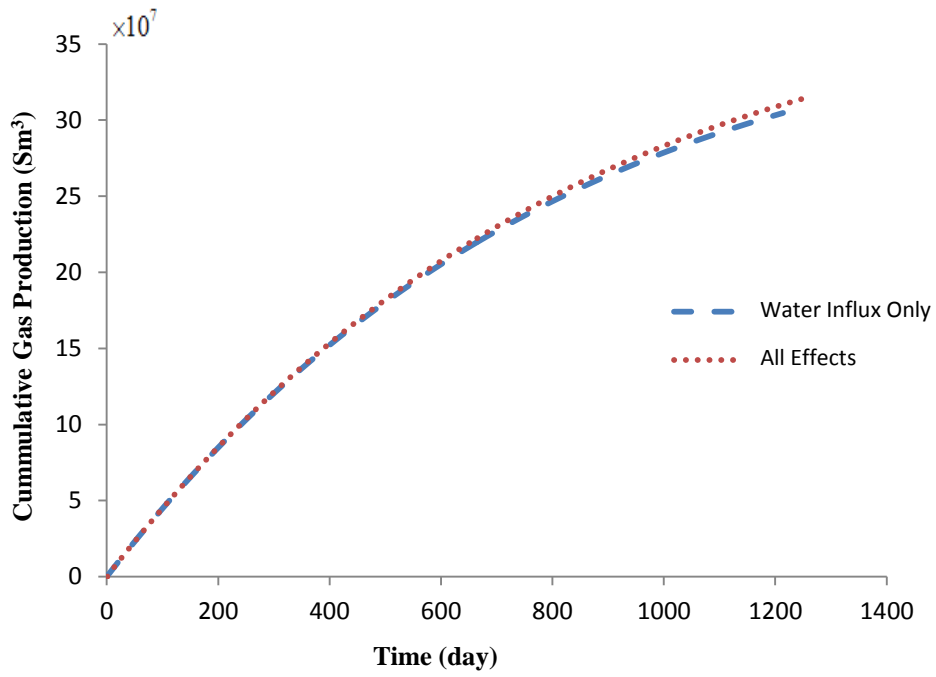


**Figure 4.12: Gas Production Profile**

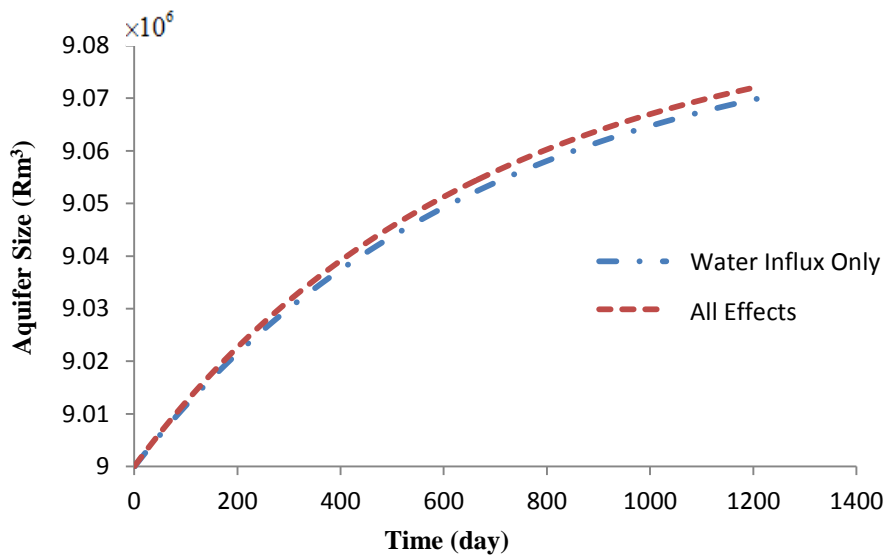


**Figure 4.13: Water Encroachment Profile**

### 4.3.3 Sensitivity Analysis

As discussed in the Section 2.2, the pore volume compressibility (PVC) is usually in the range of 0.29 to  $5.075 \times 10^{-6} \text{ kPa}^{-1}$  depending on the net overburden pressure, and the water compressibility only varies in a small range. Therefore, the value of pore volume compressibility may have a significant impact on the recovery prediction. In addition, different aquifer size and aquifer transmissibility may also affect the final results. In this section, aquifer size, aquifer transmissibility, and pore volume compressibility are chosen as the changing parameters for Model 1 and Model 2 in the sensitivity analysis, shown in the Table 4.15.

**Table 4.15: Summary of Changing Parameters in Sensitive Analysis**

Changing Variables	Values (Min)	Values (Max)
Aquifer Size ( $\text{Rm}^3$ )	$1.0 \times 10^6$	$100.0 \times 10^6$
Aquifer Transmissibility ( $\text{Sm}^3/(\text{kPa}\cdot\text{day})$ )	0, 0.1, 1, 10, 50	
Pore Volume Compressibility ( $\text{kPa}^{-1}$ )	$0.29 \times 10^{-6}$	$5.075 \times 10^{-6}$
Model Number	Model 1, Model 2	

As we can see from the results in Table 4.16, for both aquifer sizes, the relative errors of recovery factor between Model 1 and Model 2 with minimum pore volume compressibility are lower than 1%. Model 1 is the reference model (0 relative error), the relative error is obtained by the  $(\text{Model1}-\text{Model2})/\text{Model1}$ . This predicts that Model 1 is applicable for the gas model with small pore volume compressibility. However, for larger PVC, Model 1 is not applicable due to large relative errors. In another word, for reservoirs with high rock compressibility, as illustrated in Table 4.16, and the discrepancy of recovery factor in Model 1 and 2 exhibits a large error of ~13% for both small and large aquifer size. In conclusion, both models can be used for gas reservoirs with low rock compressibility, and the second model is also valid for gas reservoir with high rock compressibility.

**Table 4.16: Results from Sensitive Analysis**

<b>Model</b>	<b>PVC (kPa<sup>-1</sup>)</b>	<b>Aquifer Size (Rm<sup>3</sup>)</b>	<b>Aquifer Transmissibility (Sm<sup>3</sup>/(kPa-day))</b>	<b>Recovery Factor(%)</b>	<b>Relative Errors (%)</b>
1	N/A	1.0x10 <sup>6</sup>	0	20.89	0
			0.1	20.94	
			1	20.94	
			10	20.94	
			50	20.94	
		100.0x10 <sup>6</sup>	0	20.89	
			0.1	23.41	
			1	25.67	
			10	25.91	
			50	25.93	
2	0.29x10 <sup>-6</sup>	1.0x10 <sup>6</sup>	0	21.09	0.96
			0.1	21.14	0.96
			1	21.14	0.96
			10	21.14	0.96
			50	21.13	0.91
		100.0x10 <sup>6</sup>	0	21.09	0.96
			0.1	23.63	0.94
			1	25.88	0.82
			10	26.11	0.77
			50	26.12	0.73
	5.075 x10 <sup>-6</sup>	1.0x10 <sup>6</sup>	0	23.64	13.16
			0.1	23.69	13.13
			1	23.69	13.13
			10	23.69	13.13
			50	23.68	13.09
		100.0x10 <sup>6</sup>	0	23.64	13.16
			0.1	26.33	12.47
			1	28.45	10.83
			10	28.66	10.61
			50	28.67	10.57

## Chapter 5 Conclusions & Recommendations

### 5.1 Conclusions

The methodology and models discussed in this thesis present how the concept of multiple reservoir compartments, aquifers, and wellbore segments can be treated as an integrated system and solved as a coupled system of ordinary differential equations. One of the contributions is that a dual time step method is used to solve the system of equations. Well transmissibility and aquifer sizes are kept constant during small time steps in which pressures and flow rates are solved. The new pressure is then used to update the well indices and aquifer size over larger time steps. Another major contributions in this work is using a high order numerical method to solve the governing equations, which makes the model more accurate than the Eclipse™ models as well as Integrated Production Modeling software. One of the major drawback of Integrated Production Modeling software package developed by Petroleum Experts Ltd. (2009) is finite difference calculation, where some of the time dependent changes, such as aquifer encroachment and aquifer pressure, are not updated with the new pressure-related solutions within each numerical time step. The Eclipse™ models are also using finite different method which only offers a low order time discretization in solving governing equations. The pressure solutions in the Eclipse™ models are picked up at two ends within one time step. However, the compartmentalized reservoir model is using Runge-Kutta 4<sup>th</sup> order numerical method to solve the governing equations, which allows for an average pressure solution at each time step. Therefore, the results of reservoir pressure distribution,

cumulative oil production profile, and oil flow rate profile from both the Matlab and Eclipse<sup>TM</sup> models are presenting a small discrepancy. Comparing to the Thomas' work (Thomas 2012), the gas reservoir model is another novelty since it is not included in his work. This model is transient during a single large time step calculation and hence represents an enhancement over standard finite difference method formulations. The model could be applied to any system with appreciable pressure gradient, such as faulted reservoirs or a single wellbore draining multiple reservoirs with variable characteristics. This type of model can be efficiently used to predict production behavior from new fields to identify reservoir properties involving transmissibility, the presence of faults or baffles, the effective reservoir volume, and the support supplied by connected aquifers, or to optimize pre-drill scenarios involving well length and perforation length.

The main conclusions are:

- 1) This compartmentalized reservoir model can be used in cases where compartments are separated by large distances or for multiple compartments with variable qualities.
- 2) The fourth order Runge-Kutta numerical method provides a high order time discretization in solving pressure functions.
- 3) For black oil reservoirs, a comparison of the model with standard oil simulation software Eclipse shows a good agreement with reduced CPU time.
- 4) The gas reservoir model incorporates and compares the effects of compressibility for the gas reservoir that are not captured by traditional reservoir simulation. The sensitivity analysis shows that for gas reservoirs with low rock compressibility, water influx is sufficient to predict well performance. However, for gas reservoirs with

high rock compressibility, water compressibility and pore volume term must be used in order to obtain more realistic simulation results.

- 5) The new model developed in this thesis can be easily integrated with different numbers of reservoir compartments, aquifer compartment, and wellbore segments, etc. This shows a good flexibility of the new model.

## **5.2 Recommendations**

It is recommended that any future work consider the following:

- Variable fluid properties (e.g. density and viscosity) and compressibility for rock, water and oil in the oil reservoir model,
- Multiphase flow in the pipeline,
- The horizontal well transmissibility model calculated by Johansen et al. (2015),
- A reservoir with anisotropic permeability,
- A more rigorous approach to wellbore modeling. This work takes only friction loss into account in simple completions. This is not suitable for a variety of advanced well completions with dynamic operating conditions.
- Investigations on compositional effects in both oil and gas wells under different fluid states and conditions.
- A comparison with a case where each compartment is a standard reservoir simulation grid block with a numerical aquifer model (Eclipse) could be investigated.

## Bibliography

- Abdul Majeed, G. H., Abu Al-Soof, N. B., & Allassal, J. R. (1989, November 1). An Improved Revision to the Hagedorn and Brown Liquid Holdup Correlation. Petroleum Society of Canada. doi:10.2118/89-06-02.
- Abou-Kassem, J. H. (2008). The engineering approach versus the mathematical approach in developing reservoir simulators. *Nature Science and Sustainable Technology*, 39.
- Ahmed, PhD, PE, Tarek, & McKinney, P. (2011). *Advanced reservoir engineering*. Burlington: Gulf Professional Publishing, pp. 292.
- Al – Hussainy R., Ramey H.J., Jr., and Crawford P.B., (May 1966), The Flow of Real Gases through Porous Media, *JPT*, pp. 625 - 636.
- Allard, D. R., & Chen, S. M. (1988, May 1). Calculation of Water Influx for Bottomwater Drive Reservoirs. *Society of Petroleum Engineers*. doi:10.2118/13170-PA.
- Arya, A., & Gould, T. L. (1981, January 1). Comparison of Two Phase Liquid Holdup and Pressure Drop Correlations across Flow Regime Boundaries for Horizontal and Inclined Pipes. *Society of Petroleum Engineers*. doi:10.2118/10169-MS.
- Aziz, K., & Govier, G. W. (1972, July 1). Pressure Drop In Wells Producing Oil And Gas. Petroleum Society of Canada. doi:10.2118/72-03-04.
- Babu, D.K., Odeh, A.S. (1989, November). Productivity of a Horizontal Well, *SPERE*, pp 417.

- Beggs, D. H., & Brill, J. P. (1973, May 1). A Study of Two-Phase Flow in Inclined Pipes. Society of Petroleum Engineers.doi:10.2118/4007-PA.
- Brill, J. P., and Hemanta Mukherjee.(1999). Multiphase Flow in Wells. Richardson, TX: Henry L. Doherty Memorial Fund of AIME, Society of Petroleum Engineers,. Print.
- Brill, J. P., Schmidt, Z., Coberly, W. A., Herring, J. D., & Moore, D. W. (1981, June 1). Analysis of Two-Phase Tests in Large-Diameter Flow Lines in Prudhoe Bay Field. Society of Petroleum Engineers.doi:10.2118/8305-PA.
- Blasius, H. (1913). Das Aehnlichkeitsgesetz bei Reibungsvorgängen in Flüssigkeiten.doi:10.1007/978-3-662-02239-9\_1
- Carter, R. D., & Tracy, G. W. (1960, January 1). An Improved Method for Calculating Water Influx. Society of Petroleum Engineers.
- Cervantes, G. T. (1996, January 1). Reservoir Compartmentalisation in the Roma Area. Society of Petroleum Engineers.doi:10.2118/37004-MS
- Chen Z., Huan G., and Ma Y. (2006), Computational Methods for Multiphase Flows in Porous Media, Computational Science and Engineering Series, Vol. 2, SIAM, Philadelphia, PA.
- Chen Z. (2007), Reservoir Simulation - Mathematical Techniques in Oil Recovery, Society for Industrial and Applied Mathematics, KNOVEL, pp 4.
- Coats, K. H. (1962, March 1). A Mathematical Model Water Movement about Bottom-Water-Drive Reservoirs. Society of Petroleum Engineers. doi:10.2118/160-PA.

Courant, R.; Friedrichs, K.; Lewy, H. (1928), "Über die partiellen Differenzgleichungen der mathematischen Physik", *Mathematische Annalen* (in German) 100 (1): 32–74, doi:10.1007/BF01448839, JFM 54.0486.01, MR 1512478.

Dake, L.P. (1978). *Fundamentals of Reservoir Engineering*. Amsterdam, The Netherlands, Elsevier Inc..

Duns, H., & Ros, N. C. J. (1963, January 1). Vertical flow of gas and liquid mixtures in wells. World Petroleum Congress.

Eaton, B. A., Knowles, C. R., & Silberbrg, I. H. (1967, June 1). The Prediction of Flow Patterns, Liquid Holdup and Pressure Losses Occurring During Continuous Two-Phase Flow In Horizontal Pipelines. Society of Petroleum Engineers.doi:10.2118/1525-PA.

Ertekin, T., Abou-Kassem, J. H., and King, G. R. (2001), *Basic Applied Reservoir Simulation*. Society of Petroleum Engineers, Richardson, TX.

Evinger, H. H., & Muskat, M. (1942, December 1). Calculation of Theoretical Productivity Factor. Society of Petroleum Engineers.doi:10.2118/942126-G

Fanchi, J.R. (2006). *Principles of Applied Reservoir Simulation Third Edition*. Oxford, UK: Elsevier Inc.

Fatt, I. (1958, March 1). Pore Volume Compressibilities of Sandstone Reservoir Rocks. Society of Petroleum Engineers. doi: 10.2118/970-G.

Fetkovich, M. J. (1971, July 1). A Simplified Approach to Water Influx Calculations-Finite Aquifer Systems. Society of Petroleum Engineers. doi:10.2118/2603-PA.

- Fetkovich, M. J., Reese, D. E., & Whitson, C. H. (1998, March 1). Application of a General Material Balance for High-Pressure Gas Reservoirs (includes associated paper 51360). Society of Petroleum Engineers. doi: 10.2118/22921-PA.
- Fox, M.J., Chedburn, A.C.S., & Stewart, G. (1988, October 16). Simple Characterization of Communication between Reservoir Regions. Society of Petroleum Engineers.
- Furui, K., Zhu, D., & Hill, A. D. (2002, January 1). A Rigorous Formation Damage Skin Factor and Reservoir Inflow Model for a Horizontal Well. Society of Petroleum Engineers. doi: 10.2118/74698-MS.
- Gilbert, W. E. (1954, January 1). Flowing and Gas-lift well Performance. American Petroleum Institute.
- Goudar, C.T., Sonnad, J.R. (August 2008). Comparison of the Iterative Approximations of the Colebrook–White Equation. Hydrocarbon Processing Fluid Flow and Rotating Equipment Special Report: 79–83.
- Griffith, P., Lau, C. W., Hon, P. C., & Pearson, J. F. (1975, January 1). Two Phase Pressure Drop in Inclined and Vertical Oil Wells. Society of Petroleum Engineers.
- Guo, B., Lyons, W. C., & Ghalambor, A. (2007). Petroleum Production Engineering: A Computer-Assisted Approach. Burlington, MA: Gulf Professional Pub.
- Hagedorn, A. R., & Brown, K. E. (1965, April 1). Experimental Study of Pressure Gradients Occurring During Continuous Two-Phase Flow in Small-Diameter Vertical Conduits. Society of Petroleum Engineers. doi:10.2118/940-PA.
- Hagoort, J. (1988). Fundamentals of Gas Reservoir Engineering, Elsevier, Amsterdam, New York.

- Haaland SE. Simple and Explicit Formulas for the Friction Factor in Turbulent Pipe Flow. ASME. J. Fluids Eng. 1983; 105(1):89-90. doi:10.1115/1.3240948.
- Havlena, D. and Odeh, A.S. (1963), “The Material Balance as an Equation of a Straight Line”, J.Pet.Tech. August: 896-900. Trans., AIME, 228.
- Hughmark, G. A. and Pressburg, B. S. (1961), Holdup and pressure drop with gas-liquid flow in a vertical pipe. AIChE J., 7: 677–682. doi: 10.1002/aic.690070429.
- Hurst, W. (1958, January 1). The Simplification of the Material Balance Formulas by the Laplace Transformation. Society of Petroleum Engineers.
- Johansen, T. E. (2008). Principles of Reservoir Engineering. Memorial University of Newfoundland.
- Johansen, T. E., James, L., Cao, J. (2015) ‘Analytical Coupled Axial and Radial Productivity Model for Steady-State Flow in Horizontal Wells’ (Accept by Int. J. Petroleum Engineering).
- Johansen, T. E. (2013), “A note on modeling of dry gas reservoirs with aquifer support”, [www.petreng-thormod.ca](http://www.petreng-thormod.ca)
- Joshi, S. D. (1988, June 1). Augmentation of Well Productivity with Slant and Horizontal Wells (includes associated papers 24547 and 25308). Society of Petroleum Engineers. doi: 10.2118/15375-PA.
- Lee, A. L., Gonzalez, M. H., &Eakin, B. E. (1966, August 1). The Viscosity of Natural Gases. Society of Petroleum Engineers. doi: 10.2118/1340-PA.
- Lyons, P., &Plisga, B. (2011). Standard Handbook of Petroleum and Natural Gas Engineering (2nd ed.). Burlington: Elsevier Science.

- Minami, K., & Brill, J. P. (1987, February 1). Liquid Holdup in Wet-Gas Pipelines. Society of Petroleum Engineers. doi: 10.2118/14535-PA.
- Mukherjee, H., & Brill, J. P. (1983, May 1). Liquid Holdup Correlations for Inclined Two-Phase Flow. Society of Petroleum Engineers. doi: 10.2118/10923-PA.
- Muskat, M. (1949). In Physical Principles of Oil Production. New York: McGraw-Hill Book.
- Odeh, A. S., & Jones, L. G. (1965, August 1). Pressure Drawdown Analysis, Variable-Rate Case. Society of Petroleum Engineers. doi: 10.2118/1084-PA.
- Payne, G. A., Palmer, C. M., Brill, J. P., & Beggs, H. D. (1979, September 1). Evaluation of Inclined-Pipe, Two-Phase Liquid Holdup and Pressure-Loss Correlation Using Experimental Data (includes associated paper 8782). Society of Petroleum Engineers. doi:10.2118/6874-PA
- Peaceman, D. W. (1983, June). Interpretation of Well-Block Pressures in Numerical Reservoir Simulation with Nonsquare Grid Blocks and Anisotropic Permeability. Society of Petroleum Engineers.
- Peaceman, D. W. (1993, April 1). Representation of a Horizontal Well in Numerical Reservoir Simulation. Society of Petroleum Engineers. doi: 10.2118/21217-PA.
- Peaceman, D. W. (1995, November 1). A New Method for Representing Multiple Wells with Arbitrary Rates in Numerical Reservoir Simulation. Society of Petroleum Engineers. doi: 10.2118/29120-PA.
- Petroleum Experts Ltd. (2009, March). MBAL Online Help Manual. Petroleum Experts Ltd..

- Rahman, N.M.A., & Ambastha, A. K. (2000, September 1). Generalized 3D Analytical Model for Transient Flow in Compartmentalized Reservoirs. Society of Petroleum Engineerings. Doi: 10.2118/65106-PA.
- Rahman, N. M. A., Mattar, L., & Anderson, D. M. (2006, January 1). New, Rigorous Material Balance Equation for Gas Flow in a Compressible Formation with Residual Fluid Saturation. Society of Petroleum Engineers. doi: 10.2118/100563-MS.
- Ral, R., Singh, I., & Srinivasan, S. (1989, August 1). Comparison of Multiphase-Flow Correlations with Measured Field Data of Vertical and Deviated Oil Wells in India (includes associated paper 20380). Society of Petroleum Engineers. doi: 10.2118/16880-PA.
- Ramagost, B. P., & Farshad, F. F. (1981, January 1). P/Z Abnormally Pressured Gas Reservoirs. Society of Petroleum Engineers. doi: 10.2118/10125-MS
- Randolph, P. L. (1977, January 1). Natural Gas from Geopressed Aquifers? Society of Petroleum Engineers. doi: 10.2118/6826-MS.
- Retrieve from: [http://petrowiki.org/File%3AVol1\\_Page\\_322\\_Image\\_0001.png](http://petrowiki.org/File%3AVol1_Page_322_Image_0001.png)
- Retrieve from: [http://wiki.aapg.org/Drive\\_mechanisms\\_and\\_recovery](http://wiki.aapg.org/Drive_mechanisms_and_recovery)
- Schilthuis, R. J. (1936, December 1). Active Oil and Reservoir Energy. Society of Petroleum Engineers. doi: 10.2118/936033-G.
- Serghides, T.K (1984). Estimate Friction Factor Accurately. Chemical Engineering Journal 91(5): 63–64.

- Sinclair, I. K., Evans, J. E., Albrechtsons, E. A., and Sydora, L. J. (1999). The Hibernia Oilfield – Effects of Episodic Tectonism on Structural Character and Reservoir Compartmentalization. Geological Society, London. Doi: 10.1144/0050517.
- Stewart, G., and Whaballa, A. E. (1989, October 8). Pressure Behaviour of Compartmentalized Reservoirs. Society of Petroleum Engineers.
- Swanson, B. F. (1979, January 1). Compressibility of Geopressed Reservoirs. Society of Petroleum Engineers.
- Swami, P.K. and Jain, A.K. (1976, May). Explicit Equations for Pipe Flow Problems, J Hydraulics Div, Proc ASCE, pp. 657–664
- Thomas, B.G. (2012, May). Dynamic Reservoir Tank Modeling with Coupled Wellbore Model. Memorial University of Newfoundland.
- Van Everdingen, A. F. and Hurst, William: "The Application of the Laplace Transformation to Flow Problems in Reservoirs", Trans., AIME (1949) 186, 305.
- Vogel, J. V. (1968, January 1). Inflow Performance Relationships for Solution-Gas Drive Wells. Society of Petroleum Engineers. doi: 10.2118/1476-PA.
- Vogt, J. P., & Wang, B. (1987, January 1). Accurate Formulas for Calculating the Water Influx Superposition Integral. Society of Petroleum Engineers. doi: 10.2118/17066-MS.
- Vogel, J. V. (1968, January 1). Inflow Performance Relationships for Solution-Gas Drive Wells. Society of Petroleum Engineers. doi:10.2118/1476-PA
- Yildiz, T., & Khosravi, A. (2007, December 1). An Analytical Bottomwaterdrive Aquifer Model for Material-Balance Analysis. Society of Petroleum Engineers. doi: 10.2118/103283-PA.



# Appendix

## A Pseudo Pressure Function

---

Pseudo Pressure Function (Hagoort, 1988) is given by:

$$m(P) = (\mu B)_r \int_{P_r}^P \frac{1}{\mu B} dP \quad (\text{A.1})$$

$r$  stands for reference pressure.

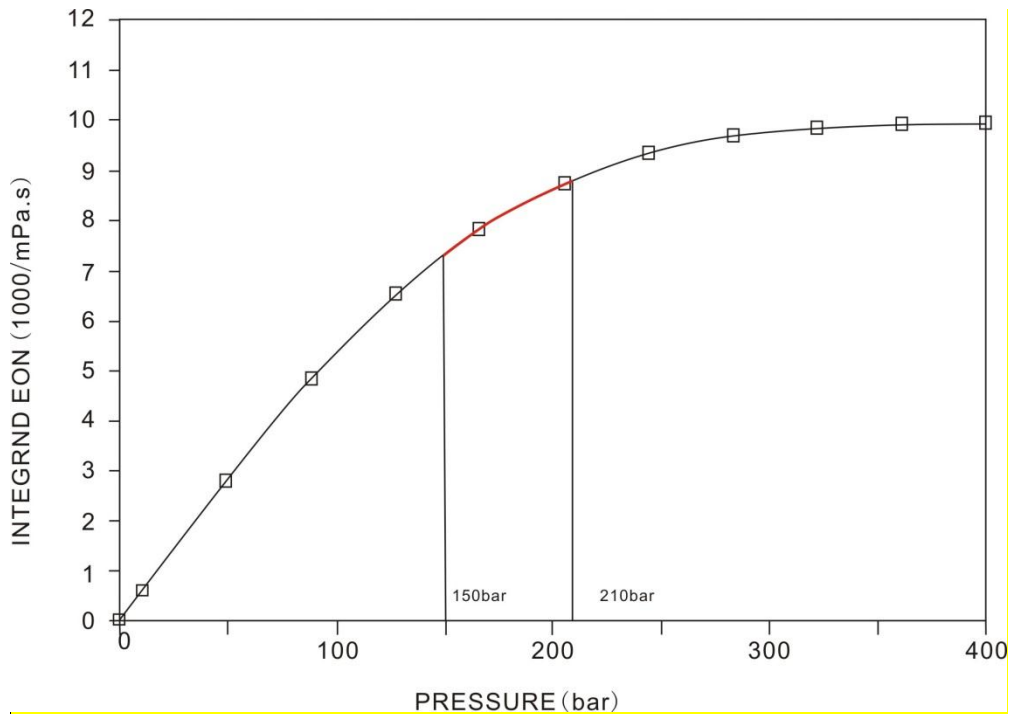


**Figure A.1: Reciprocal of Product  $\mu B$  versus Pressure (from Hagoort, 1988)**

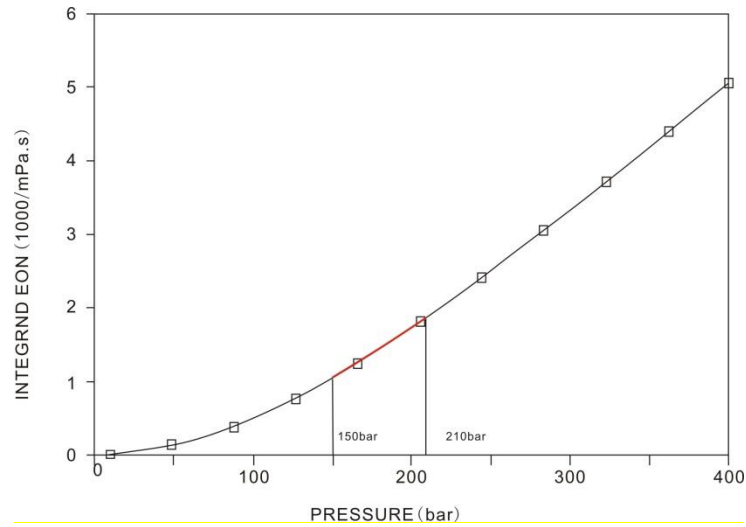


**Figure A.2: Pseudo-Pressure versus Pressure for Gas (from Hagoort, 1988)**

From figure A.1, the integrand is a distinctly nonlinear function of the pressure in the intermediate pressure range. In the case studies, the pressure interval of 150 bar to 210 bar is not too large, the pseudo-pressure curve in this interval can be approximated by a straight line shown in the figure A.2.

For the straight-line portions of the figure B.1 we can generally write

$$\frac{1}{\mu B} = aP + b, \quad (\text{A.2})$$

Where a and b are constants.

Substitution of Equation (A.2) into Equation (A.1) yields,

$$m(P) = (\mu B)_r \int_{P_r}^P (aP + b) dP, \quad (\text{A.3})$$

Integrate Equation (A.3),

$$m(P) = (\mu B)_r [a(P^2 - P_r^2) / 2 - b(P - P_r)]. \quad (\text{A.4})$$

From Equation (A.4), the difference in the corresponding pseudo-pressures can be written as,

$$m(P_1) - m(P_2) = (\mu B)_r [a(P_1^2 - P_2^2) / 2 + b(P_1 - P_2)] \quad (\text{A.5})$$

By mathematical transformation,

$$m(P_1) - m(P_2) = (\mu B)_r (P_1 - P_2) [a(P_1 + P_2) / 2 + b]. \quad (\text{A.6})$$

Therefore,

$$\frac{m(P_1) - m(P_2)}{(\mu B)_r} = (P_1 - P_2) [a(P_1 + P_2) / 2 + b]. \quad (\text{A.7})$$

From Equation (A.2), we can have

$$a(P_1 + P_2) / 2 + b = \frac{1}{(\mu B)_1} + \frac{1}{(\mu B)_2} = \frac{(\mu B)_1 + (\mu B)_2}{2(\mu B)_1(\mu B)_2}. \quad (\text{A.8})$$

Combining Equation (A.7) and Equation (A.8),

$$\frac{m(P_1) - m(P_2)}{(\mu B)_r} = \frac{(\mu B)_1 + (\mu B)_2}{2(\mu B)_1(\mu B)_2} (P_1 - P_2). \quad (\text{A.9})$$

The flow rate in Darcy's law can be written as following,

$$q_{12} = \frac{KA_c}{(\mu B)_r L} (m_2 - m_1) = \frac{KA_c}{\mu BL} (P_1 - P_2), \quad (\text{A.10})$$

where

$$\overline{\mu B} = \frac{2(\mu B)_1(\mu B)_2}{(\mu B)_1 + (\mu B)_2}. \quad (\text{A.11})$$

Gas Viscosity Correlations (Lee, Gonzalez, and Eakin, 1966) is given by:

$$\mu = K \exp[X(\rho_g / 62.43)^Y], \quad (\text{A.12})$$

Where,  $\mu$  is gas viscosity, Pa.s,  $\rho_g$  is gas density, Kg/m<sup>3</sup>,  $M$  is molecular mass, g/mol,

$P$  is pressure, Pa,  $Z$  is Z-factor,  $R$  is a gas constant, 287J/(Kg\*K),  $T$  is temperature, K.

$$K = \frac{10^{-4}(9.4 + 0.02M)T^{1.5}}{209 + 19M + T}, \quad (\text{A.13})$$

$$X = 3.5 + \frac{986}{T} + 0.01M, \quad (\text{A.14})$$

$$Y = 2.4 - 0.2X, \quad (\text{A.15})$$

$$\rho_g = \frac{MP}{ZRT}. \quad (\text{A.16})$$

## B Numerical Method Approach

---

The reservoir compartments form a series of first-order differential equations in the form of:

$$\frac{dy_i}{dx} = f(x, y_1, y_2, \dots, y_N). \quad (\text{B.1})$$

The ODEs will be solved with a known initial condition that two real numbers are given as  $x_0$  and  $y_0$ . Therefore, a solution for  $x > x_0$  can be sought as:

$$y(x_0) = y_0. \quad (\text{B.2})$$

Equation (B.1) and (B.2) can represent an initial value problem.

The 4<sup>th</sup> Order Runge-Kutta Method was selected to solve a series of ODEs generated by the system in the modeling. This method can provide a high degree of accuracy efficiently.

The 4<sup>th</sup> Order Runge-Kutta Method is governed by the following principle.

$$y_{i+1} = y_i + (a_1k_1 + a_2k_2 + a_3k_3 + a_4k_4)h. \quad (\text{B.3})$$

If we know the value at cycle ‘ $i$ ’ of  $y = y_i$  at  $x = x_i$ , we can get the value at next cycle ‘ $i+1$ ’ of  $y = y_{i+1}$  at  $x = x_{i+1}$ .

Equation (B.3) can be rewrite based on the first five terms of the Taylor series expansion.

$$y_{i+1} = y_i + \frac{dy}{dx} \Big|_{x_i, y_i} (x_{i+1} - x_i) + \frac{1}{2!} \frac{d^2 y}{dx^2} \Big|_{x_i, y_i} (x_{i+1} - x_i)^2 + \frac{1}{3!} \frac{d^3 y}{dx^3} \Big|_{x_i, y_i} (x_{i+1} - x_i)^3 + \frac{1}{4!} \frac{d^4 y}{dx^4} \Big|_{x_i, y_i} (x_{i+1} - x_i)^4. \quad (\text{B.4})$$

Equation (B.1) can be simplified in forms of

$$\frac{dy}{dx} = f(x, y). \quad (\text{B.5})$$

And we know

$$x_{i+1} - x_i = h. \quad (\text{B.6})$$

Hence, we get

$$y_{i+1} = y_i + f(x_i, y_i)h + \frac{1}{2!} f'(x_i, y_i)h^2 + \frac{1}{3!} f''(x_i, y_i)h^3 + \frac{1}{4!} f'''(x_i, y_i)h^4. \quad (\text{B.7})$$

Based on Equation (B.4) and (B.7), a popular solution is commonly used,

$$y_{i+1} = y_i + \frac{1}{6}(k_1 + 2k_2 + 2k_3 + k_4)h, \quad (\text{B.8})$$

where

$$k_1 = f(x_i, y_i)h, \quad (\text{B.9})$$

$$k_2 = f\left(x_i + \frac{1}{2}h, y_i + \frac{1}{2}k_1h\right), \quad (\text{B.10})$$

$$k_3 = f\left(x_i + \frac{1}{2}h, y_i + \frac{1}{2}k_2h\right), \quad (\text{B.11})$$

$$k_4 = f(x_i + h, y_i + k_3h). \quad (\text{B.12})$$

In this work, a system with several ODEs has to be solved simultaneously by Runge-Kutta formulas.

For a system shown in Equation (B.1), we have

$$k_{1i} = f_i(x, y_1, y_2, \dots, y_N)h, \quad (\text{B.13})$$

$$k_{2i} = f_i\left(x_i + \frac{1}{2}h, y_1 + \frac{1}{2}k_{11}h, y_2 + \frac{1}{2}k_{12}h, \dots, y_N + \frac{1}{2}k_{1N}h\right), \quad (\text{B.14})$$

$$k_{3i} = f_i\left(x_i + \frac{1}{2}h, y_1 + \frac{1}{2}k_{21}h, y_2 + \frac{1}{2}k_{22}h, \dots, y_N + \frac{1}{2}k_{2N}h\right), \quad (\text{B.15})$$

$$k_{4i} = f_i(x_i + h, y_1 + k_{31}h, y_2 + k_{32}h, \dots, y_N + k_{3N}h), \quad (\text{B.16})$$

and

$$y_{i+1} = y_i + \frac{1}{6}(k_{1i} + 2k_{2i} + 2k_{3i} + k_{4i}). \quad (\text{B.17})$$

In our case,  $x$  denotes time and  $y$  denotes pressure` in each reservoir unit. Hence, with

$N$  reservoir units, there will be  $N$  systems of equations that require solving for each

time  $x$ .

## C.1 Source Code for Dry Gas Reservoir Simulator

```

-----
% PURE GAS RESERVOIR SIMULATOR WITH WATER INFLUX CONSIDERED %%
%***** Dan Wang *****%
%***** Dec 2014 *****%
%-----

clc
clearall

%%%%%%%%%% DATA SECTION %%%%%%%%%%
timel=cputime; %CPU time record; s
Pw0=15000; %bottom hole pressure; kPa
Ja=30; %aquifer transmissibility; Sm3/(day-kPa)
Jwi=40; %well transmissibility; Sm3/(day-kPa)
Wi=9*10^6; %initial aquifer size; Rm3
Wii=Wi; %aquifer size; Rm3
Ca=1.6*10^(-6); %aquifer compressibility; /kPa
Bw=1.0; %water formation volume factor; Rm3/Sm3
G=1.08*10^9; %STGIIP; Sm3
A=0.5472; %parameter in Z-factor calculation;
C=0.0520; %parameter in Z-factor calculation;
D=1.017; %parameter in Z-factor calculation;
Pc=4.5693; %critical pressure; MPa
Tc=207.87; %critical temperature; K
Tr=370; %reservoir temperature; K
Trd=Tr/Tc; %reduced temperature;
P0=101; %pressure at standard condition; kPa
T0=288; %temperature at standard condition; K
Pr=21000; %reservoir pressure; kPa
Pa=21000; %aquifer pressure; kPa
Bgi=[0.0054;] %initial gas formation volume factor; Rm3/Sm3
Bg_Pw0=0.0076; %gas formation volume factor@Pw0; Rm3/Sm3
Vis_gi=10^(-3)/3600/24*0.0202*10^(-4); %initial viscosity; kPa.day
Vis_g_Pw0=10^(-3)/3600/24*0.0174*10^(-4); %viscosity@Pw0; kPa.day
Gpsum=0; %cumulative gas production; Sm3
dt=0.5; %time step; s

%%%%%%%%%% Z-FACTOR CALCULATIONS %%%%%%%%%%

for iii=1:7000000;
    iii; %loop variables
    Prd=Pr/(1000*Pc);
    tem_Pr=Pr;
    B=(0.62-0.23*Trd)*(Prd)+(0.066/(Trd-0.86)-0.037)*((Prd)^2)+
    (0.32/(10^(9*(Trd-1))))*((Prd)^6); %parameter in Z-factor calculation
    Z=((A+(1-A)/(exp(B))+C*((Prd)^D));
    Bg=P0*Tr/T0*Z/Pr; %Bg at time Pr(t)

Zprim=1/1000/Pc*C*D*(Prd)^(D-1)-(1-A)/(exp(B))*((0.62-0.23*Trd)+2*(0.066

```

```

/ (Trd-0.86)-0.037) * (Prd)+6*(0.32/(10^(9*(Trd-1)))) * ((Prd)^5) *1/1000/Pc;
%Z-factor derivative
Bgprim=P0*Tr/T0*(Zprim/Pr-Z/(Pr^2)); %Bg derivative

%%%%%%%%%%%%%%%%%%%%%%%%%%%%%%%%%%%%%%%%%%%%%%%%%%%%%%%%%%%%%%%%%%%%%%%% GAS VISCOSITY CALCULATIONS %%%%%%%%%%
R=10.732; %psi.ft3/lbmol.R
M=19.91;
T=Tr*9/5; %reservoir temperature; R
P=Pr*0.145; %pressure; psi
Kp=10^(-4) * (9.4+0.02*M) *T^1.5/(209+19*M+T);
X=3.5+986/T+0.01*M;
Y=2.4-0.2*X;
dens_g=M*P/Z/R/T;
vis_g=10^(-3)/3600/24*10^(-3)*Kp*exp(X*(dens_g/62.43)^Y); %kPa.day

%%%%%%%%%%%%%%%%%%%%%%%%%%%%%%%%%%%%%%%%%%%%%%%%%%%%%%%%%%%%%%%%%%%%%%%% CALCULATIONS %%%%%%%%%%
Jw=Jwi*(Bg/Bgi)*vis_g*Bg/(Vis_gi*Bgi)*...
(Vis_gi*Bgi+Vis_g_Pw0*Bg_Pw0)/(vis_g*Bg+Vis_g_Pw0*Bg_Pw0);
Prk1=(1/(G*Bgprim))*(Bg*Jw*(Pr-Pw0)-Bw*Ja*(Pa-Pr));

Pr=Pr+dt*Prk1; %reservoir pressure at time t; kPa
Pa=Pa-dt*(Ja/Ca/Wi*(Pa-tem_Pr)); %aquifer pressure at time t; kPa
Gp=Jw*(Pr-Pw0)*dt; %gas produced within a time interval; Sm3
Gpsum=Gpsum+Gp; %cumulative gas production at time t; Sm3
detW=dt*(Bw*Ja*(Pa-Pr)); %water encroachment at t; Rm3
Wii=Wii+detW; %aquifer size at time t; Rm3
if (Pr<16000) %abandon pressure limit setting
limit_t=iii;
break;
end

Jwmat(iii)=Jw;
Prmat(iii)=Pr; %reservoir pressure profile; kPa
Pamat(iii)=Pa; %aquifer pressure profile; kPa
Wiimat(iii)=Wii; %aquifer volume profile; Sm3
Gpmat(iii)=Gpsum; %cumulative gas production profile; Sm3
Bgmat(iii)=Bg; %Bg profile; Rm3/Sm3
Pro_time(iii)=iii*dt; %production life; day
end

%%%%%%%%%%%%%%%%%%%%%%%%%%%%%%%%%%%%%%%%%%%%%%%%%%%%%%%%%%%%%%%%%%%%%%%% RECOVERY FACTOR %%%%%%%%%%
RF=Gpsum/G
RF0=1-Bgi/Bg; %recover factor
T = cputime-time1 %CPU time

```

```

% PURE GAS RESERVOIR SIMULATOR WITH THREE EFFECTS CONSIDERED %%
%*****
%***** Dan Wang *****%
%***** Dec 2014 *****%
%-----

```

```

clc
clearall

```

```

%%%%%%%%%% DATA SECTION %%%%%%%%%%%

```

```

time1=cputime; %CPU time record; s
Pw0=15000; %bottom hole pressure; kPa
Ja=30; %aquifer transmissibility; Sm3/(day-kPa)
Jwi=40; %well transmissibility; Sm3/(day-kPa)
Wi=9*10^6; %initial aquifer size; Rm3
Wii=Wi; %aquifer size; Rm3
Ca=1.6*10^(-6); %aquifer compressibility;
Cw=4*10^(-7); %water compressibility; /kPa
Cr=5.075*10^(-6); %rock compressibility in range of 0.29-5.075;/kPa
Scwi=0.25; %connate water saturation;
K=Cw*Scwi/(1-Scwi)+Cr/(1-Scwi); %K# ratio;
Bw=1.0; %water formation volume factor; Rm3/Sm3
G=1.08*10^9; %STGIIP; Sm3
A=0.5472; %parameter in Z-factor calculation;
C=0.0520; %parameter in Z-factor calculation;
D=1.017; %parameter in Z-factor calculation;
Pc=4.5693; %critical pressure; MPa
Tc=207.87; %critical temperature; K
Tr=370; %reservoir temperature; K
Trd=Tr/Tc; %reduced temperature;
P0=101; %pressure at standard condition; kPa
T0=288; %temperature at standard condition; K
Pri=21000; %initial reservoir pressure; kPa
Pr=Pr; %reservoir pressure; kPa
Pai=21000; %initial aquifer pressure; kPa
Pa=Pai; %aquifer pressure; kPa
Bgi=[0.0054;] %initial gas formation volume factor; Rm3/Sm3
Bg_Pw0=0.0076; %gas formation volume factor@Pw0; Rm3/Sm3
Vis_gi=10^(-3)/3600/24*0.0202*10^(-4); %initial viscosity; kPa.day
Vis_g_Pw0=10^(-3)/3600/24*0.0174*10^(-4); %viscosity@Pw0; kPa.day
Gpsum=0; %cumulative gas production; Sm3
dt=0.5; %time step; s

```

```

%%%%%%%%%% Z-FACTOR CALCULATIONS %%%%%%%%%%%

```

```

for iii=1:700000
iii; %loop variables
Prd=Pr/(1000*Pc);
tem_Pr=Pr;
B=(0.62-0.23*Trd)*(Prd)+(0.066/(Trd-0.86)-0.037)*((Prd)^2)+
(0.32/(10^(9*(Trd-1))))*((Prd)^6); %parameter in Z-factor calculation
Z=((A+(1-A)/(exp(B))+C*((Prd)^D));
Bg=P0*Tr/T0*Z/Pr; %Bg at time Pr(t)

```

```

Zprim=1/1000/Pc*C*D*(Prd)^(D-1)-(1-A)/(exp(B))*((0.62-0.23*Trd)+2*(0.066
/(Trd-0.86)-0.037)*(Prd)+6*(0.32/(10^(9*(Trd-1))))*((Prd)^5))*1/1000/Pc;
      %Z-factor derivative
Bgprim=P0*Tr/T0*(Zprim/Pr-Z/(Pr^2));      %Bg derivative

%%%%%%%%%%%%%%%%%%%%%%%%%%%%%%%%%%%%%%%%%%%%%%%%%%%%%%%%%%%%%%%%%%%%%%%% GAS VISCOSITY CALCULATIONS %%%%%%%%%%
R=10.732;      %psi.ft3/lbmol.R
M=19.91;
T=Tr*9/5;      %reservoir temperature; R
P=Pr*0.145;      %pressure; psi
Kp=10^(-4)*(9.4+0.02*M)*T^1.5/(209+19*M+T);
X=3.5+986/T+0.01*M;
Y=2.4-0.2*X;
dens_g=M*P/Z/R/T;
vis_g=10^(-3)/3600/24*10^(-3)*Kp*exp(X*(dens_g/62.43)^Y); %kPa.day

%%%%%%%%%%%%%%%%%%%%%%%%%%%%%%%%%%%%%%%%%%%%%%%%%%%%%%%%%%%%%%%%%%%%%%%% CALCULATIONS %%%%%%%%%%

Jw=Jwi*(Bg/Bgi)*vis_g*Bg/(Vis_gi*Bgi)*...
    (Vis_gi*Bgi+Vis_g_Pw0*Bg_Pw0)/(vis_g*Bg+Vis_g_Pw0*Bg_Pw0);
Prk1=(1/(G*(Bgprim-Bg*K)))*(Bg*Jw*(Pr-Pw0)-Bw*Ja*(Pa-Pr));

Pr=Pr+dt*Prk1;      %reservoir pressure at time t; kPa
Pa=Pa-dt*(Ja/Ca/Wi*(Pa-tem_Pr)); %aquifer pressure at time t; kPa
Gp=Jw*(Pr-Pw0)*dt; %gas produced within a time interval; Sm3
Gpsum=Gpsum+Gp; %cumulative gas production at time t; Sm3
detW=dt*(Bw*Ja*(Pa-Pr)); %water encroachment at t; Rm3
Wii=Wii+detW; %aquifer size at time t; Rm3
if (Pr<16000) %abandon pressure limit setting
limit_t=iii;
break;
end

Jwmat(iii)=Jw;
Prmat(iii)=Pr; %reservoir pressure profile; kPa
Pamat(iii)=Pa; %aquifer pressure profile; kPa
Wiimat(iii)=Wii; %aquifer volume profile; Sm3
Gpmat(iii)=Gpsum; %cumulative gas production profile; Sm3
Bgmat(iii)=Bg; %Bg profile; Rm3/Sm3
Pro_time(iii)=iii*dt; %production life; day
Kmat(iii)=K;

end

%%%%%%%%%%%%%%%%%%%%%%%%%%%%%%%%%%%%%%%%%%%%%%%%%%%%%%%%%%%%%%%%%%%%%%%% RESULTS %%%%%%%%%%
RF=Gpsum/G
RF0=1-Bgi/Bg; %recover factor
T = cputime-timel %CPU time
detpa=Pai-Pa; %aquifer pressure drop; kPa
detpr=Pr-Pri;%reservoir pressure drop; kPa
detW_tot=Wi-Wii %cumulative aquifer influx; Rm3

```







```

2.0 1.7 1.65 1.85 2.0 1.5 1.8 1.3 2.0 1.5 2.0 1.7 1.65 1.85 2.0 1.5 1.8
1.3 2.0 1.5 2.0 1.7 1.65 1.85 2.0 1.5 1.8 1.3 2.0 1.5 2.0 1.7 1.65 1.85
2.0 1.5 1.8 1.3 2.0 1.5 2.0 1.7 1.65 1.85 2.0 1.5 1.8 1.3 2.0 1.5 2.0 1.7
1.65 1.85 2.0 1.5 1.8 1.3 2.0 1.5 2.0 1.7 1.65 1.85 2.0 1.5 1.8 1.3 2.0
1.5 2.0 1.7 1.65 1.85 2.0 1.5 1.8 1.3 2.0 1.5 2.0 1.7 1.65 1.85 2.0 1.5
1.8 1.3 2.0 1.5 2.0 1.7 1.65 1.85 2.0 1.5 1.8 1.3 2.0 1.5 2.0 1.7 1.65
1.85 2.0 1.5 1.8 1.3 2.0 1.5 2.0 1.7 1.65 1.85 2.0 1.5 1.8 1.3 2.0 1.5
2.0 1.7 1.65 1.85 2.0 1.5 1.8 1.3 2.0 1.5 2.0 1.7 1.65 1.85 2.0 1.5 1.8
1.3 2.0 1.5 2.0 1.7 1.65 1.85 2.0 1.5 1.8 1.3 2.0 1.5 2.0 1.7 1.65 1.85
2.0 1.5 1.8 1.3 2.0 1.5 2.0 1.7 1.65 1.85 2.0 1.5 1.8 1.3 2.0 1.5 2.0 1.7
1.65 1.85 2.0 1.5 1.8 1.3 2.0 1.5 2.0 1.7 1.65 1.85 2.0 1.5 1.8 1.3 2.0
1.5 2.0 1.7 1.65 1.85 2.0 1.5 1.8 1.3 2.0 1.5 2.0 1.7 1.65 1.85 2.0 1.5
1.8 1.3 2.0 1.5 2.0 1.7 1.65 1.85 2.0 1.5 1.8 1.3 2.0 1.5 2.0 1.7 1.65
1.85 2.0 1.5 1.8 1.3 2.0 1.5 2.0 1.7 1.65 1.85 2.0 1.5 1.8 1.3 2.0 1.5
2.0 1.7 1.65 1.85] *10^6/(n/2);
%initial HCPV volume, 100%saturation; rm3
L_com_ini=[10 15 20 15 20 10 15 10 15 20 10 15 20 15 20 10 15 10 15 20
10 15 20 15 20 10 15 10 15 20 10 15 20 15 20 10 15 10 15 20 10 15 20 15
20 10 15 10 15 20 10 15 20 15 20 10 15 10 15 20 10 15 20 15 20 10 15 10
15 20 10 15 20 15 20 10 15 10 15 20 10 15 20 15 20 10 15 10 15 20 10 15
20 15 20 10 15 10 15 20 10 15 20 15 20 10 15 10 15 20 10 15 20 15 20 10
15 10 15 20 10 15 20 15 20 10 15 10 15 20 10 15 20 15 20 10 15 10 15 20
10 15 20 15 20 10 15 10 15 20 10 15 20 15 20 10 15 10 15 20 10 15 20 15
20 10 15 10 15 20 10 15 20 15 20 10 15 10 15 20 10 15 20 15 20 10 15 10
15 20 10 15 20 15 20 10 15 10 15 20 10 15 20 15 20 10 15 10 15 20 10 15
20 15 20 10 15 10 15 20 10 15 20 15 20 10 15 10 15 20 10 15 20 15 20 10
15 10 15 20 10 15 20 15 20 10 15 10 15 20 10 15 20 15 20 10 15 10 15
20]*100/n; %the length of compartment 1 to 500; m
L_intercom_ini=[100 100 150 200 150 100 150 100 150 200 100 100 150 200
150 100 150 100 150 200 100 100 150 200 150 100 150 100 150 200 100 100
150 200 150 100 150 100 150 200 100 100 150 200 150 100 150 100 150 200
100 100 150 200 150 100 150 100 150 200 100 100 150 200 100 100 150 200
150 200 100 100 150 200 150 100 150 100 150 200 100 100 150 200 150 100
150 100 150 200 100 100 150 200 150 100 150 200 100 100 150 200 100 100
150 200

```

```

150 100 150 100 150 200 100 100 150 200 150 100 150 100 150 200 100 100
150 200 150 100 150 100 150 200 100 100 150 200 150 100 150 100 150 200
100 100 150 200 150 100 150 100 150 200 100 100 150 200 150 100 150 100
150 200 100 100 150 200 150 100 150 100 150 200 100 100 150 200 150 100
150 100 150 200 100 100 150 200 150 100 150 100 150 200 100 100 150 200
150 100 150 100 150 200 100 100 150 200 150 100 150 100 150 200 100 100
150 200 150 100 150 100 150 200 100 100 150 200 150 100 150 100 150 200
100 100 150 200 150 100 150 100 150 200 100 100 150 200 150 100 150 100
150 200 100 100 150 200 150 100 150 100 150 200 100 100 150 200 150 100
150 100 150 200 100 100 150 200 150 100 150 100 150 200 100 100 150 200
150 100 150 100 150 200 100 100 150 200 150 100 150 100 150 200 100 100
150 200 150 100 150 100 150 200 100 100 150 200 150 100 150 100 150 200
100 100 150 200 150 100 150 100 150 200 100 100 150 200 150 100 150 100
150 200 100 100 150 200 150 100 150 100 150 200 100 100 150 200 150 100
150 100 150 200 100 100 150 200 150 100 150 100 150 200 100 100 150 200
150 100 150 100 150 200 100 100 150 200 150 100 150 100 150 200 100 100
150 200 150 100 150 100 150 200 100 100 150 200 150 100 150 100 150 100
200]/(n/4);      %the length between compartment 1 to 500; m

Pw=1.5*10^4*ones(1,n); %initial wellbore pressure; kPa
Ja=Ja_ini(1:n);      %aquifer pressure; kPa
Wi=4*10^7*ones(1,n); %initial aquifer size; rm3
Jw=Jw_ini(1:n);      %well transmissibility; Sm3/(day-kPa)
J_com=J_com_ini(1:n); %inter-compartment transmissibility for
communicating case; Sm3/(day-kPa)
J_noncom=zeros(1,n);
% inter-compartment transmissibility for non-communicating case,
pipeline fraction control the value, pressure dependent,
Jw=(2DA^2/(f*density*L*pressure loss))^0.5;Sm3/(day-kPa)

%if it is multiple communicating compartments model,J_int=J_com, if it
is multiple noncommunicating compartments model, J_int=J_noncom;
if (sig==1)
J_int=J_com;
else
J_int=J_noncom;
end

W_awe=zeros(1,n); %accumulative water encroachment; rm3

```

```

Vi=Vi_ini(1:n);           %HCPV volume, 100%saturation; rm3
W_a=4*10^7*ones(1,n);    %aquifer size, initially is Wi; rm3
Cta=1.6*10^(-6)*ones(1,n); %aquifer compressibility; /kPa
Ctr=1.65*10^(-6)*ones(1,n); %total compressibility; /kPa
Bw=1.0;                  %water formation volume factor; Rms/Sm3
Bo=1.0;                  %oil formation volume factor; Rms/Sm3
Pr_avg=2.5*10^4*ones(1,n); %average reservoir pressure; kPa
Pa=2.5*10^4*ones(1,n);   %aquifer pressure; kPa
Gpsum=zeros(1,n);       %cumulative oil production profile; Sm3
Gp=zeros(1,n);          %oil production profile; Sm3
Prk=zeros(1,n);         %slope of pressure loss
detW=zeros(1,n);        %%water encroachment; Rm3
Flrat_AQ=zeros(1,n);    %aquifer influx; Rm3/day
dt=0.5;                 %time step; day

%%%%%%%%%%%%%%%%%%%%%%%%%%%%%%%%%%%%%%%%%%%%%%%%%%%%%%%%%%%%%%%%%%%%%%%% BLANK PIPE PRESSURE LOSS CALCULATIONS %%%%%%%%%

d=0.219;%wellbore diameter (m)
roughness=0.046*10^(-3);%roughness (m)
Ap=pi*d^2/4; %wellbore area Ap(m^2);
Dens=980;%Density (kg/m3);
vis=0.5*10^(-3);%Viscosity (Pa.s)
L_com=L_com_ini(1:n);%L_blank in meter,
L_intercom=L_intercom_ini(1:n);
%First value is the distance between bottomhole and compartment one, the
second value is blankpipe between compartment 1 and 2;

%%%%%%%%%%%%%%%%%%%%%%%%%%%%%%%%%%%%%%%%%%%%%%%%%%%%%%%%%%%%%%%%%%%%%%%% CALCULATIONS %%%%%%%%%

iii=1
Flratmat=zeros(1,n);
FlratmatAQ=zeros(1,n);
FlratmatAAQ=zeros(1,n);
Prmat=Pr_avg;
                %Reservoir pressure profile -KPa
Pamat=Pa;
                %Aquifer pressure profile -KPa
Pwmat=Pw;
Gpmat=zeros(1,n); %Accumulative gas production profile -Sm3
xmat_iii=iii*dt;

pathname='F:\MUNwork\figure\wd\';

Pr_avg_tot=Pr_avg;
Pa_tot=Pa;

```

```

Gp_tot=Gp;
detW_tot=detW;
Gpsum_tot=Gpsum;
W_awe_tot=W_awe;
Flrat_AQ_tot=Flrat_AQ;

for iii=2:1000

    iii;          %loop variables
    Prk(1)=-Bo*Jw(1)*(Pr_avg(1)-Pw(1))/Ctr(1)/(Vi(1)-W_awe(1))-Bw*Ja(1)*(
    Pr_avg(1)-Pa(1))/Ctr(1)/(Vi(1)-W_awe(1))+Bo*J_int(1)*(Pr_avg(2)-Pr_avg
    (1));
    forkk=2:n-1
    Prk(kk)=-Bo*Jw(kk)*(Pr_avg(kk)-Pw(kk))/Ctr(kk)/(Vi(kk)-W_awe(kk))-Bw*
    Ja(kk)*(Pr_avg(kk)-Pa(kk))/Ctr(kk)/(Vi(kk)-W_awe(kk))+Bo*J_int(kk)*(P
    r_avg(kk+1)-Pr_avg(kk))-Bo*J_int(kk-1)*(Pr_avg(kk)-Pr_avg(kk-1));
    end
    Prk(n)=-Bo*Jw(n)*(Pr_avg(n)-Pw(n))/Ctr(n)/(Vi(n)-W_awe(n))-Bw*Ja(n)*(
    Pr_avg(n)-Pa(n))/Ctr(n)/Vi(n)-Bo*J_int(n-1)*(Pr_avg(n)-Pr_avg(n-1));
    Pr_avg=Pr_avg+dt*Prk;    %Reservoir pressure in RU at time t -KPa
    forkkk=1:n
    Pa(kkk)=Pa(kkk)-dt*(Bw*Ja(kkk)/Cta(kkk)/W_a(kkk)*(Pa(kkk)-Pr_avg(kkk)
    ));
    Gp(kkk)=Bo*Jw(kkk)*(Pr_avg(kkk)-Pw(kkk))*dt;
                                     %Gas produced in RU1 within a
    time interval -Sm3
    detW(kkk)=(Bw*Ja(kkk)*(Pa(kkk)-Pr_avg(kkk)))*dt;
    %Water encroachment at t (RC)
    velocity(kkk)=Gp(kkk)/dt/24/3600/3.14/(d/2)^2;%velocity (m/s);
    NRe(kkk)=Dens*d*velocity(kkk)/vis;%Renold Number
    fric(kkk)=(1/(-1.8*log(6.9/NRe(kkk)+(roughness/d/3.7)^1.11))).^2;%fri
    ction factor
    Gpsum(kkk)=Gpsum(kkk)+Gp(kkk);
                                     %Accumulative gas production in RU1 at
    time t -Sm3
    Flrat(kkk)=Gp(kkk)/dt;          %flow rate function
    Flrat_AQ(kkk)=detW(kkk)/dt;
    W_awe(kkk)=W_awe(kkk)+detW(kkk);
    end
    forjjj=1:n-1
    Pd_bp(jjj)=fric(jjj)*Dens*(velocity(jjj)/2+velocity(jjj+1)/2)^2/2/d;
    %pressure loss Pd_bp (Pa)
    end
    Flrat_AAQ=sum(Flrat_AQ);

```

```

W_a=W_a+sum(detW);
forjj=1:n-1
Jw_noncom(jj)=(2*d*Ap^2/fric(jj)/Dens/L_intercom(jj)/Pd_bp(jj))^0.5;
end
Jw_noncom(n)=0;
Flratmat_iii=Flrat;
FlratmatAQ_iii= Flrat_AQ;
FlratmatAAQ_iii=Flrat_AAQ;
Prmat_iii=Pr_avg;           %Reservoir pressure profile -KPa
Pamat_iii=Pa;              %Aquifer pressure profile -KPa
Pwmat_iii=Pw;
Gpmat_iii=Gpsum;          %Accumulative gas production profile -Sm3
xmat_iii=iii*dt;

Pr_avg_tot=[Pr_avg_tot;Pr_avg];
Pa_tot=[Pa_tot;Pa];
Gp_tot=[Gp_tot;Gp];
detW_tot=[detW_tot;detW];
Gpsum_tot=[Gpsum_tot;Gpsum];
W_ave_tot=[W_ave_tot;W_ave];
Flrat_AQ_tot=[Flrat_AQ_tot;Flrat_AQ];
end

%%%%%%%%%%%%%%%%%%%%%%%%%%%%%%%%%%%%%%%%%%%%%%%%%%%%%%%%%%%%%%%%%%%%%%%% RESULTS %%%%%%%%%
RF=sum(Gpsum)*Bo/sum(Vi); %Recover factor
T = cputime
surf(Pr_avg_tot);shading interp;
surf(Pa_tot); shading interp;figure(gcf);
plot(Pr_avg_tot(48,:));figure(gcf);
plot(Pr_avg_tot(end,:));figure(gcf);
plot(Pr_avg_tot(:,1));figure(gcf);
plot(Pr_avg_tot(:,2));figure(gcf);
plot(Pr_avg_tot);figure(gcf);
hold on; plot(Pa,'k','linewidth',2);
hold on; plot(Pa_tot(:,3),'k','linewidth',2);

```

## D Case Study Results from Section 4.1

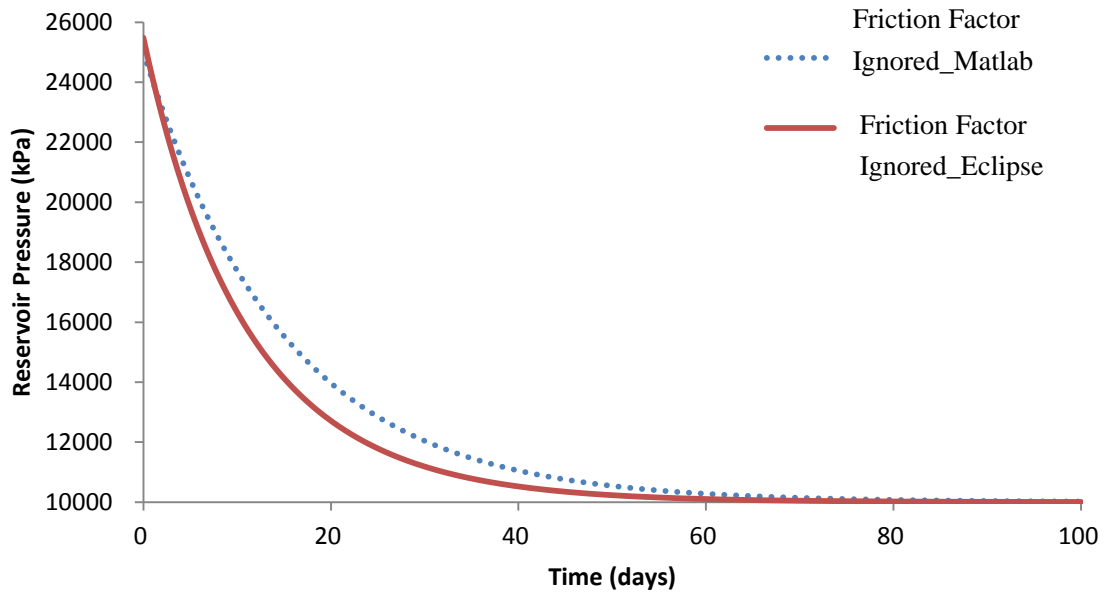


**Figure D.1: Reservoir Pressure, Friction Factor Ignored**

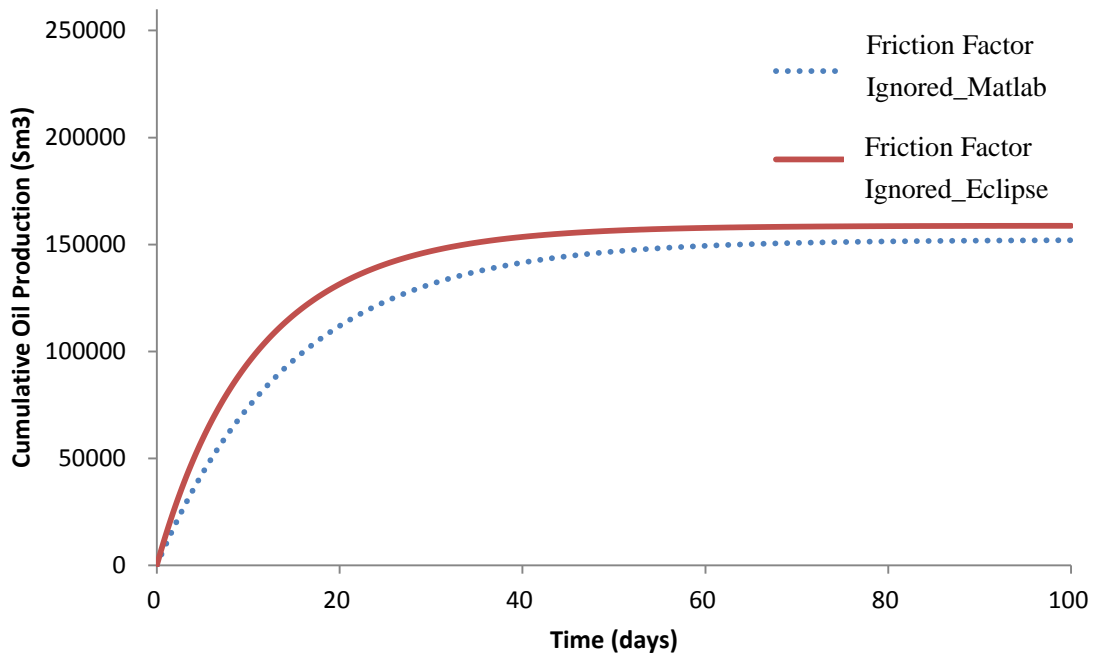


**Figure D.2: Cumulative Oil Production, Friction Factor Ignored**

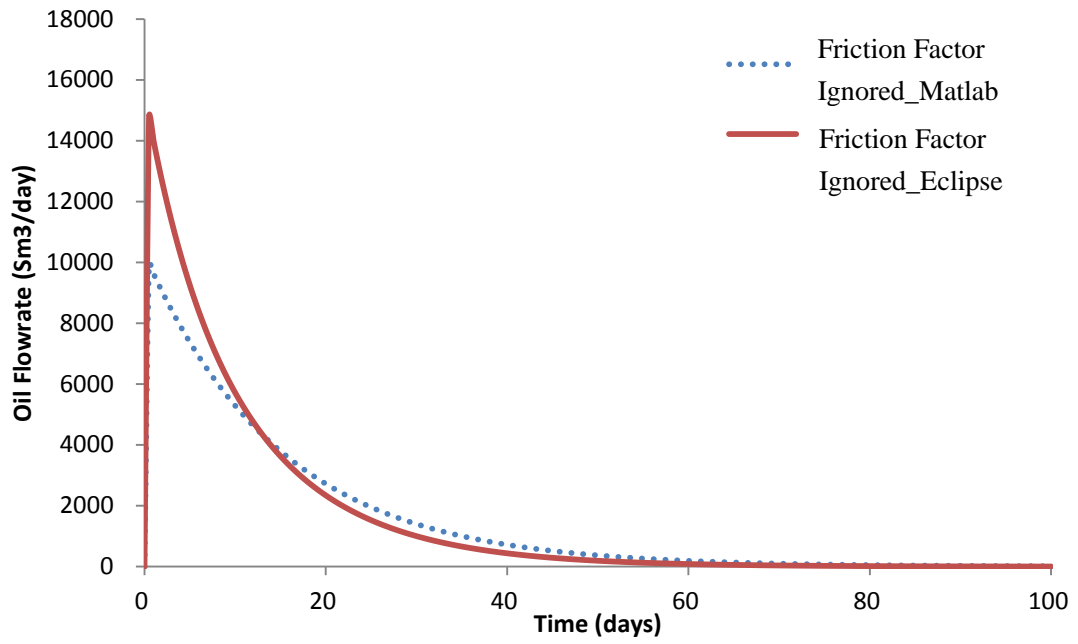


**Figure D.3: Oil Flowrate, Friction Factor Ignored**

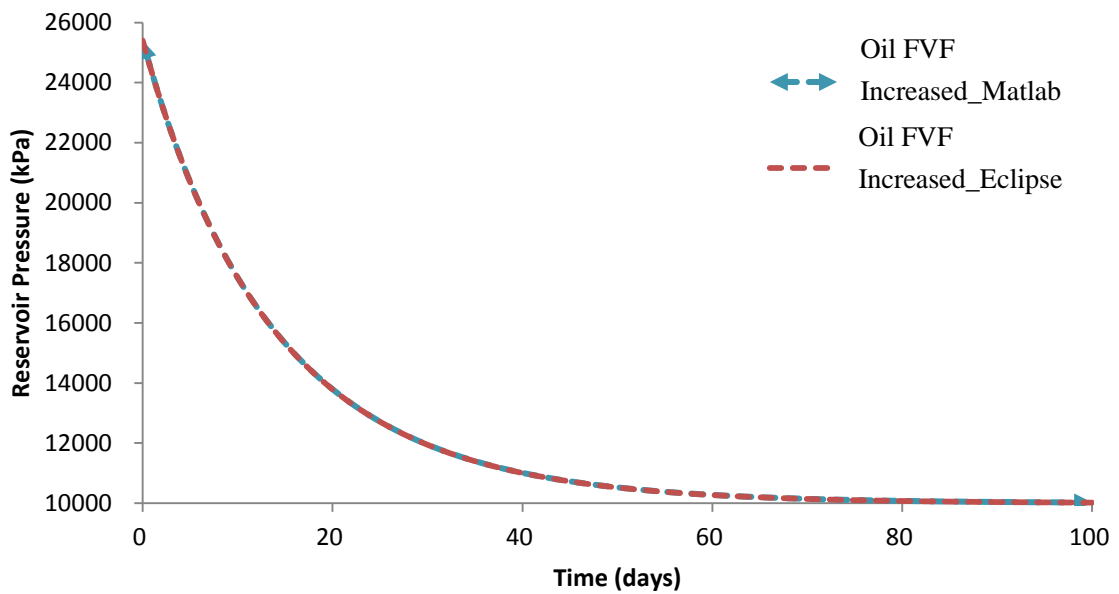


**Figure D.4: Reservoir Pressure, Oil FVF Increased**

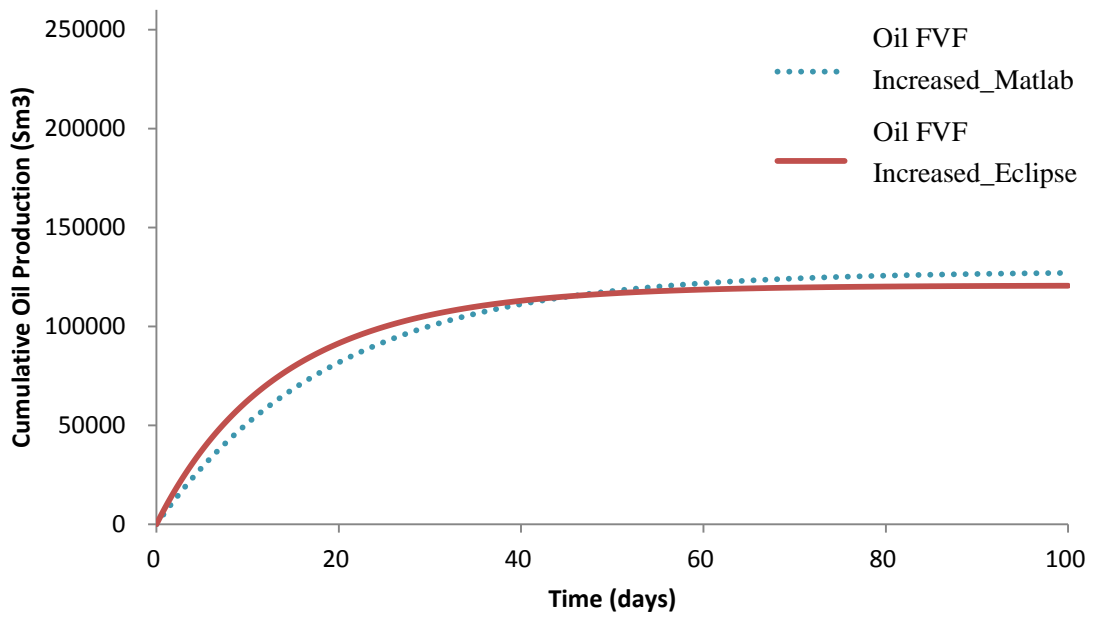


**Figure D.5: Cumulative Oil Production, Oil FVF Increased**

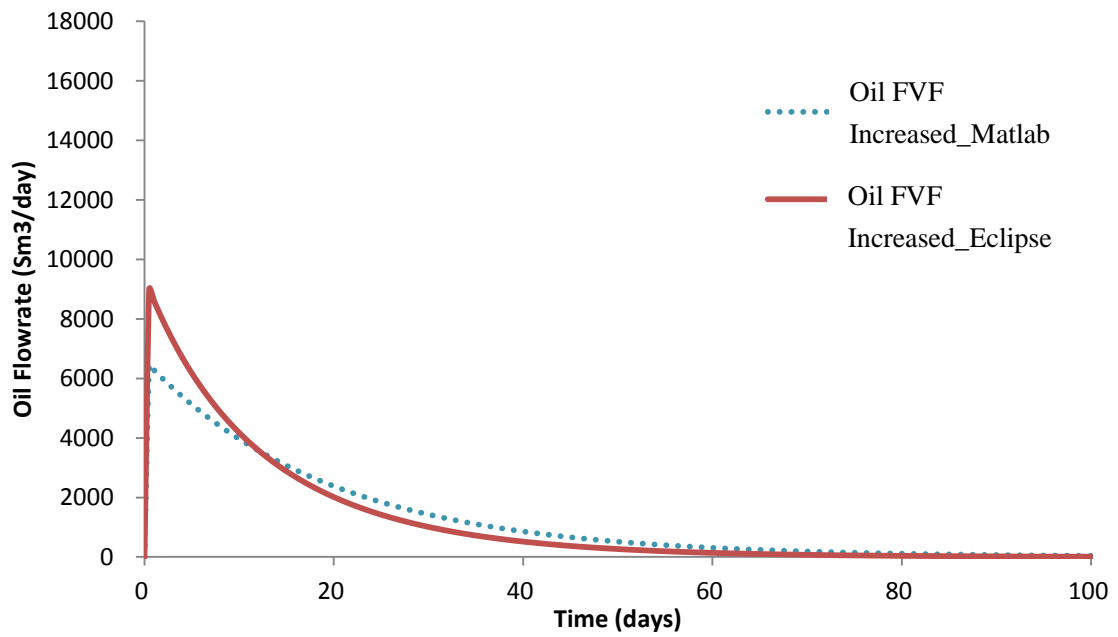


**Figure D.6: Oil Flowrate, Oil FVF Increased**

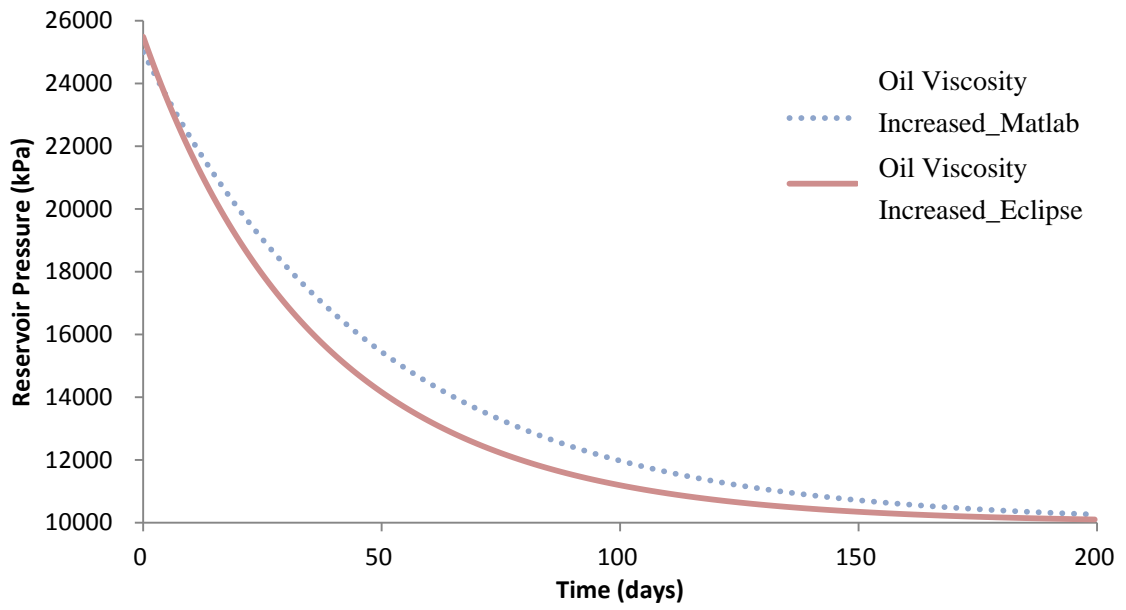


**Figure D.7: Reservoir Pressure, Oil Viscosity Increased**

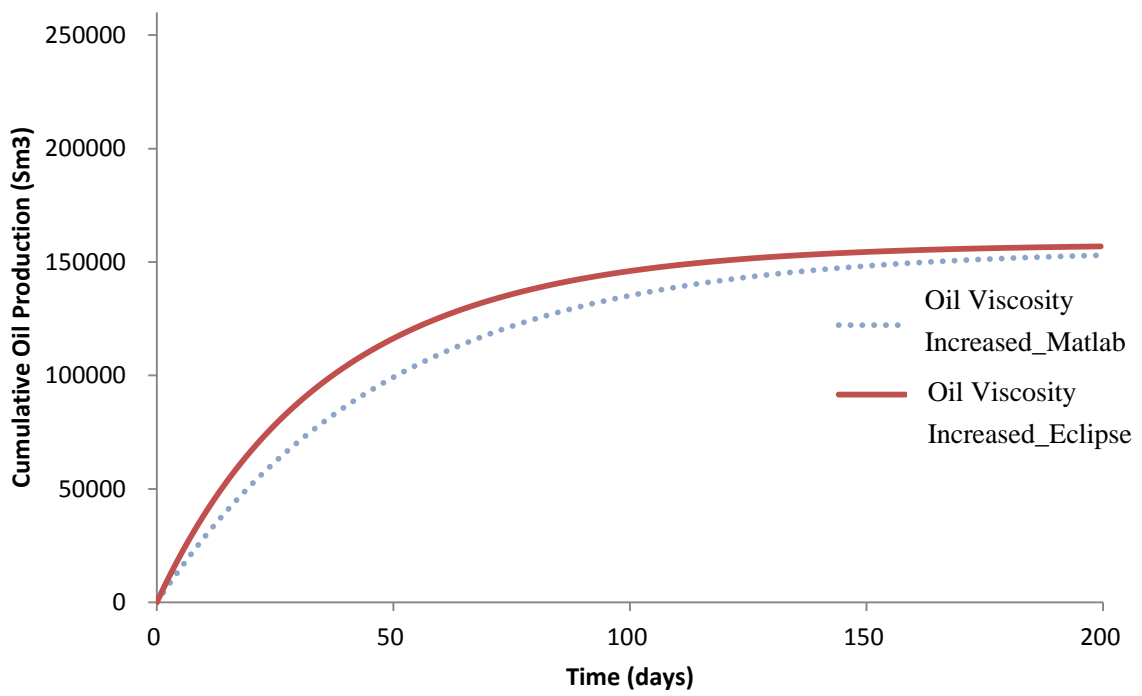


**Figure D.8: Cumulative Oil Production, Oil Viscosity Increased**

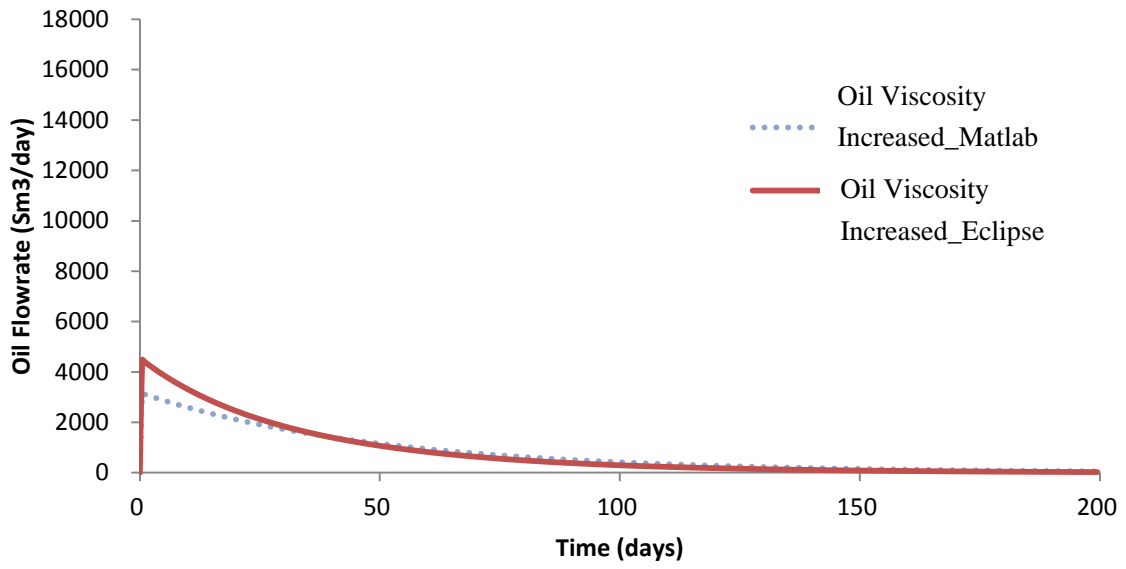


**Figure D.9: Oil Flowrate, Oil Viscosity Increased**

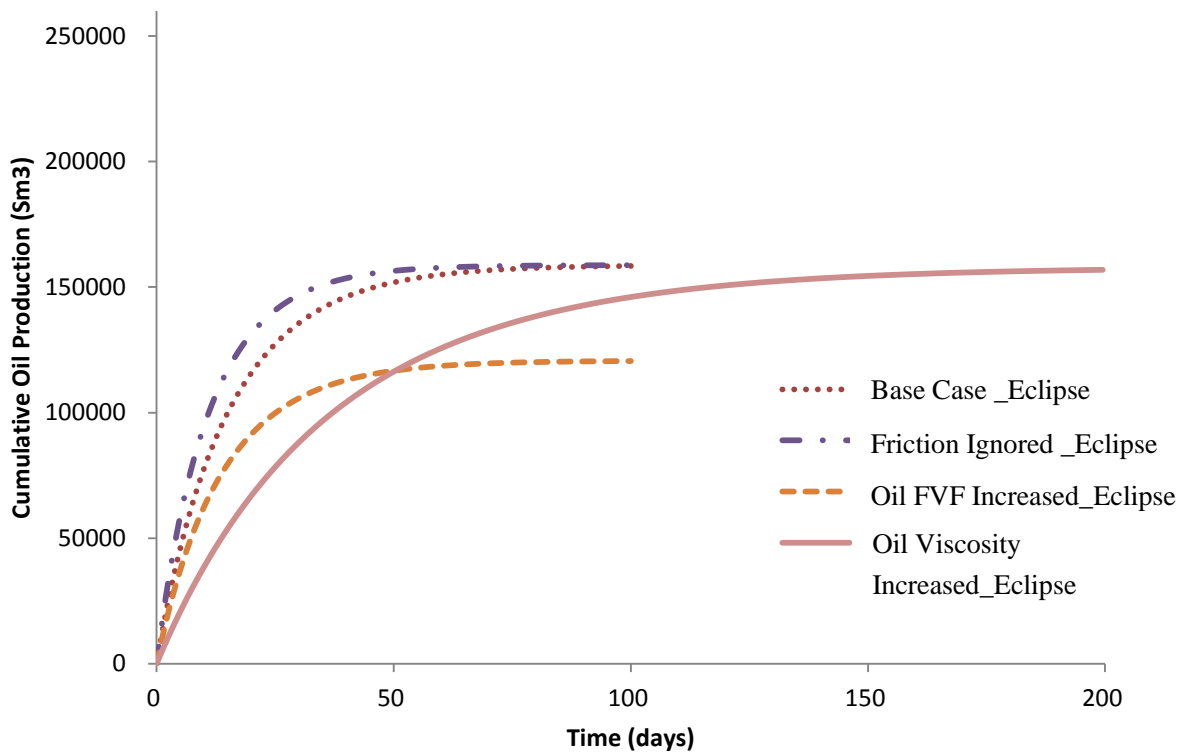


**Figure D.10: Cumulative Oil Production Profile, Eclipse**